APPROXIMATE THEORY FOR THE FLOW THROUGH A CASCADE OF CAMBERED AIRFOILS

Thesis by

Mitsuru Kurosaka

In Partial Fulfillment of the Requirements

For the Degree of

Doctor of Philosophy

California Institute of Technology

Pasadena, California

1968

(Submitted November 20, 1967)

ACKNOWLEDGMENTS

The author wishes to express his deep gratitude and appreciation to Professor W. Duncan Rannie for his most excellent guidance during the course of this investigation and throughout the author's graduate study at the California Institute of Technology.

Not only the original conceptions leading to this thesis are attributable to him, but the actual execution of the calculation and the writing of the manuscript could never have been possible without his constant advice and unfailing encouragement.

For friendly advice, encouragement, and assistance, I am grateful to Professor Frank E. Marble.

A great debt is owed to Messrs. P. N. Shankar and N. R. Thach for the painstaking care with which they read and corrected numerous linguistic mistakes in the draft.

The author also wishes to thank Mrs. Roberta Duffy for her excellent work in preparing the typed manuscript.

Financial assistance to the author in the form of California Institute of Technology Teaching and Research Assistantships and Woodrow Wilson Foundation and Ford Foundation summer scholarships has made graduate study possible and has been greatly appreciated.

Finally, my heartfelt thanks to my wife, Kumiko, who has provided the encouragement and patience which were so necessary to the completion of this work.

ABSTRACT

An approximate theory for steady irrotational flow through a cascade of thin cambered airfoils is developed. Isolated thin airfoils have only slight camber in most applications, and the well known methods that replace the source and vorticity distributions of the curved camber line by similar distributions on the straight chord line are adequate. In cascades, however, the camber is usually appreciable, and significant errors are introduced if the vorticity and source distributions on the camber line are approximated by the same distribution on the chord line.

The calculation of the flow field becomes very clumsy in practice if the vorticity and source distributions are not confined to a straight line. A new method is proposed and investigated; in this method, at each point on the camber line, the vorticity and sources are assumed to be distributed along a straight line tangent to the camber line at that point, and corrections are determined to account for the deviation of the actual camber line from the tangent line. Hence, the basic calculation for the cambered airfoils is reduced to the simpler calculation of the straight line airfoils, with the equivalent straight line airfoils changing from point to point.

The results of the approximate method are compared with numerical solutions for cambers as high as 25 per cent of the chord. The leaving angles of flow are predicted quite well, even at this high value of the camber. The present method also gives the functional relationship between the exit angle and the other parameters such as airfoil shape and cascade geometry.

TABLE OF CONTENTS

LIST OF FIGURES

LIST OF SYMBOLS

a_n	coefficient of (modified) vorticity distribution
b_n	coefficient of (modified) source distribution
c	chord length (Figure 1)
dl	infinitesimal distance measured along camber line
i	imaginary number
$m(x)$	source strength at point x
$m'(x)$	modified source strength at point x, $m'(x)=m(x)\frac{dl}{dx}$
q	velocity
q_o	induced velocity at point on camber line
q_u	upstream velocity at infinity (Figure 1)
q_d	downstream velocity at infinity (Figure 1)
q_m	geometrical mean velocity at infinity (Figure 1)
s	spacing-chord ratio of cascade (Figure 1); the reciprocal of this is solidity
$t(x)$	thickness at point x (Figure 2)
u	x component of induced velocity
v	y component of induced velocity
u_o	x component of induced velocity at a point on camber line
v_o	y component of induced velocity at a point on camber line
U_∞	x component of mean velocity q_m at infinity (Figure 1)
V_∞	y component of mean velocity q_m at infinity (Figure 1)
x, y	coordinates (Figure 1)
$y_o(x)$	vertical coordinate of camber line (Figure 2)
z_o	point on camber line where the velocity is evaluated
α	attack angle (Figure 1)

α_i	incidence angle (Figure 1)
α_n, β_n	$a_n = \alpha_n + \beta_n \cdot \tan\alpha$
α_n^*, β_n^*	$b_n = \alpha_n^* + \beta_n^* \cdot \tan\alpha$
β	stagger angle (Figure 1)
$\gamma(x)$	vorticity at point x
$\gamma'(x)$	modified vorticity at point x , $\gamma'(x) = \gamma(x)\frac{dl}{dx}$
δ_1, δ_2	angular range of expansion (see section 7, Part II)
Γ	circulation
θ	angular position of x , $\theta = \arccos\frac{x}{\frac{c}{2}}$

Subscripts

n	normal to camber line
t	tangent to camber line
$+$	just above camber line
$-$	just below camber line
i	inner range
o	outer range
u	far upstream
d	far downstream

I. INTRODUCTION

In the present investigation, the two-dimensional, inviscid, and irrotational flow past a cascade of airfoils is studied. Notable examples of cascade arrangement are found in turbomachinery. There, cascades are used to deflect the direction of flow and to change the magnitude of the velocity as the fluid passes from upstream to downstream through lattices of airfoils. Although cascade arrangements are in use in radial flow machines as well as in axial flow ones, the discussion will hereafter be limited to the axial-flow turbomachinery.

The relation between two-dimensional flow through a cascade of airfoils and the flow in an axial turbomachine is somewhat similar to the relation between two-dimensional flow around an airfoil and the flow around a three-dimensional wing. There are differences, however, that influence the type of information needed. The blades of an axial turbomachine extend between inner and outer annular walls, and in this respect operate as if they had end plates. On the other hand, the flow is never strictly two-dimensional relative to annular surfaces, because of the coupling of the centrifugal force field with the variations in the circumferential component of velocity. The flow field in the turbomachine is often strongly rotational, and although the radial component of vorticity is zero on the average, spanwise velocity components may occur having the same effect as sweepback of a three-dimensional wing.

Practical examples of a cascade are also found in the flow-deflecting devices in other technological fields, and such cascade arrangements are called by various names according to their use --

vanes, guides, or straighteners. Generally speaking, there are two important classes of cascade problems: direct and inverse problems. The direct problem is, given the inlet flow conditions and airfoil shape, to determine the flow field around the cascade. Conversely, in the inverse problem, one is interested in finding the airfoil shape such as to produce the prescribed pressure distribution along the blade surface under given inlet flow conditions.

Only the direct problem is treated in the present work. Accordingly, the question posed is the following: how does the flow pattern look for the fluid past a two-dimensional cascade of given airfoil shape under the given inlet flow conditions? It is only natural to try to analyze this cascade flow as a perturbation of the flow past an isolated airfoil. This is the approach taken by Robinson and Laurmann in ref. 1. There, the analysis is valid only for low solidity, i.e., high spacing-chord ratio. Another approach is the limiting case of high solidity, i.e., low spacing-chord ratio. In this limit, the flow between two adjacent blades can be regarded as channel flow. Everywhere except near the leading edges, the streamlines within the cascade are in a direction parallel to the blade surfaces, and this enables us to study such flow in a simple way. In most cascade arrangements of interest, however, the solidity is of the order of unity, and these cases cannot be handled adequately by either of the limiting approaches.

Various attempts have been made to treat the cascade of solidity near unity. According to the methods adopted, these may be divided into two classes; conformal mapping and the singularity method. In the conformal mapping method, the airfoil shape in the physical

plane is mapped by a series of transformations into a circle, and the flow field around the circle is determined. In the singularity method, vortices and sources are distributed along the camber line of the airfoil and the flow field is studied in the physical plane.

Perhaps the most widely-known conformal mapping method is that of Garrick (ref. 2), published in 1944. This is essentially an extension of Theodorsen's method (ref. 3) developed for isolated airfoils of arbitrary shape. In Theodorsen's method, the airfoil shape is first mapped into an intermediate mapping plane using the Joukowski transformation. If the airfoil were a flat plate, the contour in the intermediate plane would be a circle. In the case of an arbitrarily shaped airfoil, the contour becomes a pseudo-circle. This pseudo-circle is mapped into a true circle by secondary mapping, and the key of the problem is to find a suitable mapping function. Garrick followed the same procedure as Theodorsen's method, i.e., first mapping the airfoil shape in a cascade into a pseudo-circle and then to a final true circle. In transforming a cascade airfoil into a pseudo-circle, one must use some function other than the Joukowski transformation to take care of the periodicity of flow. For this purpose, Garrick used the cascade mapping function, an exact transformation which maps a cascade of flat plates into a circle. Periodicity of the flow in the physical plane is dealt with by the use of logarithmic functions in the mapping function. The final mapping from this pseudo-circle to the true circle is done exactly in the same way as Theodorsen's method.

This method has several disadvantages in practical applications. These all stem from the peculiar features of the cascade map-

ping function. The upstream and downstream infinities in the physical plane are mapped into two points close to the circle. The contour representing the blade surface is strongly distorted and very sensitive to errors near these points. It is difficult to transform the pseudo-circle into a circle with rapid convergence. These distortions make the conformal mapping technique unsuitable for practical purposes, particularly if the solidity is greater than unity.

In an attempt to by-pass the difficulties encountered in conformal mapping methods, Schlichting and his collaborators made extensive investigation of a different approach, the singularity method. This is an extension of the classical 'thin airfoil' theory to the airfoils in a cascade. By thin airfoil is meant an airfoil of small thickness and camber. Vortices and sources are located on the chord line instead of on the camber line, and the flow tangency condition is satisfied for the induced velocities obtained on the chord line. The method is discussed in more detail elsewhere; here, we merely remark that approximations valid for the single airfoil become cruder for airfoils in a cascade. Therefore, results based on Schlichting's method involve inevitable errors ab initio, even for the case of a slightly cambered airfoil to which his method is strictly applicable.

Practical isolated airfoils have small camber, and the approximation made by placing the vorticity and source distributions on the straight chord line is not seriously in error. The blades in cascades, however, have high camber in general, to conform to the large change in flow direction through the cascade. Conventional thin airfoil theory is not adequate; it is necessary to extend the theory to cambered air-

foils if it is to be useful.

Recently, another approach requiring the use of a high-speed digital computer (refs. 6-8) has been quite successful. In this method, vortices are distributed on the surface of the airfoil. With a sufficient number of vortices (100 or more), one can obtain an accurate representation of the flow even for thick airfoils. From the condition for tangential flow at the blade surface, the magnitudes of the vortices can be determined by direct numerical procedure. By this method, a cascade of any airfoil shape, thick or thin, at any solidity, can be studied with any desired accuracy.

The availability of this method, however, does not provide the final answer to the problem. Being numerical from the beginning to the end, it cannot give any insight to the functional relationship between some desired characteristic and the various factors affecting it. In general, the designer is more in need of such functional relationship in its simplest possible form rather than the detailed, accurate results for a few specific examples. Such functional relationship would enable him, firstly, to compute families of results for the different combinations of parameters, secondly, to study the optimum design condition analytically,and thirdly, to furnish guidelines for the systematic correlation of experimental data. Specifically, the main interest of the cascade designer in the flow analysis will be to find the dependence of airfoil surface pressure distribution and the exit flow angle on parameters such as airfoil shape, cascade geometry, and inlet flow direction. The velocity or pressure distribution is important in estimating the boundary layer behavior over the airfoil

surface.

Because induced drag is of no importance in the turbomachine, optimum performance of the blades occurs at a much higher lift coefficient than for a three-dimensional wing. The pressure distribution on the blade surfaces is at least helpful in estimating the stall margin for the cascade.

Aside from pressure distribution, the designer needs to know the overall performance of the cascade quite accurately, and for this purpose the leaving angle is the most convenient parameter (ref. 18). The leaving angle gives the deflection of the flow through the cascade, and it is found to be not strongly dependent on incidence angle. Hence, it is a better indicator of overall performance than the lift coefficient, for instance, which varies appreciably with incidence angle. It is clear that one cannot expect accurate information for pressure distribution near the leading edges of the airfoil. Such information cannot be found easily for the isolated airfoil, and for airfoils in a cascade the situation is worse. Knowledge of the flow close to the leading edge of the blade, however, is of little practical use compared with similar knowledge for the airplane wing.

One should be able to predict the exit angle through analytical treatment, because it is largely determined by the general outline of the airfoil and cascade geometry; local leading edge contours have small effect on the flow downstream. Methods used in the past have not been very successful. For example, in Schlichting's work, loc. cit., it is possible to express exit angle in terms of incidence angle only after all other parameters are given in numbers explicitly.

Further, his work is applicable only to slightly cambered airfoils in the cascade. Therefore, the principal objective of the present study is to develop a theory without restriction to small camber that will predict exit angle and pressure distribution with reasonable accuracy and a minimum of numerical computation.

A remark about the degree of accuracy needed is pertinent here. The Reynolds number for blades in a turbomachine is lower than that appropriate to an airplane wing by a factor of 100 or more. Hence, boundary layers are relatively much thicker; this, combined with unavoidable errors in manufacture of blades and damage in operation, implies that there is little point in attempting a very exact theory of flow around blades of precisely given contour.

A brief outline of the present method is given below. The singularity method is adopted here. The essential difference between the present singularity method and those of Schlichting and Mellor is that the sources and vortices are distributed on the camber line of airfoils in the cascade instead of on the straight chord line. The calculation of the flow field becomes very awkward in practice, however, unless the vortices and sources are not confined to a straight line. At a point on the camber line of an airfoil in a cascade, the major contribution to the induced velocity comes from the sources and vortices located near the point on the same airfoil. This contribution can be represented approximately by the source and vorticity distribution on the straight line tangent to the airfoil camber line at that point. Therefore, at each point on the camber line, the vortices and sources are first assumed to be distributed along the tangent line,

and corrections are made to account for the deviation of the actual camber line from the tangent line and for the velocities induced by the other airfoils in the cascade. Hence, basically, the calculation is reduced to the similar case of straight line airfoils, with the equivalent straight line airfoils changing from point to point. From the flow tangency condition, the strengths of source and vortex distribution are determined.

II. THEORY AND ANALYSIS

In this part, first the problem will be defined and formulated by distributing the vortices and sources on the camber line. Then, in section 2, the technique of the method of 'tangent slope,' as it is called in the present work, will be introduced for the simplest case of the isolated airfoil. Then, before applying this method to the cascade problem, several preliminary steps will be described in sections 3 and 4. In section 5, we will see the application of the tangent slope method to the cascade problem with some ensuing discussion in sections 6 and 7. In sections 8 and 9, the boundary condition and the method of satisfying it will be discussed. In section 10, the main steps of the calculation procedure will be summarized.

1. Formulation of the Problem.

In Figure 1, the fluid approaches the cascade from far upstream with velocity q_u at an angle α_u and leaves far downstream of the cascade with velocity q_d at an angle α_d. The vectorial mean of q_u and q_d is called the mean velocity q_m at a mean angle α_m. Although usually q_u and α_u are the given quantities, it is more convenient to regard q_m and α_m as given for theoretical treatment. The conversion of these mean values to q_u and α_u can be made easily once the circulation around an airfoil is determined. The angle which q_u makes with the tangent to the mean camber line of the airfoil at the leading edge is the incidence angle α_i. β is called the stagger angle, and if β is positive, the cascade is a compressor cascade; if negative, a turbine cascade.

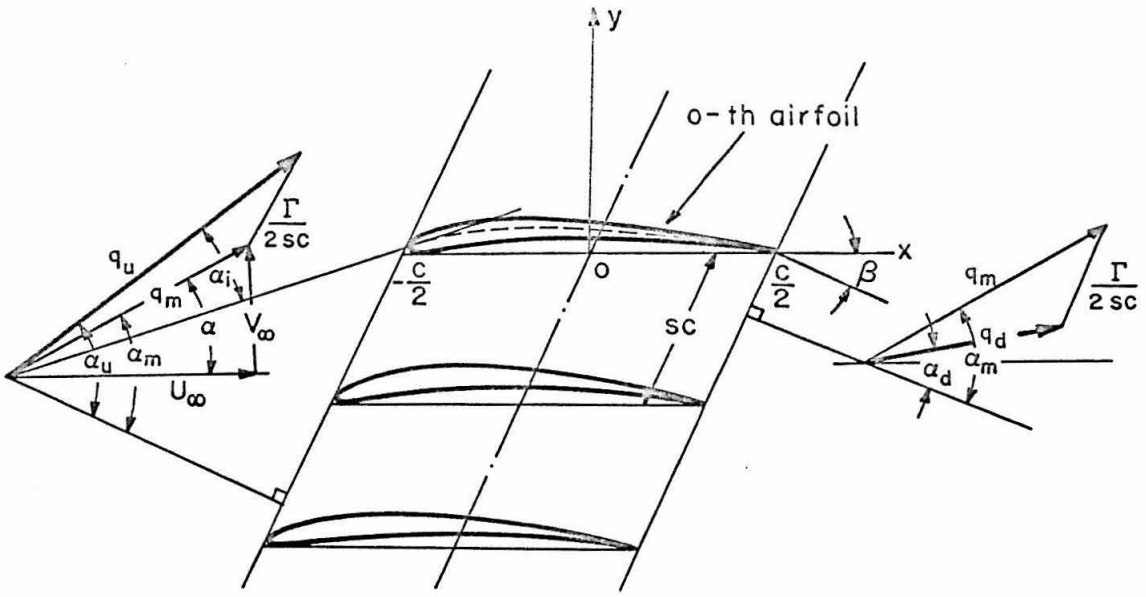

Figure 1. Cascade geometry and nomenclature.

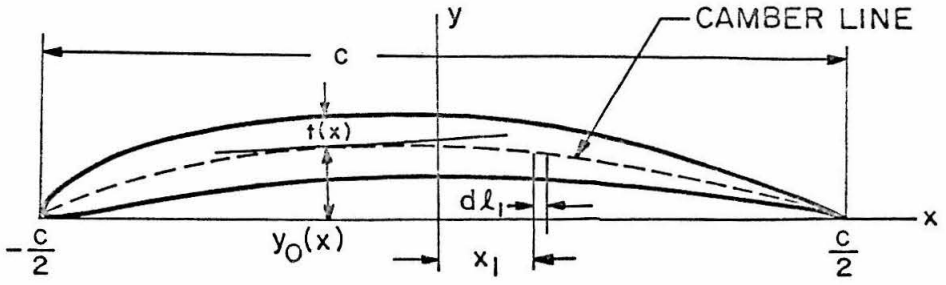

Figure 2. Airfoil Sections.

The spacing chord ratio is s , and the reciprocal of s is called solidity. As for the airfoil section, the chord c connects the two points of greatest curvature, the leading and trailing edges. A camber line $y_o(x)$ is specified along the chord and, normal to the camber line, the profile thickness $t(x)$ is superposed, see Figure 2.

The fluid is assumed to be in steady, inviscid, irrotational flow. The flow at infinity is uniform.

If the airfoil is thin, the induced velocity at a given point $z = x + iy$ can be obtained by distributing vorticity γ and source m over the camber of each airfoil. From the periodicity of the cascade flow, the strength of these singularities is the same on each airfoil at the correspoinding points. If the position at which these singularities are located on the 0^{th} airfoil is $x_1 + iy_o(x_1) = z_1$, then the corresponding point on the N^{th} airfoil can be given as $x_1 + nsc\sin\beta + iy_o(x) + insc\cdot\cos\beta$, and the induced velocity at z is

$$u - iv = \frac{1}{2\pi}\int (m(x_1) + i\gamma(x_1))\left(\sum_{n=-\infty}^{\infty} \frac{1}{z - z_1 - nsc\sin\beta - insc\cos\beta}\right) dl_1 \qquad (2.1)$$

where dl_1 is the segment of camber line, and the integration is carried out over the entire camber line.

The sum inside the integral can be identified as the hyperbolic cotangent function (ref. 9), and the above relation can then be rewritten as

$$u - iv = \frac{1}{2sc} e^{i\beta}\int (m(x_1) + i\gamma(x_1)) \coth\left[\frac{\pi(z - z_1)}{sc} e^{i\beta}\right] dl_1 \qquad (2.2)$$

It is convenient here to change the integration variable from ℓ_1 to x_1 and define 'modified' source and vorticity as

$$\left.\begin{aligned} m(x_1)\,d\ell_1 &= m'(x_1)\,dx_1 \\ \gamma(x_1)\,d\ell_1 &= \gamma'(x_1)\,dx_1 \end{aligned}\right\} \qquad (2.3)$$

Then (2. 2) becomes

$$u - iv = \frac{1}{2sc} e^{i\beta} \int_{-\frac{c}{2}}^{\frac{c}{2}} \left(m'(x_1) + i\,\gamma'(x_1)\right) \coth\left[\frac{\pi(z - z_1)}{sc} e^{i\beta}\right] dx_1 \qquad (2.4)$$

2. The Case of the Isolated Airfoil of Zero Thickness: Method of Tangent Slope.

To illustrate the main idea of what, in the present work, is called the 'method of tangent slope,' consider the simplest case of isolated airfoil of zero thickness. This corresponds to $s \to \infty$, $m' = 0$ in (2. 4) of the previous section.

$$u - iv = \frac{i}{2\pi} \int_{-\frac{c}{2}}^{\frac{c}{2}} \gamma'(x_1) \frac{1}{z - z_1}\, dx_1$$

Let $z = z_0$ be the point on the camber line; then the induced velocities on the camber line u_0 , v_0 are given by

$$\begin{aligned} u_0 - iv_0 &= \frac{i}{2\pi} \int_{-\frac{c}{2}}^{\frac{c}{2}} \gamma'(x_1) \frac{1}{\left[x + iy_0(x)\right] - \left[x_1 + iy_0(x_1)\right]}\, dx_1 \\ &= \frac{i}{2\pi} \int_{-\frac{c}{2}}^{\frac{c}{2}} \gamma'(x_1) \frac{1}{x - x_1 + i\left[y_0(x) - y_0(x_1)\right]}\, dx_1 \end{aligned} \qquad (2.5)$$

Now, even if $y_0(x)$ is a relatively simple polynomial, it is difficult to carry out this integration. To overcome this difficulty, expand the

camber line $y_o(x_1)$ about x in a Taylor series.

$$y_o(x)-y_o(x_1) = -y_o'(x)(x_1-x) - \frac{1}{2}y_o''(x)(x_1-x)^2 - \frac{1}{6}y_o^{(3)}(x)(x_1-x)^3 - \cdots\cdots$$

$$- \frac{1}{n!}y_o^{(n)}(x)(x_1-x)^n - \cdots\cdots$$

Then

$$\begin{aligned} & x - x_1 + i\left[y_o(x) - y_o(x_1)\right] \\ &= (x-x_1)\Big\{1 + iy_o'(x) - \frac{i}{2}y_o''(x)(x-x_1) + \frac{i}{6}y_o^{(3)}(x)(x-x_1)^2 + \cdots + \frac{i}{n!}(-1)^{n-1}y_o^{(n)}(x)(x-x_1)^{n-1} \\ &\qquad + \cdots\cdots\Big] . \\ &= \left(1+iy_o'(x)\right)(x-x_1)\Big\{1 - \Big[\frac{i}{2}\frac{y_o''(x)}{1+iy_o'(x)}(x-x_1) - \frac{i}{6}\frac{y_o^{(3)}(x)}{1+iy_o'(x)}(x-x_1)^2 + \cdots\cdots \\ &\qquad + \frac{i}{n!}(-1)^n\frac{y_o^{(n)}(x)}{1+iy_o'(x)}(x-x_1)^{n-1} + \cdots\cdots\Big]\Big\} \end{aligned}$$

and

$$\begin{aligned} & \frac{1}{x - x_1 + i\left[y_o(x) - y_o(x_1)\right]} \\ &= \frac{1}{1+iy_o'(x)}\cdot\frac{1}{x-x_1} \\ &\quad \times \frac{1}{1 - \Big[\frac{i}{2}\frac{y_o''(x)}{1+iy_o'(x)}(x-x_1) - \frac{i}{6}\frac{y_o^{(3)}(x)}{1+iy_o'(x)}(x-x_1)^2 + \cdots\cdots + \frac{i}{n!}(-1)^n\frac{y_o^{(n)}(x)}{1+iy_o'(x)}(x-x_1)^{n-1} + \cdots\Big]} \\ &= \frac{1}{1+iy_o'(x)}\cdot\frac{1}{x-x_1} \\ &\quad \times \Big\{1 + \sum_{m=1}^{\infty}\Big[\frac{i}{2}\cdot\frac{y_o''}{1+iy_o'}(x-x_1) - \frac{i}{6}\cdot\frac{y_o^{(3)}}{1+iy_o'}(x-x_1)^2 + \cdots + \frac{i}{n!}(-1)^n\cdot\frac{y_o^{(n)}(x)}{1+iy_o'}(x-x_1)^{n-1} + \cdots\Big]^m\Big\} \end{aligned}$$

In the last step, the formula $\frac{1}{1-a} = \sum_{m=0}^{\infty} a^m$ is used. Carrying out the expansion in the bracket, one gets

$$\frac{1}{X-X_1+i[Y_0(x)-Y_0(x_1)]}$$

$$= \frac{1}{1+iY_0'(x)} \frac{1}{x-x_1}$$

$$\times\Bigg[1+\frac{i}{2}\frac{Y_0''}{1+iY_0'}(x-x_1)+\frac{1}{12}\cdot\frac{-3Y_0''^2-2iY_0^{(3)}(1+iY_0')}{(1+iY_0')^2}(x-x_1)^2$$

$$+\frac{-3iY_0''^3+4(1+iY_0')Y_0''Y_0^{(3)}+iY_0^{(4)}(1+iY_0')^2}{24(1+iY_0')^3}(x-x_1)^3$$

$$+\frac{-6iY_0^{(5)}(1+iY_0')^3-(20(Y_0^{(3)})^2+30Y_0''Y_0^{(4)})(1+iY_0')^2+90iY_0''^2\cdot Y_0^{(3)}(1+iY_0')+45Y_0''^4}{720(1+iY_0')^4}$$

$$\times(x-x_1)^4$$

$$+\Big\{2iY_0^{(6)}(1+iY_0')^4+(12Y_0''Y_0^{(5)}+20Y_0^{(3)}Y_0^{(4)})(1+iY_0')^3-(45i(Y_0'')^2Y_0^{(4)}+60iY_0''(Y_0^{(3)})^2$$

$$\times(1+iY_0')^2-120(Y_0'')^3Y_0^{(3)}(1+iY_0')+45i(Y_0'')^5\Big\}\times\frac{1}{1440(1+iY_0')^5}$$

$$\times(x-x_1)^5+\cdots\Bigg]$$

It is to be noticed here that all the derivatives in the bracket $\Big[\quad\Big]$ are evaluated at the point x and independent of the integration variable x_1.

Thus, the induced velocities (2.5) can be written in the following form.

$$u_o(x) - iv_o(x) = \frac{i}{2\pi}\left[\frac{1}{1+iy_o'} \int_{-\frac{c}{2}}^{\frac{c}{2}} \frac{\gamma'(x_1)\,dx_1}{x - x_1} + \frac{iy_o''}{2(1+iy_o')^2} \int_{-\frac{c}{2}}^{\frac{c}{2}} \gamma'(x_1)\,dx_1 \right.$$

$$+ \frac{-3y_o''^2 - 2iy_o^{(3)}(1+iy_o')}{12(1+iy_o')^3} \int_{-\frac{c}{2}}^{\frac{c}{2}} \gamma'(x_1)(x - x_1)\,dx_1$$

$$+ \frac{-3iy_o''^3 + 4(1+iy_o')y_o''y_o^{(3)} + iy_o^{(4)}(1+iy_o')^2}{24(1+iy_o')^4} \int_{-\frac{c}{2}}^{\frac{c}{2}} \gamma'(x_1)(x - x_1)^2\,dx_1$$

$$+ \left\{ -6iy_o^{(5)}(1+iy_o')^3 - \left(20(y_o^{(3)})^2 + 30y_o''\cdot y_o^{(4)}\right)(1+iy_o')^2 + 90iy_o''^2\cdot y_o^{(3)}(1+iy_o') + 45y_o''^4 \right\}$$

$$\times \frac{1}{720(1+iy_o')^5} \int_{-\frac{c}{2}}^{\frac{c}{2}} \gamma'(x_1)(x - x_1)^3\,dx_1$$

$$+ \left\{ 2iy_o^{(6)}(1+iy_o')^4 + \left(12y_o''\cdot y_o^{(5)} + 20y_o^{(3)}\cdot y_o^{(4)}\right)(1+iy_o')^3 - \left(45i(y_o'')^2\cdot y_o^{(4)} + 60iy_o''\cdot(y_o^{(3)})^2\right.\right.$$

$$\left.\left. \times (1+iy_o')^2 - 120(y_o'')^3\cdot y_o^{(3)}(1+iy_o') + 45i(y_o'')^5 \right\}\right.$$

$$\left. \times \frac{1}{1440(1+iy_o')^6} \int_{-\frac{c}{2}}^{\frac{c}{2}} \gamma'(x_1)(x - x_1)^4\,dx_1 + \text{----} \right] \qquad (2.6)$$

Notice that due to Taylor series expansion of the camber line about x all the factors associated with y_o are taken outside of the integral and the integrand involves only $x - x_1$ and vorticity γ', and once the form of γ' is given, they are in forms ready to be integrated.

The above expression for the induced velocities has a simple physical interpretation. If one considers the velocity due to the first term in the bracket,

$$u_o^{(1)} - iv_o^{(1)} = \frac{i}{2\pi} \frac{1}{1+iy_o'(x)} \int_{-\frac{c}{2}}^{\frac{c}{2}} \frac{\gamma'(x_1)\,dx_1}{x - x_1} \qquad (2.7)$$

then, for the special case of $y_o'(x) = 0$, this reduces to

$\frac{v}{2\pi}\int_{-\frac{c}{2}}^{\frac{c}{2}} \frac{\gamma'(x_1)dx_1}{x-x_1}$, and this is the familiar induced velocity on the chord due to the vorticity distributed over a flat plate lying along x axis. In the general case of $y_0'(x) \neq 0$, (2.7) can be identified as a rotation of this flat plate in such a way that it becomes tangent to the camber line at point x , where the velocity on the camber line is computed, as shown in Figure 3. This can be demonstrated in the following way. Equating the real and imaginary parts of both sides of equation (2.7), one gets

$$u_0^{(1)} = \frac{1}{2\pi}\cdot\frac{y_0'(x)}{1+(y_0'(x))^2}\int_{-\frac{c}{2}}^{\frac{c}{2}} \frac{\gamma'(x_1)dx_1}{x-x_1} = \frac{1}{2\pi}\cdot\frac{y_0'(x)}{(1+y_0'^2)^{\frac{1}{2}}}\int_{-\frac{c}{2}}^{\frac{c}{2}} \frac{\gamma(x_1)dx_1}{x-x_1}$$

$$v_0^{(1)} = \frac{-1}{2\pi}\cdot\frac{1}{1+(y_0'(x))^2}\int_{-\frac{c}{2}}^{\frac{c}{2}} \frac{\gamma'(x_1)dx_1}{x-x_1} = \frac{-1}{2\pi}\cdot\frac{1}{(1+y_0'^2)^{\frac{1}{2}}}\int_{-\frac{c}{2}}^{\frac{c}{2}} \frac{\gamma(x_1)dx_1}{x-x_1} \qquad (2.8)$$

On the other hand, let us consider the induced velocity at point P due to the vorticity at Q with the same strength as at the corresponding point Q' on the camber line, but instead distributed on the straight-line ξ axis, which is tangent at P to the camber line. Then, in ξ , η coordinates,

$$u_\xi - iv_\eta = \frac{v}{2\pi}\int_{-\frac{c^{(2)}}{2}}^{\frac{c^{(1)}}{2}} \frac{\gamma(\xi_1)d\xi_1}{\xi-\xi_1} \quad , \qquad \gamma(\xi_1) = \gamma(x_1)$$

$$\therefore \quad u_\xi = 0 \quad , \quad v_\eta = -\frac{1}{2\pi}\int_{-\frac{c^{(2)}}{2}}^{\frac{c^{(1)}}{2}} \frac{\gamma(x_1)d\xi_1}{\xi-\xi_1}$$

Substituting $\xi = \frac{x}{\cos\varphi_0}$, $\xi_1 = \frac{x_1}{\cos\varphi_0}$, we get

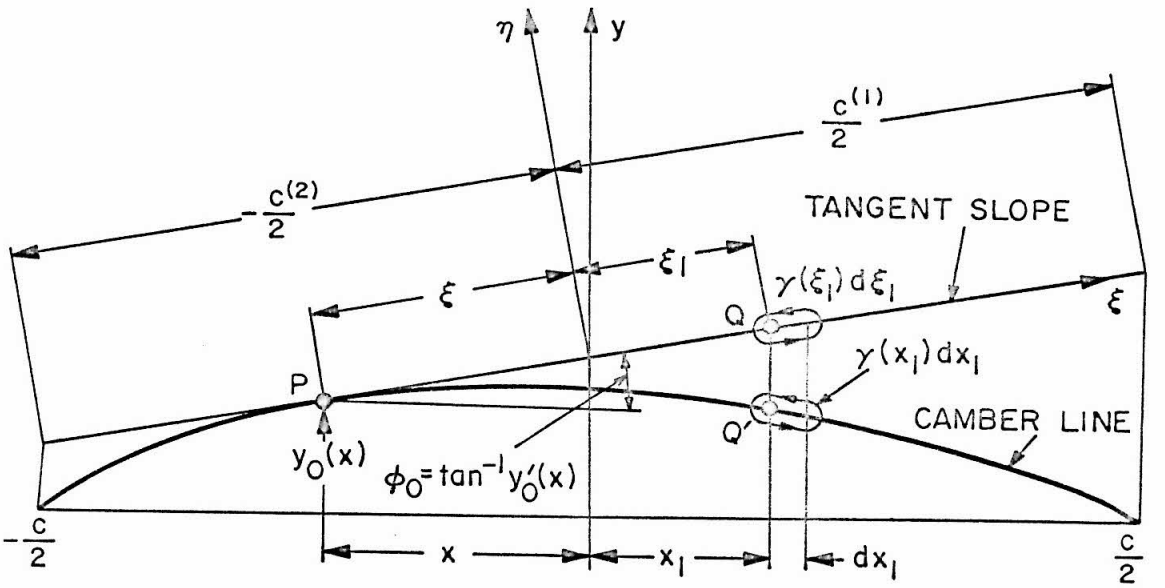

Figure 3. Tangent slope method.

$$u_\xi = 0 \quad , \quad v_\eta = -\frac{1}{2\pi}\int_{-\frac{c}{2}}^{\frac{c}{2}} \frac{\gamma(x_1)\,dx_1}{x - x_1}$$

Transforming to x , y coordinate system,

$$u_x = u_\xi \cos\varphi_0 - v_\eta \sin\varphi_0 = -v_\eta \sin\varphi_0 = \frac{1}{2\pi}\,\frac{y_0'}{(1+y_0'^2)^{\frac{1}{2}}}\int_{-\frac{c}{2}}^{\frac{c}{2}} \frac{\gamma(x_1)\,dx_1}{x - x_1} ,$$

$$u_y = u_\xi \sin\varphi_0 + v_\eta \cos\varphi_0 = v_\eta \cos\varphi_0 = -\frac{1}{2\pi}\,\frac{1}{(1+y_0'^2)^{\frac{1}{2}}}\int_{-\frac{c}{2}}^{\frac{c}{2}} \frac{\gamma(x_1)\,dx_1}{x - x_1} ,$$

Comparing these expressions with equation (2. 8), we see these expressions are identical. Hence, we can conclude that the first term in the velocity equation of (2. 6) is due to the vorticity with the same strength as at the corresponding point on a curved camber line, but distributed on the tangent to the mean camber line at the point where the velocity is being evaluated. The remaining terms are all correction terms to this first one, and each has its own physical meaning: the second term is due to the single vortex, the amount of which is equal to the total circulation. This single vortex is located on the concave side of the camber line, because by the first term the vorticity distribution is displaced from the camber line to the tangent line, which is located on the convex side, and the second term, the largest of all remaining terms, must be placed in such a way as to cancel this effect. The third term is due to the moment of vorticity or doublet, ; the fourth term is due to the triplet, and so forth. Usually, the first term gives the most significant contribution, and from its characteristic feature, the Taylor series expansion leading to

equation (2.6) is called the 'tangent slope' method in this study. The rate of convergence of series expression in (2.6) will be examined in Part III; in the following sections, the 'tangent slope' method will be applied to the cascade problem. First, let us study the nature of the singularity of the integrand in the cascade.

3. Two Types of Series Expansion of the Cotangent Hyperbolic Function in the Integral for the Cascade.

For simplicity, let ξ be defined as

$$\xi(z, z_1) \equiv \frac{\pi(z - z_1)}{sc} e^{i\beta}$$

then equation (2.4) can be written as

$$u - iv = \frac{1}{2sc} e^{i\beta} \int_{-\frac{c}{2}}^{\frac{c}{2}} (m'(x_1) + i\gamma'(x_1)) \coth \xi(z, z_1)\, dx_1, \qquad (2.9)$$

$$z = x + iy, \quad z_1 = x_1 + iy_0(x_1)$$

Now the only singularity of the integrand in (2.9) comes from the point $z = z_1$; namely, if we fix the point z to be a point on the O^{th} blade, $z = z_0 = x + iy_0(x)$, then the singularity occurs when the integration variable x_1 crosses the point x . The form of the singularity at the point z_0 in question is apparent from equation (2.1), for from that equation, the singular term at z_0 is found to be given by $n = 0$,

$$\frac{1}{2\pi} \int (m(x_1) + i\gamma(x_1)) \frac{1}{z_0 - z_1} dl_1$$

i.e., the velocities induced by the sources and vortices on the airfoil where the point z_0 is also situated. Such singular behavior of the integrand can be brought out in explicit form, if we expand $\coth \xi$ near $z - z_1$ or $\xi = 0$ (e.g. ref. 10).

$$\coth\xi = \frac{1}{\xi} + \frac{1}{3}\xi - \frac{1}{45}\xi^3 + \frac{2}{945}\xi^5 + \cdots + \frac{(-1)^{n-1}\,2^{2n}}{(2n)!}B_n\xi^{2n-1} + \cdots \qquad (2.10)$$

$$|\xi| < \pi$$

where the B_n's are Bernoulli numbers. The first term of the expansion gives the above-mentioned singularity of the isolated airfoil, and the corrections to this are provided by the rest of the series. When ξ is small, a few terms in this expansion provide a good approximation.

Since the radius of convergence of this series is π, the validity of (2.10) over the entire chord is restricted to

$$|\xi| = \frac{\pi|z - z_1|}{sc} < \pi$$

or

$$|z - z_1| < sc \qquad (2.11)$$

But since $|z - z_1|_{max} = c$, the expansion above is valid over the entire chord line only if $s > 1$. Thus, except for cascades of high spacing-chord ratio, expansion (2.10) cannot be used over the entire chord, and another type of expansion of $\coth\xi$ for large ξ is needed. This is

$$\coth\xi = 1 + 2e^{-2\xi} + 2e^{-4\xi} + 2e^{-6\xi} + \cdots + 2e^{-2n\xi} + \cdots \qquad (2.12)$$

$$Re\,\xi > 0$$

The leading term of the right hand side corresponds to the limiting case of $\xi \longrightarrow \infty$, i.e., $s \longrightarrow 0$ for a finite value of $z - z_1$. Physically, $s \longrightarrow 0$ means a closely-spaced cascade, and in this case, instead of the discontinuous vorticity distribution along the

direction parallel to the cascade axis for a finite spacing s, the vorticity distribution becomes uniform -- in other words, smeared out -- along the cascade axis. The remaining terms correct for the periodicity of vorticity distribution for the finite spacing s.

These two expansions, (2. 10) and (2. 12), of the same function $\coth\xi$ are suitable in different ranges of ξ and to evaluate the integral of equation (2. 9), the chord line is split in such a way that in each division we can replace $\coth\xi$ by the correspondingly appropriate form. Hereafter, equation (2. 10) type expansions are called inner expansions, while those like (2. 12) are called outer expansions, denoting each with subscripts i and o respectively. Then (2. 9) can be written into two integrals as

$$\begin{aligned} u_o(x) - iv_o(x) &= \frac{1}{2sc} e^{i\beta} \int_i \left(m'(x_1) + i\gamma'(x_1)\right)(\coth\xi)_i \, dx_1 \\ &\quad + \frac{1}{2sc} e^{i\beta} \int_o \left(m'(x_1) + i\gamma'(x_1)\right)(\coth\xi)_o \, dx_1 \\ &= \frac{1}{2sc} e^{i\beta} \int_i \left(m'(x_1) + i\gamma'(x_1)\right)\left(\frac{1}{\xi} + \frac{1}{3}\xi - \frac{1}{45}\xi^3 + \cdots\right) dx_1 \\ &\quad + \frac{1}{2sc} e^{i\beta} \int_o \left(m'(x_1) + i\gamma'(x_1)\right)\left(1 + 2e^{-2\xi} + 2e^{-4\xi} + \cdots\right) dx_1 \end{aligned} \qquad (2.13)$$

4. Range of Inner and Outer Expansion.

In this section, we study the method of determining the range of the inner - outer expansion. Near $\xi = 0$, the inner expansion of equation (2. 10) is valid, while for $|\xi| \gg 1$, an equation (2.12) type outer expansion is suitable. In the overlapping region where the two types of expansion are both valid, however, there is no unique way to determine which expansion is preferable. For example, if one type

of expansion results in easier integration along the chord up to the higher order terms, then it might be wise to widen the range of such expansion within the overlapping region. But whatever the choice of range might be, the final induced velocity of equation (2. 13) should be independent of such choice. In reality, however, this would be so only if the infinite series are kept in their full form, and when one truncates such series expansions, then the final approximate expression for the induced velocity does depend on the choice of inner - outer expansion range. Nevertheless, we can anticipate that even such approximate velocities would not be too sensitive to the choice of such range. This is because such velocities consist of outer and inner expansion integrals, and if the range of inner expansion integral is taken to be narrower, then compensation will be made by widening the range of outer expansion. Such cancelling effect does not appreciably influence the sum of these two integrals.

Now let us first decide how to truncate the series expansions. As for the inner expansion series of equation (2. 10), after assuming proper forms for sources and vortices, every term is found to be integrated, explicitly and without difficulty, and we can retain any number of terms as we like. But for the purpose of the present investigation of obtaining as simple a method as possible, it would be best to take as small a number of terms as possible. So let us try the first and second terms in the inner expansion, equation (2. 10),

$$(\coth\xi)_i = \frac{1}{\xi} + \frac{1}{3}\xi \qquad (2.14)$$

and choose the range of expansion in such a way as the other terms are negligible.

As for the outer expansion, the terms of the form $2\bar{e}^{2n\xi}$ are found to make the integration difficult, so let us take only the first term in equation (2. 12),

$$(\coth \xi)_o = 1 \tag{2. 15}$$

and again we hope that there exists a range of expansion where the remaining terms can be neglected.

Of course, if we could not find a suitable range of ξ where both (2. 14) and (2. 15) are valid, then we would have to add extra terms, but as we will see in the next paragraph, such a range exists. First, consider the following problem, with $\beta = 0$, $x = X$, $x_1 = X_1$, and

$$\xi = \frac{\pi (X - X_1)}{SC}$$

Let us choose the range of expansion in such a way that $\coth\xi$ can be best represented by $(\coth\xi)_i$ and $(\coth\xi)_o$ over the entire chord range with the least possible error. Defining $F(\xi)$ as

$$F(\xi) = \begin{cases} (\coth\xi)_i = \frac{1}{\xi} + \frac{1}{3}\xi \ , & 0 < \xi < \xi_{cr} \\ \\ (\coth\xi)_o = 1 \ , & \xi_{cr} < \xi < \frac{\pi(X + \frac{C}{2})}{SC} \end{cases}$$

where $\xi_{cr} = \frac{\pi(X - X_{cr})}{SC}$ corresponds to the limit of inner expansion to the left of the fixed position of x . Then the square of the error in expressing $\coth\xi$ by $F(\xi)$ can be written as

$$E^2 = \int_0^{\frac{\pi(x+\frac{c}{2})}{sc}} (\coth\xi - F(\xi))^2 d\xi$$

$$= \int_0^{\xi_{cr}} (\coth\xi - \frac{1}{\xi} - \frac{1}{3}\xi)^2 d\xi + \int_{\xi_{cr}}^{\frac{\pi(x+\frac{c}{2})}{sc}} (\coth\xi - 1)^2 d\xi$$

Choose ξ_{cr} in such a way that E^2 is a minimum,

$$\frac{\partial E^2}{\partial \xi_{cr}} = 0$$

or

$$(\coth\xi_{cr} - \frac{1}{\xi_{cr}} - \frac{1}{3}\xi_{cr})^2 - (\coth\xi_{cr} - 1)^2 = 0$$

or

$$(1 - \frac{1}{\xi_{cr}} - \frac{1}{3}\xi_{cr}) \cdot (2\coth\xi_{cr} - 1 - \frac{1}{\xi_{cr}} - \frac{1}{3}\xi_{cr}) = 0$$

$$1 - \frac{1}{\xi_{cr}} - \frac{1}{3}\xi_{cr} = 0 \qquad \text{or} \qquad 2\coth\xi_{cr} - 1 - \frac{1}{\xi_{cr}} - \frac{1}{3}\xi_{cr} = 0$$

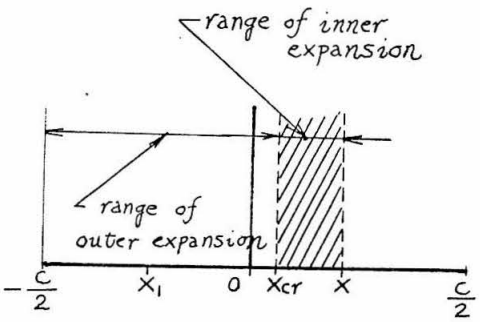

The first equation does not possess any real ξ_{cr} solution, while the second equation yields

$$\xi_{cr} = 1.6400$$

Similarly, it can be shown that the range of inner expansion to the right of x can be found to be the same as those to the left of x. Therefore,

$$(\coth\xi)_i = \frac{1}{\xi} + \frac{1}{3}\xi \quad , \quad 0 < |\xi| < |\xi_{cr}| \qquad (2.16)$$

$$(\coth\xi)_o = 1 \quad , \quad \text{outside of the above range}$$

$$|\xi_{cr}| = \frac{\pi|x - x_{cr}|}{sc} = 1.6400 \qquad (2.17)$$

In Figure 4, the graph of $\coth\xi$ is plotted against $(\coth\xi)_i$ and $(\coth\xi)_o$. There, it is seen that the inner expansion provides a good approximation over a large portion of the inner expansion range, while in the outer expansion range, the outer expansion $(\coth\xi)_o$ gives a satisfactory approximation. The largest error between $\coth\xi$ and two types of approximation occurs at $\xi = \xi_{cr} = 1.6400$, where

$$\coth\xi_{cr} = 1.0782,$$

$$(\coth\xi_{cr})_i = 1.1564, \quad (\coth\xi_{cr})_o = 1.000$$

and the discrepancies between the exact values and the two approximations are almost the same and about 8 per cent; the inner expansion over-estimates the true value while the outer expansion underestimates. Thus, these two errors almost cancel each other in the integral evaluation of equation (2.13). Furthermore, the largest contribution to this integral comes from the integrand near $x_1 = x$ or $\xi = 0$, and since inner expansion approximates well near such a point, these errors are almost completely negligible. We will see in Part III, after making comparison with the exact solution for the flat plate, that this is indeed so. It might be noteworthy to add that the accuracy of this approximation does not change from a cascade of one solidity to another, if we join the two expansions according to (2.16) and (2.17). This is due to the fact that ξ is given as the ratio of the distance on the chord to spacing sc, and if this ratio is kept

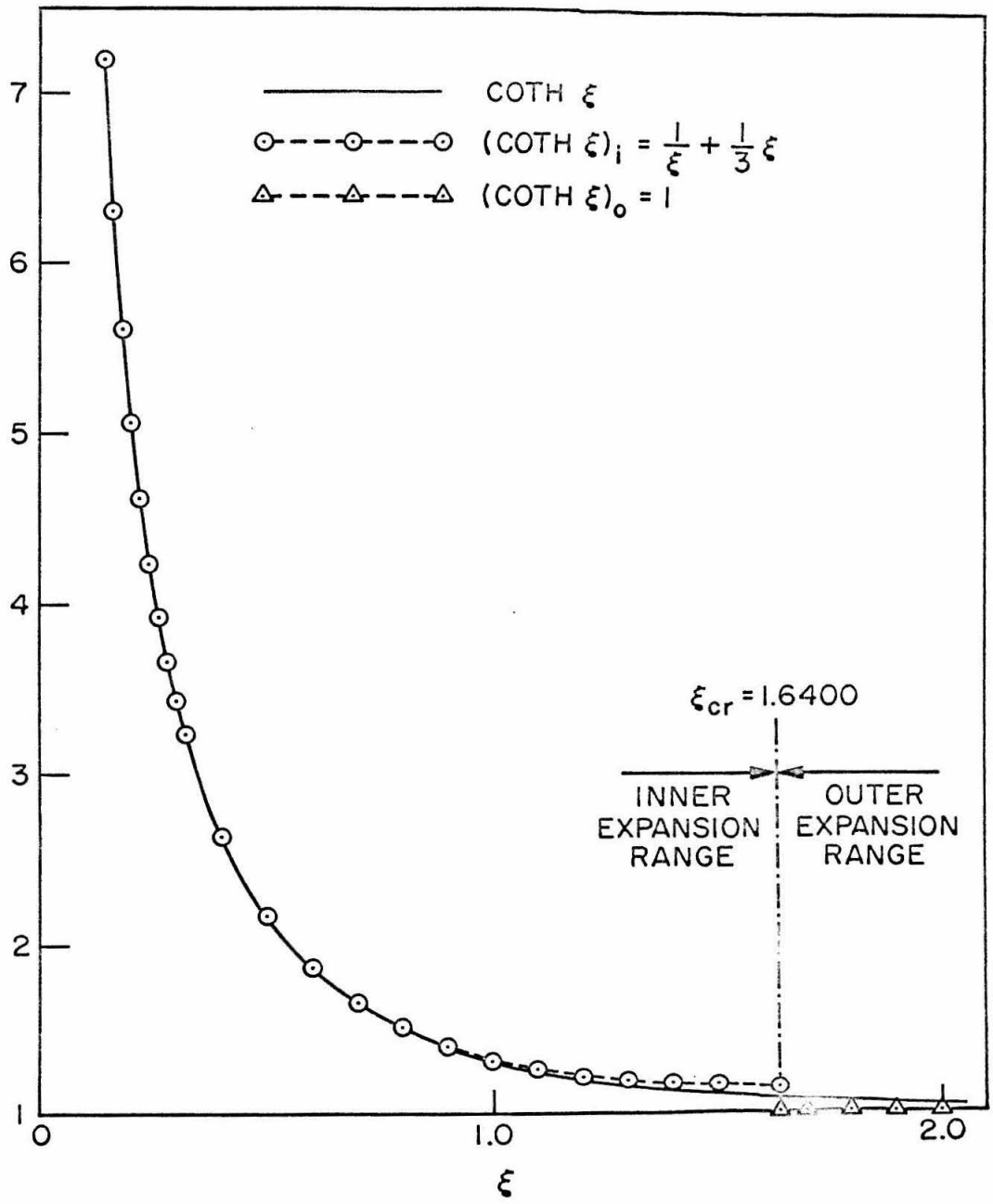

Figure 4. Approximation by inner-outer expansion.

constant, then the degree of approximation becomes similar for the cascade of any solidity.

Now the above method of determining the optimum expansion range applies only to a particular simple configuration related to the cascade. For the general case of a staggered and cambered cascade, we should compute such a range case by case, but such a procedure would complicate the problem. Instead, it is more useful for the present purpose to determine the range of expansion in some simple, uniform manner. This we will do by simply assuming that the expansion range x_{cr}, determined by (2. 17) and a function of both position on chord x and spacing-chord ratio s, is applicable to a cascade of staggered, cambered airfoils. We will see, in Part III, numerical justification of this assumption, too. The validity of this somewhat crude determination of expansion range comes from the aforementioned insensitivity of final results to such a split-up. Having determined the expansion range, we will apply the method of tangent slope to the cascade problem in the next section.

5. Application of Method of 'Tangent Slope' to the Cascade Problem.

Truncating the series expression in the integral of equation (2. 13) according to section 4, one gets

$$
\begin{aligned}
&u_0(x) - iv_0(x) \\
&= \frac{1}{2sc} e^{i\beta} \int_i (m'(x_1) + i\gamma'(x_1)) \left(\frac{1}{\xi} + \frac{1}{3}\xi \right) dx_1 \\
&\quad + \frac{1}{2sc} e^{i\beta} \int_0 (m'(x_1) + i\gamma'(x_1)) dx_1 \\
&= \frac{1}{2sc} e^{i\beta} \int_i (m'(x_1) + i\gamma'(x_1)) \left[\frac{sc\bar{e}^{i\beta}}{\pi(z_0 - z_1)} + \frac{1}{3} \frac{\pi(z_0 - z_1)}{sc} e^{i\beta} \right] dx_1 \\
&\quad + \frac{1}{2sc} e^{i\beta} \int_0 (m'(x_1) + i\gamma'(x_1)) dx_1 \\
&= \frac{1}{2\pi} \int_i (m'(x_1) + i\gamma'(x_1)) \frac{1}{z_0 - z_1} dx_1 + \frac{\pi e^{2i\beta}}{6(sc)^2} \int_i (m'(x_1) + i\gamma'(x_1))(z_0 - z_1) dx_1 \\
&\quad + \frac{1}{2sc} e^{i\beta} \int_0 (m'(x_1) + i\gamma'(x_1)) dx_1
\end{aligned}
\qquad (2.18)
$$

Now the first term in the equation corresponds to the isolated airfoil, and the method of 'tangent slope' of section 2 can be directly applied to evaluate the integral.

As for the second term, we can use the similar technique of Taylor expansion about x , such as

$$
z_0 - z_1 = (1 + iy_0'(x))(x - x_1) - \frac{i}{2} y_0''(x)(x - x_1)^2 + \frac{i}{6} y_0^{(3)}(x)(x - x_1)^3 + \cdots
$$
$$
+ \frac{i}{n!} (-1)^{n-1} y_0^{(n)}(x)(x - x_1)^n + \cdots
$$

Thus, (2.18) can be written in the following form.

$$
\begin{aligned}
&u_0(x) - i v_0(x) \\
&= \frac{1}{2\pi}\Bigg[\frac{1}{1+iy_0'}\int_i \big(m'(x_1)+i\gamma'(x_1)\big)\frac{dx_1}{x-x_1} + \frac{iy_0''}{2(1+iy_0')^2}\int_i \big(m'(x_1)+i\gamma'(x_1)\big)\,dx_1 \\
&\quad + \frac{-3y_0''^2 - 2iy_0^{(3)}(1+iy_0')}{12(1+iy_0')^3}\int_i \big(m'(x_1)+i\gamma'(x_1)\big)(x-x_1)\,dx_1 \\
&\quad + \frac{-3iy_0''^3 + 4(1+iy_0')y_0''y_0^{(3)} + iy_0^{(4)}(1+iy_0')^2}{24(1+iy_0')^4} \\
&\qquad \times \int_i \big(m'(x_1)+i\gamma'(x_1)\big)(x-x_1)^2\,dx_1 \\
&\quad + \Big\{ -6iy_0^{(5)}(1+iy_0')^5 - \big(20(y_0^{(3)})^2 + 30y_0''\cdot y_0^{(4)}\big)(1+iy_0')^2 + 90iy_0''^2\cdot y_0^{(3)}(1+iy_0') \\
&\qquad + 45y_0''^4 \Big\} \frac{1}{720(1+iy_0')^5}\int_i \big(m'(x_1)+i\gamma'(x_1)\big)(x-x_1)^3\,dx_1 \\
&\quad + \Big\{ 2iy_0^{(6)}(1+iy_0')^4 + \big(12y_0''\cdot y_0^{(5)} + 20y_0^{(3)}\cdot y_0^{(4)}\big)(1+iy_0')^3 \\
&\qquad - \big(45i(y_0'')^2 y_0^{(4)} + 60iy_0''\cdot(y_0^{(3)})^2\big)(1+iy_0')^2 - 120(y_0'')^3\cdot y_0^{(3)}(1+iy_0') \\
&\qquad + 45i(y_0'')^5 \Big\} \frac{1}{1440(1+iy_0')^6}\int_i \big(m'(x_1)+i\gamma'(x_1)\big)(x-x_1)^4\,dx_1 + \cdots \Bigg] \\
&+ \frac{\pi c}{6(sc)^2} e^{2i\beta}\Bigg[(1+iy_0')\int_i \big(m'(x_1)+i\gamma'(x_1)\big)(x-x_1)\,dx_1 \\
&\qquad - \frac{i}{2}y_0''\int_i \big(m'(x_1)+i\gamma'(x_1)\big)(x-x_1)^2\,dx_1 \\
&\qquad + \frac{i}{6}y_0^{(3)}\int_i \big(m'(x_1)+i\gamma'(x_1)\big)(x-x_1)^3\,dx_1 + \cdots \\
&\qquad + \frac{i}{n!}(-1)^{n-1}\cdot y_0^{(n)}\int_i \big(m'(x_1)+i\gamma'(x_1)\big)(x-x_1)^n\,dx_1 + \cdots \Bigg] \\
&+ \frac{1}{2sc} e^{i\beta}\int_0 \big(m'(x_1)+i\gamma'(x_1)\big)\,dx_1
\end{aligned}
\tag{2.19}
$$

Once the form of sources $m'(x_1)$ and vortices $\gamma'(x_1)$ are given, then all the integrals are in the forms ready to be integrated. In the next section, such forms will be discussed.

6. Series Form for Source and Vorticity Distribution.

Physically it is obvious that source $m(x_1)$ and vorticity $\gamma(x_1)$ are the differences of the velocities normal and tangential to the camber line, respectively, when they are evaluated just off the camber line,

$$m(x) = q_{n,+}(x) - q_{n,-}(x)$$

$$\gamma(x) = q_{t,+}(x) - q_{t,-}(x)$$

where suffixes + and - denote just above and below the camber line, respectively. Mathematical proof of this relation for the case of isolated airfoil is given in ref. 11, and the proof for the case of a cascade is given in Appendix 1 of the present work.

Introducing the auxiliary variable defined by

$$\theta = \cos^{-1}\left(\frac{x}{\frac{c}{2}}\right) \tag{2.20}$$

we take this variable θ to be positive for the point just above the camber line and negative for the point just below the camber line. Using this convention and dropping suffixes

$$m(\theta) = q_n(\theta) - q_n(-\theta)$$

$$\gamma(\theta) = q_t(\theta) - q_t(-\theta)$$

Also, from Appendix 1,

$$q_n(\theta) = \frac{1}{2} m(\theta) = -q_n(-\theta),$$

$$q_t(\theta) = \frac{1}{2}\gamma(\theta) = -q_t(-\theta)$$

From these relations, q_n and q_t are odd functions, and therefore m and γ are also odd functions of θ. Thus, the modified singularities m' and γ' are also odd functions of θ.

As for the source distribution m, the total sum of these sources should be zero for the trailing edge to be closed. From the relation of equation (2.3), the total sum of the sources is equal to the total sum of modified sources, and thus m' should satisfy

$$\int m(x_1)\,dl = \int_{-\frac{c}{2}}^{\frac{c}{2}} m'(x_1)\,dx_1 = 0 \tag{2.21}$$

Therefore, one should choose the form of $m'(\theta)$ and $\gamma'(\theta)$ as the odd function of θ, satisfying the closure condition. Assume modified sources to be Allen type series (ref. 12), as

$$m'(\theta) = U_\infty \left[b_0 \tan\frac{\theta}{2} + \sum_{n=1}^{\infty} b_n \sin n\theta \right], \quad b_1 = -2b_0 \tag{2.22}$$

This series satisfies the above requirements, and the first term in the bracket corresponds to an isolated, thin, symmetrical Joukowski airfoil. The unknown coefficients in this and in the following series are going to be determined from the flow tangency condition, as we will see later.

Modified vorticity is assumed to be a Birnbaum type series (ref. 13), as

$$\gamma'(\theta) = U_\infty \left[a_0 \tan\frac{\theta}{2} + \sum_{n=1}^{\infty} a_n \sin n\theta \right] \tag{2.23}$$

For the isolated airfoil, the first term corresponds to a flat plate at an angle of attack and the second term to a parabolic-arc airfoil with small camber. The singularity near the leading edge comes from the first term.

Notice in (2. 23) that $\gamma'(0)=0$, i. e., the vorticity distribution has the zero value at the trailing edge, satisfying the Kutta condition automatically. Were it not so, the flow would turn around the trailing edge.

Having assumed the form of the distribution of the singularities, we are now ready to perform the integration to obtain the explicit formula for the induced velocity.

7. Explicit Expressions for the Induced Velocity.

Before substituting the series form obtained in section 6 to equation (2. 19), we express the range of expansions obtained in section 4 in terms of the auxiliary variable θ . There, the range of inner expansion was given by

$$\left[x-P,\ x+P \right]$$

where

$$\frac{\pi P}{SC} = 1.6400$$

or, in terms of θ ,

$$\left[\theta+\delta_2,\ \theta-\delta_1 \right]$$

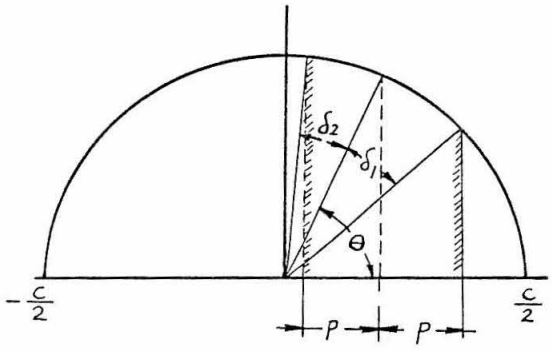

where

$$x+P = \frac{c}{2}\cos(\theta-\delta_1)$$

$$x-P = \frac{c}{2}\cos(\theta+\delta_2)$$

The integral over the inner range $\int_i$ in equation (2. 19) should be carried out within this range. The left hand side of the limit of the

range can be written more explicitly as

$$\delta_2 = \arccos\left(\frac{x-p}{\frac{c}{2}}\right) - \theta$$

$$= \arccos\left(\frac{x}{\frac{c}{2}} - 1.0440S\right) - \arccos\frac{x}{\frac{c}{2}}$$

$$\text{provided} \quad \left|\frac{x}{\frac{c}{2}} - 1.0440S\right| \leq 1$$

If $\left|\frac{x}{\frac{c}{2}} - 1.0440S\right| > 1$, then the left hand side of the limit of inner expansion should not be extended beyond the leading edge, namely,

$$\delta_2 = \pi - \arccos\frac{x}{\frac{c}{2}}$$

$$\text{provided} \quad \left|\frac{x}{\frac{c}{2}} - 1.0440S\right| > 1$$

Similarly,

$$\delta_1 = -\arccos\left(\frac{x}{\frac{c}{2}} + 1.0440S\right) + \arccos\frac{x}{\frac{c}{2}}$$

$$\text{provided} \quad \left|\frac{x}{\frac{c}{2}} + 1.0440S\right| \leq 1$$

If $\left|\frac{x}{\frac{c}{2}} + 1.0440S\right| > 1$, then the right hand side limit of inner expansion should not be extended beyond the trailing edge, i. e.,

$$\delta_1 = \arccos\frac{x}{\frac{c}{2}}$$

$$\text{provided} \quad \left|\frac{x}{\frac{c}{2}} + 1.0440S\right| > 1$$

Correspondingly, the integral over the outer range $\int_o$ is carried out within two separated regions outside of the inner range, $\left[0, \theta - \delta_1\right]$ and $\left[\theta + \delta_2, \pi\right]$. Notice once more that the range of expansion at a point x is determined by the point X itself and the spacing-chord

ratio, S .

Now, with the assumed series form, it is clear that the integrals of section 5, equation (2. 19), come out as the sum of the two terms proportional to a_n and b_n , respectively. Define

$$\int_i \left(m'(x_1) + i\gamma'(x_1) \right)(x - x_1)^{m-2} dx_1$$

$$\equiv U_\infty \left[\sum_{n=0}^{\infty} b_n \cdot A_{nm} + i \sum_{n=0}^{\infty} a_n \cdot A_{nm} \right] \left(\frac{c}{2}\right)^{m-1} \equiv I_m \tag{2. 24}$$

where A_{nm} 's are all real and dimensionless. The similarity of the assumed form of the sources and vortices leads to the above results, where the same expression A_{nm} appears twice in the first and second series. The explicit forms of A_{nm} and the following B_n will be given in Appendix 2. Also, write

$$\int_0 \left(m'(x_1) + i\gamma'(x_1) \right) dx_1 = U_\infty \left[\sum_{n=0}^{\infty} b_n \cdot B_n + i \sum_{n=0}^{\infty} a_n \cdot B_n \right] \left(\frac{c}{2}\right) \tag{2. 25}$$

where B_n are all real and dimensionless.

The induced velocity can be written as

$$u_0(x) - i v_0(x) = U_\infty \left[\sum_{n=0}^{\infty} b_n (-g_n - i f_n) + \sum_{n=0}^{\infty} a_n (f_n - i g_n) \right] \tag{2. 26}$$

where f_n and g_n are real. We would like to obtain the explicit forms of f_n and g_n , and this is accomplished, without loss of generality, by putting $b_n = 0$ ($n = 0, 1, \cdots$) in (2. 26). Substituting (2. 24), (2. 25), and (2. 26) into equation (2. 19), and equating the coefficients of a_n on both sides of the equation,

$$
\begin{aligned}
&f_n - i g_n \\
&= -\frac{i}{2\pi}\Bigg[\frac{1}{1+iy_0'} A_{n1} + \frac{iy_0''}{2(1+iy_0')^2}\left(\frac{c}{2}\right) A_{n2} + \frac{-3y_0''^2 - 2iy_0^{(3)}(1+iy_0')}{12(1+iy_0')^3}\left(\frac{c}{2}\right)^2 A_{n3} \\
&\quad + \frac{-3iy_0''^3 + 4(1+iy_0')y_0''y_0^{(3)} + iy_0^{(4)}(1+iy_0')^2}{24(1+iy_0')^4}\left(\frac{c}{2}\right)^3 A_{n4} \\
&\quad + \Big\{ -6iy_0^{(5)}(1+iy_0')^3 - \left(20(y_0^{(3)})^2 + 30y_0''y_0^{(4)}\right)(1+iy_0')^2 + 90iy_0''^2 y_0^{(3)}(1+iy_0') \\
&\qquad + 45y_0''^4 \Big\} \frac{1}{720(1+iy_0')^5}\left(\frac{c}{2}\right)^4 A_{n5} \\
&\quad + \Big\{ 2iy_0^{(6)}(1+iy_0')^4 + \left(12y_0''y_0^{(5)} + 20y_0^{(3)}y_0^{(4)}\right)(1+iy_0')^3 \\
&\qquad - \left(45i(y_0'')^2 y_0^{(4)} + 60iy_0''(y_0^{(3)})^2\right)(1+iy_0')^2 - 120(y_0'')^3 y_0^{(3)}(1+iy_0') \\
&\qquad + 45i(y_0'')^5 \Big\} \frac{1}{1440(1+iy_0')^6}\left(\frac{c}{2}\right)^5 A_{n6} + \cdots \Bigg] \\
&+ \frac{\pi}{6(sc)^2} e^{2i\beta} i \Big[(1+iy_0')\left(\frac{c}{2}\right)^2 A_{n3} - \frac{i}{2}y_0''\left(\frac{c}{2}\right)^3 A_{n4} + \frac{i}{6}y_0^{(3)}\left(\frac{c}{2}\right)^4 A_{n5} \\
&\qquad - \frac{i}{24}y_0^{(4)}\left(\frac{c}{2}\right)^5 A_{n6} + \cdots \Big] \\
&+ \frac{1}{2sc} e^{i\beta} \cdot i\left(\frac{c}{2}\right) B_n
\end{aligned}
$$

Separating real and imaginary parts on the right hand side, one obtains, for f_n and g_n :

$$
\begin{aligned}
&f_n\left(\frac{x}{\frac{c}{2}}\,;\,y_0\,;\,s,\beta\right)\\
&=\frac{1}{2\pi}\Bigg[\frac{y_0'}{1+y_0'^2}An1-\frac{1}{2}\,\frac{y_0''(1-y_0'^2)}{(1+y_0'^2)^2}\left(\frac{c}{2}\right)An2\\
&\quad+\frac{2y_0^{(3)}(1-3y_0'^2)+(3y_0''^2-2y_0'\cdot y_0^{(3)})(-3y_0'+y_0'^3)}{12(1+y_0'^2)^3}\left(\frac{c}{2}\right)^2An3\\
&\quad-\Big\{(-3y_0''^3+4y_0'y_0''y_0^{(3)}+(1-y_0'^2)y_0^{(4)}(1-6y_0'^2+y_0'^4)+(4y_0''\cdot y_0^{(3)}-2y_0'\cdot y_0^{(4)})\\
&\qquad\times(-4y_0'+4y_0'^3)\Big\}\frac{1}{24(1+y_0'^4)^4}\left(\frac{c}{2}\right)^3An4\\
&\quad-\Big\{\Big\{-6y_0^{(5)}(1-3y_0'^2)-40y_0'\cdot(y_0^{(3)})^2-60y_0'\cdot y_0''\cdot y_0^{(4)}+90y_0''^2\cdot y_0^{(3)}\Big\}\\
&\qquad\times(1-10y_0'^2+5y_0'^4)-\Big\{6y_0^{(5)}(3y_0'-y_0'^3)-20(y_0^{(3)})^2(1-y_0'^4)\\
&\qquad-30y_0''\cdot y_0^{(4)}(1-y_0'^2)-90y_0'\cdot y_0''^2\cdot y_0^{(3)}+45y_0''^4\Big\}\cdot(5y_0'-10y_0'^3+y_0'^5)\Big\}\\
&\qquad\times\frac{1}{720(1+y_0'^2)^5}\left(\frac{c}{2}\right)^4An5\\
&\quad+\Big\{\Big\{-8y_0'\cdot y_0^{(6)}(1-y_0'^2)+(12y_0''\cdot y_0^{(5)}+20y_0^{(3)}y_0^{(4)})(1-3y_0'^2)\\
&\qquad+2y_0'(45(y_0'')^2y_0^{(4)}+60y_0''\cdot(y_0^{(3)})^2)-120(y_0'')^3y_0^{(3)}\Big\}(6y_0'-20y_0'^3+6y_0'^5)\\
&\qquad-\Big\{2y_0^{(6)}(1-6y_0'^2+y_0'^4)+(12y_0''y_0^{(5)}+20y_0^{(3)}y_0^{(4)})(3y_0'-y_0'^3)\\
&\qquad-(45(y_0'')^2y_0^{(4)}+60y_0''\cdot(y_0^{(3)})^2)(1-y_0'^2)-120(y_0'')^3y_0^{(3)}y_0'+45(y_0'')^5\Big\}\\
&\qquad\times(1-15y_0'^2+15y_0'^4-y_0'^6)\Big\}\frac{1}{1440(1+y_0'^2)^6}\left(\frac{c}{2}\right)^5An6+\cdots\Bigg]\\
&+\frac{\pi}{6(sc)^2}\Bigg[(-y_0'\cos2\beta-\sin2\beta)\left(\frac{c}{2}\right)^2An3+\cos2\beta\cdot\frac{1}{2}y_0''\left(\frac{c}{2}\right)^3An4-\cos2\beta\cdot\frac{1}{6}y_0^{(3)}\left(\frac{c}{2}\right)^4An5\\
&\qquad+\cos2\beta\cdot\frac{1}{24}y_0^{(4)}\left(\frac{c}{2}\right)^5An6+\cdots\Bigg]\\
&-\frac{1}{2sc}\left(\frac{c}{2}\right)\sin\beta\cdot Bn
\end{aligned}
$$

(2. 27)

$$
\begin{aligned}
&q_n\left(\frac{x}{\frac{c}{2}}\,;\,y_0\,;\,s,\beta\right)\\
&=\frac{1}{2\pi}\Bigg[-\frac{1}{1+y_0'^2}An1-\frac{y_0'\cdot y_0''}{(1+y_0'^2)^2}\left(\frac{c}{2}\right)An2\\
&\quad+\frac{(3y_0''^2-2y_0'\cdot y_0^{(3)})(1-3y_0'^2)-2y_0^{(3)}(-3y_0'+y_0'^3)}{12(1+y_0'^2)^3}\left(\frac{c}{2}\right)^2An3\\
&\quad-\Big\{(4y_0''\cdot y_0^{(3)}-2y_0'\cdot y_0^{(4)})(1-6y_0'^2+y_0'^4)-(-3y_0''^3+4y_0'\cdot y_0''\cdot y_0^{(3)}+(1-y_0'^2)y_0^{(4)})\\
&\qquad\times(-4y_0'+4y_0'^3)\Big\}\frac{1}{24(1+y_0'^2)^4}\left(\frac{c}{2}\right)^3An4\\
&\quad-\Big\{\Big\{6y_0^{(5)}(3y_0'-y_0'^3)-20(y_0^{(3)})^2(1-y_0'^2)-30y_0''\cdot y_0^{(4)}(1-y_0'^2)\\
&\qquad-90y_0'\cdot y_0''^2y_0^{(3)}+45y_0''^4\Big\}(1-10y_0'^2+5y_0'^4)\\
&\qquad+\Big\{-6y_0^{(5)}(1-3y_0'^2)-40y_0'\cdot(y_0^{(3)})^2-60y_0'\cdot y_0''y_0^{(4)}+90y_0''^2\cdot y_0^{(3)}\Big\}\\
&\qquad\times(5y_0'-10y_0'^3+y_0'^5)\Big\}\frac{1}{720(1+y_0'^2)^5}\left(\frac{c}{2}\right)^4An5\\
&\quad-\Big\{\Big\{-8y_0'\cdot y_0^{(6)}(1-y_0'^2)+(12y_0''\cdot y_0^{(5)}+20y_0^{(3)}y_0^{(4)})(1-3y_0'^2)\\
&\qquad+2y_0'(45(y_0'')^2y_0^{(4)}+60y_0''\cdot(y_0^{(3)})^2)-120(y_0'')^3y_0^{(3)}\Big\}(1-15y_0'^2+15y_0'^4-y_0'^6)\\
&\qquad+\Big\{2y_0^{(6)}(1-6y_0'^2+y_0'^4)+(12y_0''\cdot y_0^{(5)}+20y_0^{(3)}y_0^{(4)})(3y_0'-y_0'^3)\\
&\qquad-(45(y_0'')^2y_0^{(4)}+60y_0''(y_0^{(3)})^2)(1-y_0'^2)-120(y_0'')^3y_0^{(3)}y_0'+45(y_0'')^5\Big\}\\
&\qquad\times(6y_0'-20y_0'^3+6y_0'^5)\Big\}\frac{1}{1440(1+y_0'^2)^6}\left(\frac{c}{2}\right)^5An6+\cdots\Bigg]\\
&-\frac{\pi c}{6(sc)^2}\Bigg[(\cos2\beta-y_0'\sin2\beta)\left(\frac{c}{2}\right)^2An3+\sin2\beta\cdot\frac{1}{2}y_0''\left(\frac{c}{2}\right)^3An4-\sin2\beta\,\frac{1}{6}y_0^{(3)}\left(\frac{c}{2}\right)^4An5\\
&\qquad+\sin2\beta\cdot\frac{1}{24}y_0^{(4)}\left(\frac{c}{2}\right)^5An6+\cdots\Bigg]\\
&-\frac{1}{2sc}\left(\frac{c}{2}\right)\cos\beta\cdot Bn
\end{aligned}
$$

(2. 28)

f_n and g_n are functions of position on the chord $\frac{x}{\frac{c}{2}}$, airfoil shape $y_0(x)$ and its derivatives, stagger angle β, and spacing-chord ratio S. Only the dependence on S is implicit, and this comes from the fact that the A_{nm} are dependent upon S through δ_1 and δ_2. As mentioned before, complete derivations of A_{nm} and B_n are given in Appendix 2. The following are samples of A_{nm}.

$$A_{01}\left(\frac{x}{\frac{c}{2}};S\right)=(\delta_1+\delta_2)-\frac{1-\cos\theta}{\sin\theta}\log\left|\frac{\sin(\theta+\frac{1}{2}\delta_2)\sin\frac{1}{2}\delta_1}{\sin(\theta-\frac{1}{2}\delta_1)\sin\frac{1}{2}\delta_2}\right|,$$

$$A_{02}\left(\frac{x}{\frac{c}{2}};S\right)=(\delta_1+\delta_2)-\left[\sin(\theta+\delta_2)-\sin(\theta-\delta_1)\right]$$

Although A_{nm} and B_n are such simple combinations of logarithmic and trigonometric functions and can be evaluated without difficulty for any $\frac{x}{\frac{c}{2}}$ and S, the numerical values of these coefficients are tabulated in Appendix 3 as functions of the two parameters $\frac{x}{\frac{c}{2}}$ and S so as to facilitate the computation. Hence, once the values of A_{nm} and B_n are taken from these tables for a given point $\frac{x}{\frac{c}{2}}$ and specified spacing-chord ratio S, f_n and g_n are expressed as functions depending explicitly on airfoil shape $y_0(x)$ and stagger angle β. Thus, we can express the functional relationship between the desired aerodynamic parameters and the other factors, once the spacing-chord ratio is specified. We will come back to this point in Part III, where a number of examples of such relationships are given.

After f_n and g_n are obtained, the induced velocities on the camber line can be determined from equation (2.26) as

$$\frac{u_0(x)}{U_\infty} = \sum_{n=0}^{\infty} a_n \cdot f_n - \sum_{n=0}^{\infty} b_n \cdot g_n$$

$$\frac{v_0(x)}{U_\infty} = \sum_{n=0}^{\infty} a_n \cdot g_n + \sum_{n=0}^{\infty} b_n \cdot f_n \qquad (2.29)$$

From the flow tangency condition on the surface of the airfoil, the coefficients a_n and b_n determining the unknown strength of singularities are obtained. In the following section, this boundary condition will be discussed.

8. Boundary Conditions.

Since we are treating the fluid as inviscid, the boundary condition on the surface of the airfoil is that the flow should be tangent to the slope of the airfoil surface. For a thin airfoil, except for the vicinity of the leading edge, the surface velocities can be obtained by superposing one-half of the strength of singularity on the velocity at a point on the camber line. Referring to the figure at the right,

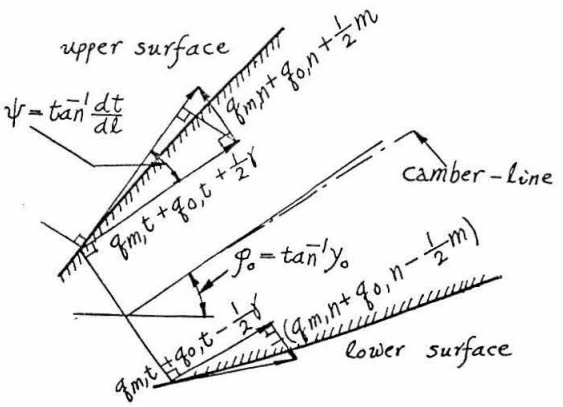

velocity normal to the upper surface:

$$= -(q_{m,t} + q_{o,t} + \tfrac{1}{2}\gamma)\sin\psi + (q_{m,n} + q_{o,n} + \tfrac{1}{2}m)\cos\psi$$

$$= -(q_{m,t} + q_{o,t} + \tfrac{1}{2}\gamma)\frac{\frac{dt}{d\ell}}{\sqrt{1+\left(\frac{dt}{d\ell}\right)^2}} + (q_{m,n} + q_{o,n} + \tfrac{1}{2}m)\frac{1}{\sqrt{1+\left(\frac{dt}{d\ell}\right)^2}} = 0 \qquad (2.30)$$

velocity normal to the lower surface:

$$= -(q_{m,t} + q_{o,t} - \tfrac{1}{2}\gamma)\sin\psi - (q_{m,n} + q_{o,n} - \tfrac{1}{2}m)\cos\psi$$

$$= -(q_{m,t} + q_{o,t} - \tfrac{1}{2}\gamma)\frac{\frac{dt}{d\ell}}{\sqrt{1+\left(\frac{dt}{d\ell}\right)^2}} - (q_{m,n} + q_{o,n} - \tfrac{1}{2}m)\frac{1}{\sqrt{1+\left(\frac{dt}{d\ell}\right)^2}} = 0 \qquad (2.31)$$

Adding (2.30) and (2.31), we get

$$\tfrac{1}{2}m(x) = (q_{m,t} + q_{o,t})\frac{dt}{d\ell} \qquad (2.32)$$

and physically, this means that the flux of fluid out of two adjacent surfaces normal to the camber line is balanced by the flow produced from the sources.

Subtracting (2.30) from (2.31), we get

$$q_{m,n} + q_{o,n} - \tfrac{1}{2}\gamma\frac{dt}{d\ell} = 0 \qquad (2.33)$$

and this means that the velocity is not quite tangent to the camber line due to the unsymmetrical flow pattern on the upper and lower surfaces of the airfoil. For a thin airfoil, the term $\frac{1}{2}\gamma\frac{dt}{d\ell}$ is small, except near the leading edge, where $\frac{dt}{d\ell}$ becomes infinitely large; elsewhere the velocity is almost tangent to the camber line.

Expressing normal and tangential components of the induced velocity on the camber line by x, y components, u_o and v_o, which in turn are given in terms of a_n and b_n by equation (2.29),

we obtain

$$q_{m,n} = -U_\infty \sin\varphi_0 + V_\infty \cos\varphi_0 = \frac{U_\infty}{\sqrt{1+y_0'^2}}(\tan\alpha - y_0')$$

$$q_{0,n} = \frac{U_\infty}{\sqrt{1+y_0'^2}}\left[\sum_{n=0}^{\infty} a_n (g_n - y_0' f_n) + \sum_{n=0}^{\infty} b_n (f_n + y_0' g_n)\right]$$

$$q_{m,t} = U_\infty \cos\varphi_0 + V_\infty \sin\varphi_0 = \frac{U_\infty}{\sqrt{1+y_0'^2}}(1 + y_0' \tan\alpha)$$

$$q_{0,t} = \frac{U_\infty}{\sqrt{1+y_0'^2}}\left[\sum_{n=0}^{\infty} a_n (f_n + y_0' g_n) - \sum_{n=0}^{\infty} b_n (g_n - y_0' f_n)\right]$$

Substituting these into (2. 32) and (2. 33),

$$b_0 \tan\frac{\theta}{2} + \sum_{n=1}^{\infty} b_n \sin n\theta + 2\frac{dt}{dX}\frac{1}{\sqrt{1+y_0'^2}}\sum_{n=0}^{\infty} b_n (g_n - y_0' f_n)$$
$$- 2\frac{dt}{dX}\frac{1}{\sqrt{1+y_0'^2}}\sum_{n=0}^{\infty} a_n (f_n + y_0' g_n) = 2\frac{dt}{dX}\frac{1}{\sqrt{1+y_0'^2}}(1 + y_0' \tan\alpha) \qquad (2.34)$$

$$\sum_{n=0}^{\infty} a_n (g_n - y_0' f_n) + \sum_{n=0}^{\infty} b_n (f_n + y_0' g_n) - \frac{1}{2}\frac{dt}{dX}\frac{1}{\sqrt{1+y_0'^2}}\left(a_0 \tan\frac{\theta}{2} + \sum_{n=1}^{\infty} a_n \sin n\theta\right)$$
$$= y_0' - \tan\alpha \qquad (2.35)$$

Once the airfoil shape and cascade geometry are specified, the only unknown factors in these equations are a_n's and b_n's. One remark is pertinent here. It is usual in the isolated thin airfoil theory to simplify the boundary conditions (2. 32) and (2. 33). For example, the induced velocity $q_{0,t}$ in the equation and the unsymmetrical term $\frac{1}{2}\gamma\frac{dt}{dl}$ are ordinarily neglected and, more important, in a version of equation (2. 33),

$$\frac{V_\infty + v_0}{U_\infty + u_0} = y_0'$$

the x component of the induced velocity u_0 is neglected in comparison with the undisturbed velocity U_∞. Such linearization is not made in the present work in anticipation of the importance of some of these terms in cascade flow. This point will be taken up again in Part III, but in passing, let us see in the following paragraph that the results of the isolated thin airfoil theory can be formally recovered, without making these assumptions a priori.

For simplicity, consider the isolated airfoil of small camber and zero thickness. Then $t(x) = 0$ and from (2.34), $b_n \equiv 0$, and equation (2.35) becomes

$$\sum_{n=0}^{\infty} a_n (g_n - y_0' f_n) = y_0' - \tan\alpha \qquad (2.36)$$

From equations (2.27) and (2.28), we get for the isolated airfoil, i.e., $S \to \infty$,

$$g_n - y_0' f_n = -\frac{1}{2\pi} A_{n1}$$

for small camber $\epsilon = \frac{y_0(x)}{\frac{c}{2}} \ll 1$

to the first order of ϵ. Now, from Appendix 2, A_{n1} can be obtained by putting $\delta_1 = \theta$ and $\delta_2 = \pi - \theta$ for $S \to \infty$, yielding

$$A_{n1} = \pi \cos n\theta$$

(2.36) becomes

$$-\frac{1}{2}\sum_{n=0}^{\infty} a_n \cos n\theta = y_0' - \tan\alpha$$

or

$$a_0 = -\frac{2}{\pi}\int_0^{\pi} (y_0' - \tan\alpha)\, d\theta, \quad a_n = -\frac{4}{\pi}\int_0^{\pi} y_0' \cos n\theta \cdot d\theta \quad (n \geq 1)$$

These final results are the familiar ones for the case of the 'thin airfoil theory' for an isolated airfoil, valid up to the order ϵ .

Now, in this special case, the boundary condition (2.36) is satisfied everywhere on the chord. In the general case of a highly-cambered airfoil, if we try to satisfy (2.34) and (2.35) everywhere on the chord line by a method such as Fourier analysis, the procedure would lead to a more complicated result, and the numerical work does not justify the higher accuracy that might be attained. Instead, the collocation method is adopted here. Namely, by computing f_n , g_n , y_0' , $\frac{dt}{dx}$, $\tan\frac{\theta}{2}$, and $\sin n\theta$ at a suitable number of discrete points on the chord and truncating the series at the corresponding number of terms in (2.34) and (2.35), linear simultaneous equations for the a_n's and b_n's are obtained. Of course, if we increase the number of such 'control points' -- the points where the boundary conditions are satisfied -- then presumably the accuracy of the values of a_n and b_n obtained would improve. For practical purposes, however, there is no need to take the number of control points more than necessary for reasonable engineering estimates. The choice of number of control points is discussed in the section following.

Before leaving this section, a final remark is in order. Notice that equations (2.34) and (2.35) are linear with respect to attack angle $\tan\alpha$; the fact enables us to separate (2.34) and (2.35) into two parts, one independent of α .and one proportional to $\tan\alpha$. If we express

a_n and b_n as

$$a_n = \alpha_n + \beta_n \cdot \tan\alpha$$

$$b_n = \alpha_n^* + \beta_n^* \cdot \tan\alpha \tag{2.37}$$

then equations (2.34) and (2.35) can be decomposed into two sets of equations, each set independent of the other, i.e.,

$$\left.\begin{aligned} &\alpha_0^* \tan\frac{\theta}{2} + \sum_{n=1}^{\infty} \alpha_n^* \sin n\theta + 2\frac{dt}{dx}\frac{1}{\sqrt{1+y_0'^2}}\sum_{n=0}^{\infty}\alpha_n^*(g_n - y_0' f_n) \\ &\qquad - 2\frac{dt}{dx}\frac{1}{\sqrt{1+y_0'^2}}\sum_{n=0}^{\infty}\alpha_n(f_n + y_0' g_n) = 2\frac{dt}{dx}\frac{1}{\sqrt{1+y_0'^2}} \\ &\sum_{n=0}^{\infty}\alpha_n(g_n - y_0' f_n) + \sum_{n=0}^{\infty}\alpha_n^*(f_n + y_0' g_n) \\ &\qquad - \frac{1}{2}\left(\alpha_0 \tan\frac{\theta}{2} + \sum_{n=1}^{\infty}\alpha_n \sin n\theta\right)\frac{1}{\sqrt{1+y_0'^2}}\frac{dt}{dx} = y_0' \end{aligned}\right\} \tag{2.38}$$

$$\left.\begin{aligned} &\beta_0^* \tan\frac{\theta}{2} + \sum_{n=1}^{\infty} \beta_n^* \sin n\theta + 2\frac{dt}{dx}\frac{1}{\sqrt{1+y_0'^2}}\sum_{n=0}^{\infty}\beta_n^*(g_n - y_0' f_n) \\ &\qquad - 2\frac{dt}{dx}\frac{1}{\sqrt{1+y_0'^2}}\sum_{n=0}^{\infty}\beta_n(f_n + y_0' g_n) = 2\frac{dt}{dx}\frac{y_0'}{\sqrt{1+y_0'^2}} \\ &\sum_{n=0}^{\infty}\beta_n(g_n - y_0' f_n) + \sum_{n=0}^{\infty}\beta_n^*(f_n + y_0' g_n) \\ &\qquad - \frac{1}{2}\left(\beta_0 \tan\frac{\theta}{2} + \sum_{n=1}^{\infty}\beta_n \sin n\theta\right)\frac{1}{\sqrt{1+y_0'^2}}\frac{dt}{dx} = -1 \end{aligned}\right\} \tag{2.39}$$

Once α_n , β_n , α_n^* , and β_n^* are determined from these equations, a_n and b_n are computed for any arbitrary attack angle α and thus we can obtain an explicit functional relationship involving α .

9. Choice of Control Points.

It is clear from the very beginning that the choice of control points involves some arbitrariness. We require that such control points be well distributed over the chord and representative of the general shape of the airfoil, but otherwise there is no unique way of determining the distribution of such points. If a point P is a control point, then any other points in the neighborhood of P can take the place of P. There are certain points, however, which cannot be used as control points. The leading edge and its neighboring points cannot be candidates for control points, because there the previous formulation of boundary condition is invalid. Also, for the series form of source distribution assumed, the trailing edge cannot be used for such a purpose unless the trailing edge has a cusp. This arises from the fact that at $\theta = 0$, the source strength at the left hand side of equation (2.32) becomes zero, while the right hand side does not vanish unless $\frac{dt}{d\ell} = 0$. Otherwise, any other points can be chosen for control points. In ref. 4, Schlichting uses the 'three-quarter chord method' to determine such points. These are the points chosen in such a way as, for n-points collocation, the chord is divided into n equally-spaced segments, and for each segment a control point is allocated at three-quarters of the segment. For example, for three-point collocation, the control points are located at $\frac{x}{\frac{c}{2}} = -\frac{1}{2}$, $\frac{1}{6}$, and $\frac{5}{6}$. For four-point collocation, they are located at $\frac{x}{\frac{c}{2}} = -\frac{5}{8}$, $-\frac{1}{8}$, $\frac{3}{8}$, and $\frac{7}{8}$, and so forth.

As is well known, this three-quarter method comes from an attempt to improve Prandtl's lifting line theory so as to obtain chord-

wise distribution of load. In the Prandtl's lifting line theory, a single vortex is placed at the aerodynamic center of the airfoil, which is about one-quarter chord from the leading edge. To see the special meaning of the three-quarter point, consider the simple case of the flat plate at an angle of attack. Let Γ be the magnitude of circulation of the vortex, and we try to determine Γ by satisfying the boundary condition at a single control point. If we happen to choose the three-quarter chord point as such a point, then the downwash there, w_0, is given by

$$w_0 = \frac{1}{2\pi} \cdot \frac{\Gamma}{\frac{3}{4}c - \frac{1}{4}c} = \frac{1}{2\pi} \cdot \frac{\Gamma}{\frac{c}{2}}$$

and from the boundary condition $w_0 = U_\infty \sin\alpha$, we get

$$\Gamma = \pi c U_\infty \sin\alpha$$

and this agrees with the exact result. Therefore, the three-quarter point is the best single collocation point to obtain the overall aerodynamic factors for a flat plate.

Since concentration of lift in one vortex does not furnish information about the chordwise distribution of the load, an attempt was made to improve this by using two or more vortex lines. In ref. 15, Wieghardt generalized the above approach. For a number n of vortices Γ_1, Γ_2, ... and Γ_n, he put a lifting line at the quarter points of the n equal divisions of the chord and satisfied the boundary condition at each control point located at the three-quarter point of the segment. For the flat plate, the sum of the circulations $\Gamma = \Gamma_1 + \Gamma_2 + \cdots + \Gamma_n$ can be shown to be the same as the exact magnitude of the circulation (ref. 16).

It is obvious, however, that the advantage of the three-quarter method is a result of the particular distribution of vorticity on an isolated flat plate, and for the more general vortex distribution for a cascade such as treated in this investigation, the method loses some of its significance. The best that it can offer in this case is to provide us some conventional standard for determining the control points. Any other well-distributed points could be used for control points, and in the preliminary numerical experiments performed by changing the position of control points, the results obtained by the three-quarter method are found to be no better than those by different choice of control points. But since we apparently do not have a way to determine a method definitely superior, in the present study the three-quarter method is adopted. In Appendix 3, the values of A_{nm} are tabulated at the lower part of the table at the control points corresponding to three- and four-point collocation chosen according to the three-quarter method.

10. Summary of Calculation Procedure and Various Aerodynamic Parameters.

In this section, we give a brief summary of steps of calculation procedure developed so far. They are:

(1) decide the number of control points N and choose them according to the three-quarter method;

(2) compute the derivatives y_0', y_0'', ---- from the given camber line equation at these points;

(3) calculate f_n and g_n in equations (2.27) and (2.28) at the control points for $n = 0$ to N for given solidity

(A_{nm}'s in these expressions are tabulated in Appendix 3 as functions of solidity and collocation points);

(4) compute $\frac{dt}{dx}$ from the thickness distribution equation;

(5) solve α_n , β_n and α_n^* , β_n^* from equations (2.38) and (2.39); the number of α_n's and β_n's are N , respectively, while the number of α_n^*'s and β_n^*'s are $N+1$, respectively. The additional coefficients α_{N+1}^* and β_{N+1}^* come from the fact, by the closure condition, that b_1 is not independent but given by $b_1 = -2b_0$; and

(6) determine $a_n (n = 0, N-1)$ and $b_n (n = 0, N)$ from equation (2.37).

Once a_n and b_n are determined, various aerodynamic parameters can be deduced easily in the following way.

surface velocity and pressure distribution:

$$q_{\pm} \doteq (q_{m,t} + q_{0,0} \pm \frac{1}{2}\gamma) = \frac{U_\infty}{\sqrt{1+y_0'^2}}\Big[1 + y_0'\tan\alpha + \sum_{n=0}^{\infty} a_n (f_n + y_0' g_n) - \sum_{n=0}^{\infty} b_n (g_n - y_0' f_n) \pm \frac{1}{2}\Big(b\tan\frac{\theta}{2} + \sum_{n=1}^{\infty} b_n \sin n\theta\Big)\Big]$$

The ± sign in the brackets corresponds to the upper and lower surfaces, respectively. From the Bernoulli equation, the pressure distribution on the surface can be computed.

circulation and lift coefficients:

$$\Gamma = \int \gamma\, dl = \int_{\frac{c}{2}}^{\frac{c}{2}} \gamma' dx = \frac{c}{2}\pi U_\infty \Big(a_0 + \frac{1}{2}a_1\Big)$$

or, expressing a_0 and a_1 in terms of α_n and β_n,

$$\frac{\Gamma}{cq_m} = \frac{\pi}{2}\left[\left(\alpha_0 + \frac{\alpha_1}{2}\right)\cos\alpha + \left(\beta_0 + \frac{\beta_1}{2}\right)\sin\alpha\right]$$

From the Kutta-Joukowski theorem, lift perpendicular to mean velocity q_m can be given by

$$L = \rho q_m \Gamma$$

and the lift coefficient is expressed by

$$C_L \equiv \frac{L}{\frac{1}{2}\rho q_m^2 C} = \pi\left[\left(\alpha_0 + \frac{\alpha_1}{2}\right)\cos\alpha + \left(\beta_0 + \frac{\beta_1}{2}\right)\sin\alpha\right]$$

zero-lift angle and ideal angle of attack:

The zero lift angle δ is expressed as:

$$\tan\delta = -\frac{\alpha_0 + \frac{1}{2}\alpha_1}{\beta_0 + \frac{1}{2}\beta_1}$$

The ideal angle of attack, defined as the angle at which the velocity is finite at the leading edge (shockless entry in steam turbine terminology), can be obtained by putting $a_0 = 0$, i.e.,

$$\tan\delta^* = -\frac{\alpha_0}{\beta_0}$$

upstream and downstream directions of flow:

The upwash at infinity parallel to the frontal line of the cascade is given by $\frac{\Gamma}{2sc}$. Thus, referring to Figure 1,

$$\tan\alpha_d = \frac{\sin(\alpha+\beta) - \frac{\Gamma}{2sc q_m}}{\cos(\alpha+\beta)},$$

$$\tan\alpha_u = \frac{\sin(\alpha+\beta) + \frac{\Gamma}{2sc q_m}}{\cos(\alpha+\beta)}$$

III. RESULTS AND DISCUSSION

The results based upon the theory developed in Part II are discussed here. For convenience, the cascades are divided into three classes according to the camber; slightly, moderately, and highly cambered cascades. A slightly cambered cascade is one which deviates slightly from the flat plate. A moderately cambered cascade is one with a maximum camber of about 10 per cent; cascades with greater camber than this are referred to as highly cambered cascades.

In section 1, the present method is compared to the known exact solution for the flat plate cascade and is found to be in close agreement. The next three sections deal with the slightly cambered cascade. First, Schlichting's method is outlined and its weaknesses discussed. In section 3, an example of the functional relationship of the exit angle with other parameters is derived. In section 4, as an aside, the formula for widely spaced cascades is deduced and the results are found to agree with those given in other references. In sections 5 and 6, the cases of moderately and highly cambered cascades are studied numerically by hand and compared with the results obtained by the direct use of a digital computer. The comparison indicates that the present method can predict the overall factors with reasonable accuracy. In section 7, and example of the functional relationship of the exit angle to other parameters is derived for highly cambered cascades. In the final section, closely spaced blades are discussed.

1. Case of the Flat Plate Cascade.

In section 4 of Part II, the optimum range of two different types

of expansions is determined. First, the optimum range for the unstaggered flat-plate cascade is determined; this result is applied to the staggered cascade. In this section, a numerical investigation is made concerning the validity of this optimum range for the case of the flat-plate cascade of zero thickness, which has been solved exactly by conformal mapping. According to the present method, (2.28) is reduced, for the flat plate, to

$$g_n = -\frac{1}{2\pi}A_{n1} - \frac{\pi}{6(sc)^2}\cos 2\beta\cdot\left(\frac{c}{2}\right)^2 A_{n3} - \frac{1}{2sc}\left(\frac{c}{2}\right)\cos\beta\cdot B_n \qquad (3.1)$$

Of these terms, the A_{n1}, A_{n3} and B_n are affected by the choice of expansion range. The a_n's are determined from equation (2.35), which becomes, in this case,

$$\sum_{n=0}^{\infty} a_n g_n = -\tan\alpha, \quad b_n \equiv 0 \qquad \text{for all } n \qquad (3.2)$$

If we take the number of control points to be three, then, according to the three-quarter method, they are $\frac{x}{\frac{c}{2}} = -0.5$, 0.16667, and 0.8333. Corresponding to the optimum range, the necessary values A_{n1}, A_{n3} and B_n at the control points are read from the tables of Appendix 3, the g_n's are computed, and equation (3.2) can be solved for a_0, a_1, and a_2. The comparison of the results obtained by the present method and the exact conformal mapping method are made in Figures 5 and 6 for the unstaggered cascade of $\beta = 0$. Figure 5 is for a solidity of unity; that is, a spacing-chord ratio of $s = 1.0$. Figure 6 is for a solidity of two. It can be noted in these figures that the agreement between the present method (approximate) and the conformal mapping method (exact) is extremely

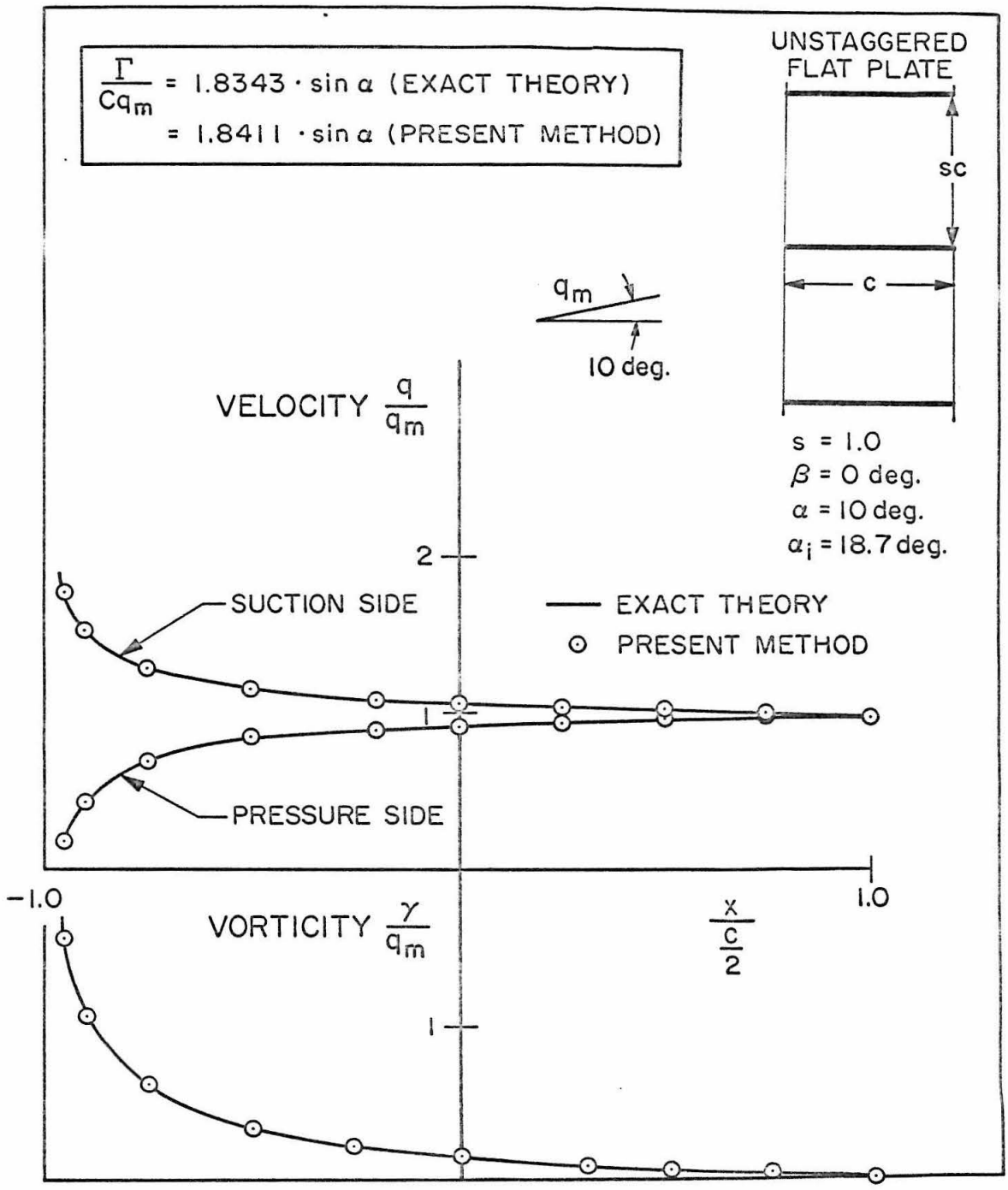

Figure 5. Unstaggered cascade of flat-plate airfoils with S = 1.0.

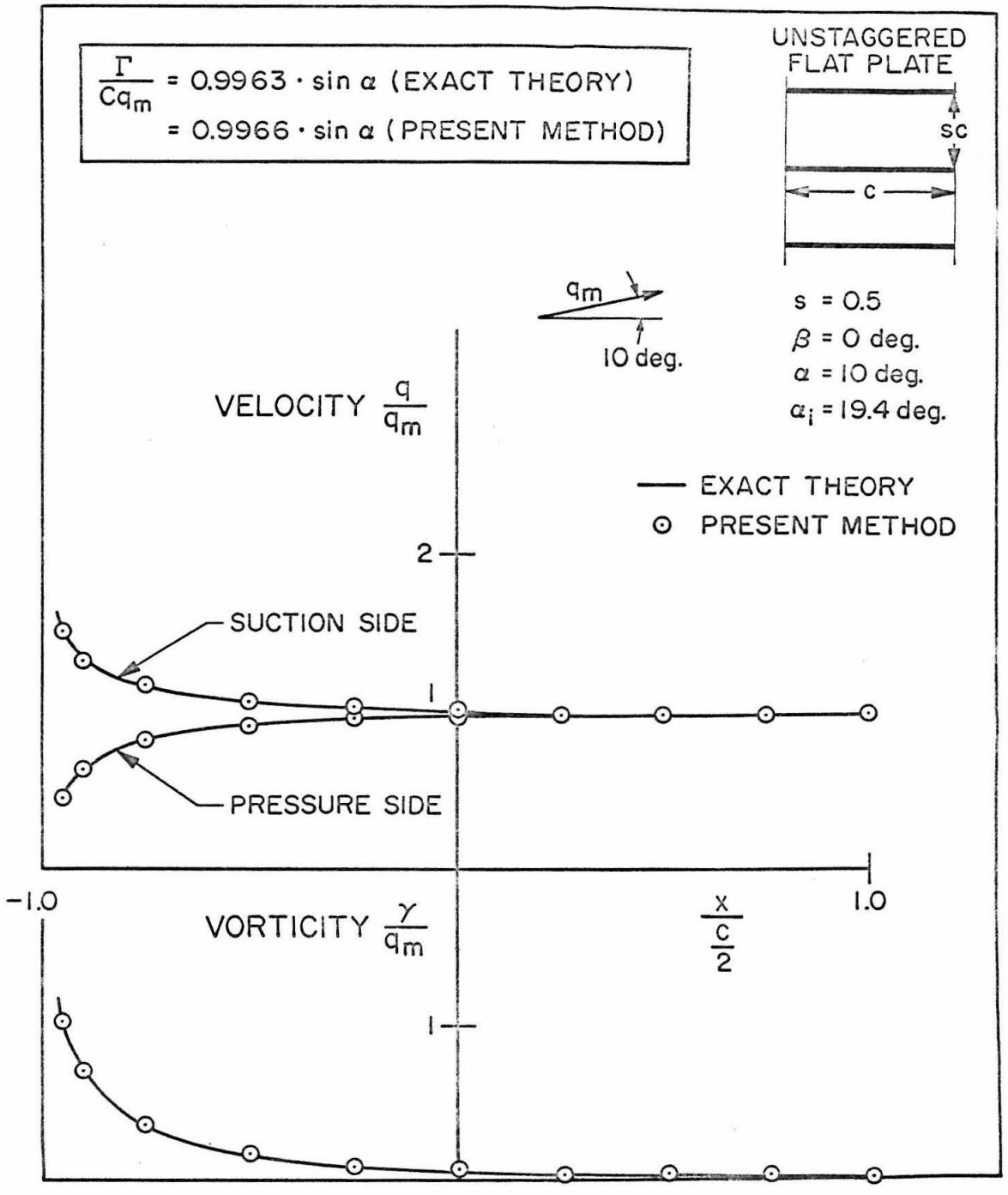

Figure 6. Unstaggered cascade of flat-plate airfoils with S = 0.5.

good with respect to both velocity and vorticity distribution. Although these two figures are drawn for the attack angle, α = 10 degrees, the agreement between the two methods is equally good for any other attack angle, as shown by the comparison of circulation, written in the box in the figures. The assumption that the optimum range determined for the unstaggered cascade is also applicable to the staggered cascade is verified in Figure 7. This is the case of stagger angle β = 30 degrees, with solidity 2 . Again, the agreement between the two methods is seen to be good. An interesting point pertinent to these examples is that, although the a_n terms vanish except for the leading term a_0 in the case of the isolated flat-plate airfoil, the aerodynamic interference between the airfoils gives rise to higher terms of a_n in the cascade. For example, the values of a_n 's in Figure 5 are as follows:

$$a_0 = 1.49318 \cdot \tan\alpha \ , \ a_1 = -0.64221 \cdot \tan\alpha \ , \ a_2 = 0.04279 \cdot \tan\alpha$$

Thus, there are non-zero values of a_1 , a_2 even in the flat-plate airfoil cascade.

Having confirmed the present method for the case of flat-plate cascade, the slightly cambered cascade is treated in the following three sections.

2. A Critical Discussion of Schlichting's and Mellor's Methods for Slightly Cambered Cascades.

In this section, a critical review of the Schlichting and related Mellor's method is given. Schlichting's work (ref. 4) essentially parallels the so-called 'thin airfoil' theory of an isolated airfoil.

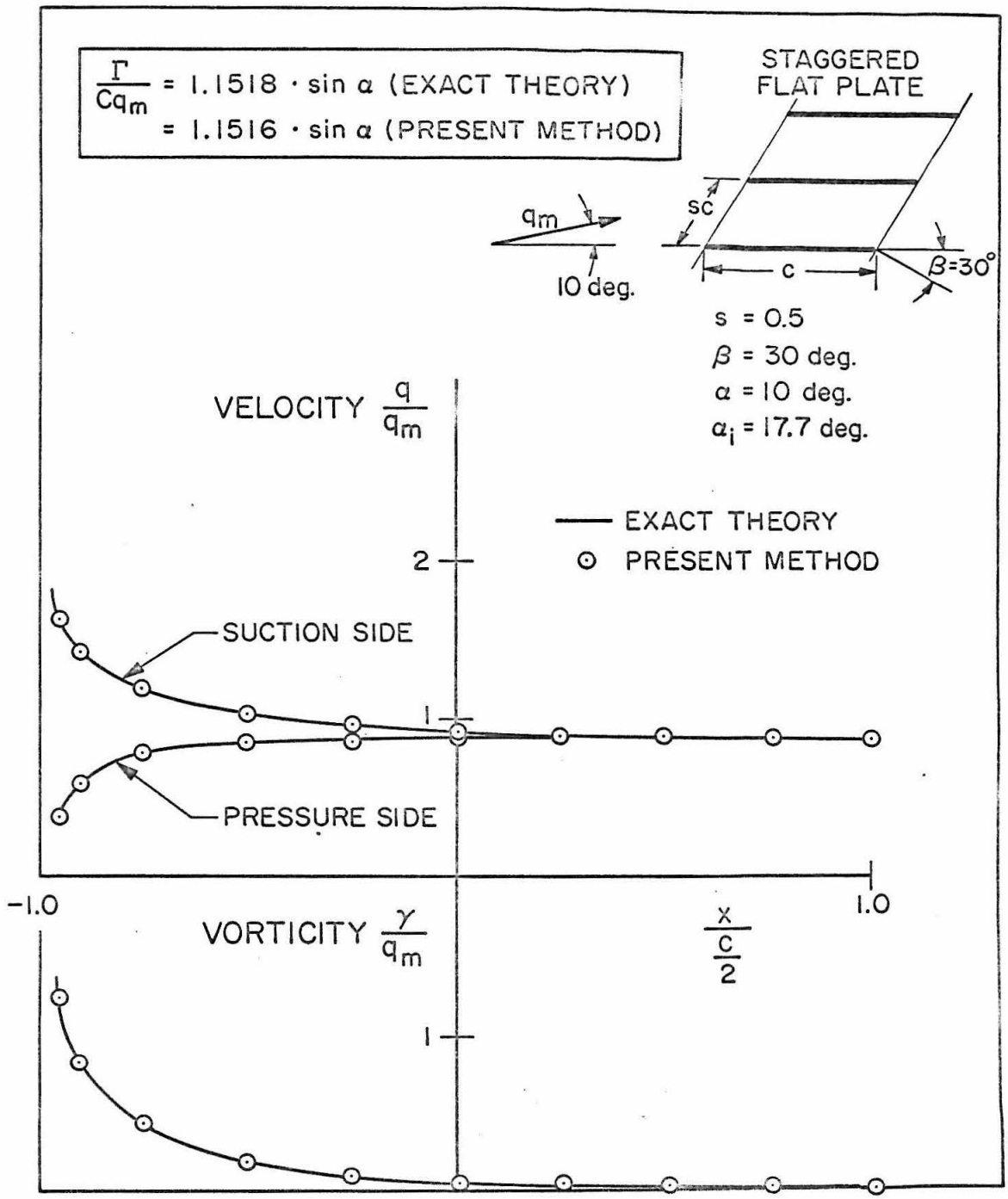

Figure 7. Staggered cascade of flat-plate airfoils, $S = 0.5$, $\beta = 30^{\circ}$.

Usually, thin airfoil theory is based upon two key assumptions:

(1) the vortices can be displaced from the camber line to chord line and the induced velocities on the camber line can be approximated by those on the chord line; and

(2) the x component of the induced velocity u_o is negligible as compared to the undisturbed velocity component U_∞, i.e.,

$$\frac{v_o + V_\infty}{\cancel{u_o}^{\,0} + U_\infty} = y_o'$$

In Schlichting's analysis, although in the flow tangency condition the x component of the induced velocity is retained, assumption (1) is adopted. We will see in a moment that, by extending this approach to the case of a cascade, the results obtained are more crude than the corresponding isolated airfoil flow problem, and for more satisfactory treatment, the present method should be used instead. But for the time being, let us skip this point and follow the outline of Schlichting's method. In equation (2.4), he puts

$$\xi = x, \quad \xi_1 = x_1$$

and rewrites the equation as

$$u(x,0) - iv(x,0) = \frac{1}{2\pi}\int_{-\frac{c}{2}}^{\frac{c}{2}} (m(x_1) + i\gamma(x_1))\frac{dx_1}{x - x_1}$$
$$+ \frac{1}{2sc}\int_{-\frac{c}{2}}^{\frac{c}{2}} \left\{ e^{i\beta} \coth\left[\frac{\pi(x - x_1)}{sc} e^{i\beta}\right] - \frac{1}{\pi}\frac{sc}{x - x_1}\right\}(m(x_1) + i\gamma(x_1))dx_1$$

The first integral represents the induced velocity by the single airfoil, namely, that due to the singularity located on the same airfoil at which the induced velocity is being computed. It is separated from the

rest so that the second integral becomes non-singular. Assuming the series forms for source $m(x_1)$ and vorticity distribution $\gamma(x_1)$, the integration can be carried out easily in the first integral in the same way as in thin airfoil theory. The second integral, however, does not lend itself to easy integration, and Schlichting prepared extensive tables, based on direct numerical integration, to compute this. If we express induced velocity, after substituting the series form for the singularity, as

$$u(x,0) - iv(x,0) = \sum a_n F_n\left(\beta; s; \frac{x}{\frac{c}{2}}\right) + \sum b_n G_n\left(\beta; s; \frac{x}{\frac{c}{2}}\right)$$

where F_n and G_n's are universal functions of three parameters -- stagger angle β, solidity s, and position on chord $\frac{x}{\frac{c}{2}}$ -- then they can be found from the compiled tabulation for the combinations of these parameters. These universal functions, being the results of numerical integration, cannot be obtained easily for the values of parameters other than the ones listed in the table, and one has to use interpolation in such cases. In the present method, the corresponding universal functions A_{nm} are simple combinations of logarithmic and trigonometric functions, and they can be computed for any solidity s and the position on the chord $\frac{x}{\frac{c}{2}}$, the only parameters. As for the effect of stagger angle β, this appears explicitly in the expressions of f_n and of g_n in section 7, Part II. Therefore, by the present method, one can study the functional dependence of aerodynamic parameter on the stagger angle β, while in Schlichting's method, this effect is embedded implicitly in the numerical tables. Thus, in this respect, the present method is more flexible

than his method. An example of the functional relationship between the exit angle and the various parameters will be given in section 3. As for the effect of solidity, it has to be given a priori in both methods. The rest of the calculation procedure of Schlichting's method is quite similar to the present one. Substitution of the velocity expression in the flow tangency condition yields a simultaneous linear equation for a_n's and b_n's. Collocating these boundary conditions at control points chosen according to the three-quarter point method and truncating the series, we can solve those equations for a_n's and b_n's.

One of the drawbacks of Schlichting's method is that the flow tangency condition is not satisfied everywhere but only at discrete points. To improve this, Mellor (ref. 5) uses a Fourier analysis, i.e., expresses both sides of the flow tangency condition in a Fourier series and equating these coefficients. This requires a second integration. Some of these double integrals are not a universal function, but depend on the airfoil shape and have to be worked out numerically each time for a new airfoil shape. From the practical point of view, such improvements, made at the cost of time required for one computation, might not be justified.

Now let us return to the basic assumption made in Schlichting's analysis, commensurate with the assumption (1) in thin airfoil theory for an isolated airfoil. To investigate its validity, let us see whether such an assumption follows from the present method for the slightly cambered cascade, which, since the singularity is located <u>on</u> the camber line instead of on the chord line, can be made to be exact, at least for the airfoil of zero thickness. To simplify the treatment, ex-

press the airfoil camber line for slight camber as

$$y_o = -\epsilon\left(\frac{c}{2}\right)F(x) \quad , \quad \epsilon \ll 1$$

where $F(x)$ is some function of x. The thickness is assumed to be zero. Noting all the derivatives of camber line $y_o^{(n)}(x)$ are of the order of ϵ, q_n in (2.28) can be written as

$$q_n = -\frac{1}{2\pi}A_{n1} - \frac{\pi}{6(sc)^2}\left\{(\cos 2\beta - y_o' \sin 2\beta)\left(\frac{c}{2}\right)^2 A_{n3} + \frac{1}{2}y_o'' \sin 2\beta\left(\frac{c}{2}\right)^3 A_{n4} + \cdots\right\} - \frac{1}{2sc}\left(\frac{c}{2}\right)\cos\beta \cdot B_n$$

to the order of ϵ, while f_n in (2.27) can be written as

$$f_n = -\frac{\pi}{6(sc)^2}\sin 2\beta\left(\frac{c}{2}\right)^2 A_{n3} - \frac{1}{2sc}\left(\frac{c}{2}\right)\sin\beta \cdot B_n$$

to the order of unity. Thus, to the order of ϵ,

$$q_n - y_o' f_n = \left[-\frac{1}{2\pi}A_{n1} - \frac{\pi}{6(sc)^2}\cos 2\beta \cdot \left(\frac{c}{2}\right)^2 A_{n3} - \frac{1}{2sc}\left(\frac{c}{2}\right)\cos\beta \cdot B_n\right] - \frac{\pi}{6(sc)^2}\left[-2y_o' \sin 2\beta\left(\frac{c}{2}\right)^2 A_{n3} + \frac{1}{2}y_o'' \sin 2\beta\left(\frac{c}{2}\right)^3 A_{n4} - \cdots\right] + \left[\frac{1}{2sc}\left(\frac{c}{2}\right)y_o' \sin\beta \cdot B_n\right]$$

The expression in the first bracket is of the order of unity, while the expressions in the second and third brackets are of the order of ϵ. The flow tangency conditions, (2.38) and (2.39), become

$$\sum_{n=0}^{\infty}\alpha_n\Big\{\underbrace{\left[-\frac{1}{2\pi}A_{n1} - \frac{\pi}{6(sc)^2}\cos 2\beta\left(\frac{c}{2}\right)^2 A_{n3} - \frac{1}{2sc}\left(\frac{c}{2}\right)\cos\beta \cdot B_n\right]}_{O(1)} - \underbrace{\frac{\pi}{6(sc)^2}\left[-2y_o' \sin 2\beta\left(\frac{c}{2}\right)^2 A_{n3} + \frac{1}{2}y_o'' \sin 2\beta\left(\frac{c}{2}\right)^3 A_{n4} - \cdots\right]}_{O(\epsilon)} + \underbrace{\frac{1}{2sc}\left(\frac{c}{2}\right)y_o' \sin\beta \cdot B_n}_{O(\epsilon)}\Big\} = \underbrace{y_o'}_{O(\epsilon)} \qquad (3.3)$$

$$\sum_{n=0}^{\infty}\beta_n\Big\{\Big[\underbrace{-\frac{1}{2\pi}A_{n1}-\frac{\pi}{6(sc)^2}\cos 2\beta\left(\frac{c}{2}\right)^2 A_{n3}-\frac{1}{2sc}\left(\frac{c}{2}\right)\cos\beta\cdot B_n}_{O(1)}\Big]$$

$$\underbrace{-\frac{\pi}{6(sc)^2}\Big[-2y_0'\sin 2\beta\left(\frac{c}{2}\right)^2 A_{n3}+\frac{1}{2}y_0''\cdot\sin 2\beta\cdot\left(\frac{c}{2}\right)^3 A_{n4}-\cdots\Big]}_{O(\epsilon)}$$

$$+\underbrace{\frac{1}{2sc}\left(\frac{c}{2}\right)y_0'\cdot\sin\beta\cdot B_n}_{O(\epsilon)}\Big\}=\underbrace{-1}_{O(1)} \qquad (3.4)$$

where $a_n=\alpha_n+\beta_n\cdot\tan\alpha$. Let us notice first that in the limiting case of $s\to\infty$, corresponding to an isolated airfoil, all the $O(\epsilon)$ terms and some of the $O(1)$ terms in the left hand side of the equation vanish, and (3. 3) and (3. 4) become

$$\sum_{n=0}^{\infty}\alpha_n\left(-\frac{1}{2\pi}A_{n1}\right)=y_0',$$

$$\sum_{n=0}^{\infty}\beta_n\left(-\frac{1}{2\pi}A_{n1}\right)=-1,$$

and as $s\to\infty$,

$$A_{n1}=\pi\cos n\theta$$

The familiar result for thin airfoil theory is recovered, as pointed out in section 8, Part II. Namely, the α_n 's are of order ϵ , given by

$$\alpha_0=-\frac{2}{\pi}\int_0^{\pi}y_0'\,d\theta \quad , \quad \alpha_n=-\frac{4}{\pi}\int_0^{\pi}y_0'\cos n\theta\cdot d\theta \quad (n\geq 1)$$

while the β_n 's are of the order of unity, given by

$$\beta_0=2 \quad , \qquad \beta_n=0 \quad (n\geq 1)$$

or, in terms of a_n ,

$$a_0=-\frac{2}{\pi}\int_0^{\pi}(y_0'-\tan\alpha)\,d\theta \quad , \quad a_n=-\frac{4}{\pi}\int_0^{\pi}y_0'\cos n\theta\cdot d\theta \quad (n\geq 1)$$

valid up to the order of ϵ . Thus, the two assumptions made in the thin airfoil theory for the isolated airfoil are legitimate if we are concerned only with the values of vorticity distribution up to the order of ϵ . Returning to the case of a cascade where $S \neq \infty$, the terms of the order of ϵ are found to be non-vanishing in general in equations (3.3) and (3.4). If we started from the beginning using assumption (1) in the previous section, then the results would be the same as putting $y_0 = 0$ in the left hand side of equations (3.3) and (3.4). Then it is seen that all the terms of the order of ϵ vanish there.

This vanishing of the ϵ term in the left hand side of the equations does not affect the values of α_n up to the order of ϵ . For, if for the time being we perform the collocation at a large number of discrete points on the chord and solve (3.3) by Cramer's rule for α_n 's, then, since the right hand side of the equations is of the order of ϵ , the α_n 's must be of the order of ϵ , and only the terms of order unity in the bracket of the left hand side of the equation matter.

The vanishing of the term does affect the value of β_n up to the order of ϵ , however, as can be seen easily if we perform the same operation as above for equation (3.4). Therefore, if we adapt assumption (1) in thin airfoil theory to the case of a cascade, then part of the term of the order of ϵ will be lost in the final expression of vorticity strength $a_n = \alpha_n + \beta_n \cdot \tan\alpha$ and the difference between the flat-plate cascade, which corresponds to the $O(1)$ term, and the cambered-airfoil cascade will not be fully brought out. Physically, this means that in the case of a cascade, the velocity field near the

airfoil is quite different from that near the isolated airfoil, and the displacement of the coordinate points resulting from assumption (1) of thin airfoil theory causes an appreciable error in the magnitude of the velocities. A question might be raised that equations (3. 3) and (3. 4) are not exact. This does not invalidate the present conclusion, for even if we express $\coth\zeta$ in an infinite series as (2. 13) -- where it becomes exact -- the forms of equations (3. 3) and (3. 4) are of the same nature only with the additional terms. Thus, right from the beginning, Schlichting's method is based on an assumption which is a cruder approximation for a cascade than for the isolated airfoil; and accordingly in his analysis, the important difference between the flat-plate cascade and cambered cascade is partly lost, unless the spacing-chord ratio is sufficiently large.

3. Functional Relationship of the Exit Angle to Other Parameters for a Slightly Cambered Cascade.

In this section, let us obtain the relation of the exit angle to various parameters by retaining the term of the order of ϵ in equation (3. 4). Express the camber line equation as

$$y_0 = -\frac{\epsilon}{\frac{c}{2}}\left[x^2-\left(\frac{c}{2}\right)^2\right]\left(K_0 + K_1\frac{x}{\frac{c}{2}}\right) \quad , \qquad \epsilon \ll 1$$

and take the solidity as

$$s = 1.0$$

Selecting a three-point collocation chosen according to the three-quarter method and reading A_{nm} and B_n from the tables of Appendix 3, the α_n's and β_n's are solved from equations (3. 3) and (3. 4). The final result can be expressed in terms of the exit angle α_d

in the following way.

$$\tan\alpha_d = \tan(\alpha+\beta) - \frac{\pi}{4}\sec(\alpha+\beta)\left[\epsilon\,\frac{K_0 R_1(\beta)+K_1 R_2(\beta)}{R_0(\beta)}\cos\alpha + \frac{R_6(\beta)+\epsilon\{K_0 R_7(\beta)+K_1 R_8(\beta)\}}{R_3(\beta)+\epsilon\{K_0 R_4(\beta)+K_1 R_5(\beta)\}}\sin\alpha\right] \quad (3.5)$$

where $R_n(\beta)$ are partial sums of the Fourier series in terms of stagger angle such as

$$R_n(\beta) = C_0^{(n)} + \sum_{m=1}^{\infty} C_m^{(n)}\cos m\beta + \sum_{m=1}^{\infty} S_m^{(n)}\sin m\beta$$

and the C_m's and S_m's are tabulated in Appendix 4. This expression, though not as simple as desired, does provide, by straightforward computation, the relation between the exit angle α_d in terms of the attack angle α, stagger angle β, and airfoil shape ϵ, K_0 and K_1 for given solidity $S = 1.0$. Equivalent expressions for the other values of solidity or more complicated airfoil shapes can be worked out easily in a similar way. It is of interest to note that if the number of control points is increased, the number of coefficients in the series $R_n(\beta)$ would be augmented proportionally, and in the limiting case of satisfying the boundary condition everywhere, one obtains the Fourier series expansion of certain functions of stagger angle β, instead of the truncated forms $R_n(\beta)$. Some of such closed forms can be obtained explicitly if we consider the special case of a flat-plate cascade. Putting $\epsilon = 0$ in (3.5), we get

$$\tan\alpha_d = \tan(\alpha+\beta) - \frac{\pi}{4}\sec(\alpha+\beta)\left[\frac{R_6(\beta)}{R_3(\beta)}\right]\sin\alpha \quad (3.6)$$

On the other hand, the exact solution based upon the conformal mapping provides us with the following expression for the case of a flat-plate cascade.

$$\tan\alpha_d = \tan(\alpha+\beta) - \frac{\pi}{4}\sec(\alpha+\beta)\left[\frac{4}{\pi}\frac{\sqrt{2}}{\sqrt{\cosh 2\psi + \cos 2\beta}}\right]\sin\alpha \qquad (3.7)$$

where $\psi(s,\beta)$ is given as the solution of the following transcendental equation:

$$\frac{\pi}{s} = \cos\beta \cdot \log\left[\frac{\sqrt{\cosh 2\psi + \cos 2\beta} + \sqrt{2}\cos\beta}{\sqrt{\cosh 2\psi + \cos 2\beta} - \sqrt{2}\cos\beta}\right] + 2\sin\beta \cdot \tan^{-1}\left(\frac{\sqrt{2}\sin\beta}{\sqrt{\cosh 2\psi + \cos 2\beta}}\right) \qquad (3.8)$$

Comparison of (3.6) and (3.7) shows that the truncated Fourier series expression $\frac{R_6(\beta)}{R_3(\beta)}$ corresponds to $\left[\frac{4}{\pi}\frac{\sqrt{2}}{\sqrt{\cosh 2\psi + \cos 2\beta}}\right]$. It is also seen that from the transcendental dependence of ψ on solidity s and stagger angle β in the exact solution for the flat plate that a rather involved expression for stagger angle β_n effect and the specification of the solidity as a number at the beginning are of somewhat unavoidable consequence.

Returning to a cambered cascade, Klingemann discovered the velocity expression which satisfies approximately the boundary condition on a cascade of parabolic airfoils as well as the condition at infinity (ref. 19). The approximation is based on the two assumptions in isolated thin airfoil theory which were described in the preceding section. Therefore, as far as the basic assumption is concerned, his method is no better than Schlichting's. In this connection, Rannie first pointed out in ref. 18 that the application of the assumptions of isolated airfoil theory to the cascade problem should be made with

more reservation than for the corresponding isolated airfoil problem. Apart from this defect, the advantage of Klingemann's result is that for the parabolic airfoil, the exit angle can be expressed as a function of each of the influencing factors, including the solidity s .

Following the descriptions given in ref. 18, a brief outline of Klingemann's method will be given below, along with an improvement of Rannie. The cascade mapping function that maps a unit circle in the ζ plane into a flat-plate cascade in the z plane is given by

$$z = \frac{sc}{2\pi}\left[\bar{e}^{i\beta} \log \frac{\zeta + e^{\psi}}{\zeta - e^{\psi}} + e^{i\beta} \log \frac{\zeta + \bar{e}^{\psi}}{\zeta - \bar{e}^{\psi}} \right] \tag{3.9}$$

where ψ is given by (3.8). Consider the following expression for the complex velocity:

$$\frac{dw}{dz} = q_m \cdot \frac{(\bar{e}^{-i(\alpha+\beta)+\psi} + e^{i(\alpha+\beta)-\psi})\zeta^2 - (e^{i(\alpha+\beta)+\psi} + \bar{e}^{-i(\alpha+\beta)-\psi})}{(\bar{e}^{i\beta+\psi} + e^{i\beta-\psi})\zeta^2 - (e^{i\beta+\psi} + \bar{e}^{i\beta-\psi})}$$

$$+ \frac{2i}{\pi} s v_1 \zeta e^{i\beta} \frac{\left[e^{\psi}(\bar{e}^{i\beta+\psi} + e^{i\beta-\psi}) - \bar{e}^{\psi}(e^{i\beta+\psi} + \bar{e}^{i\beta-\psi}) \right] \log(\coth \psi)}{(\bar{e}^{i\beta+\psi} + e^{i\beta-\psi})\zeta^2 - (e^{i\beta+\psi} + \bar{e}^{i\beta-\psi})}$$

$$- \frac{2i}{\pi} s v_1 e^{i\beta} \log\left(\frac{\zeta + \bar{e}^{\psi}}{\zeta - \bar{e}^{\psi}}\right) + \frac{i\Gamma}{s} \frac{s \sinh 2\psi}{(\bar{e}^{i\beta+\psi} + e^{i\beta-\psi})\zeta^2 - (e^{i\beta+\psi} + \bar{e}^{i\beta-\psi})}$$

where v_1 is a yet unspecified velocity. It can be shown that this satisfies the flow condition at infinity. If we put $\zeta = e^{i\phi}$ corresponding to the chord line $-\frac{c}{2} \leq x \leq \frac{c}{2}$, then the following velocity components on the airfoil chord line are obtained:

$$u = q_m \cos\alpha + \frac{2}{\pi} s\vartheta_1 \left[\sin\beta \cdot \log \frac{\cosh\psi + \cos\phi}{\cosh\psi - \cos\phi} - 2\cos\beta \cdot \tan^{-1} \frac{\sin\phi}{\sinh\psi} \right]$$

$$+ \frac{\sinh 2\psi}{\cosh\psi \cdot \cos\beta \cdot \sin\phi - \sinh\psi \cdot \sin\beta \cdot \cos\phi} \left[\frac{\Gamma}{2sc} + s\frac{\vartheta_1}{\pi} \log(\coth\psi) \right.$$

$$\left. - \frac{q_m \cdot \sin\alpha}{\sinh 2\psi} (\cosh\psi \cdot \sin\beta \cdot \sin\phi + \sin\psi \cdot \cos\beta \cdot \cos\phi) \right]$$

$$v = 2\vartheta_1 \frac{x}{c}$$

The circulation Γ can be determined by applying the Kutta condition at the trailing edge. The substitution of $\zeta = e^{i\phi}$ is commensurate with assumption (1) in thin airfoil theory.

So far, nothing has been mentioned about the shape of the airfoil. The slope of the streamline on the x axis is given by

$$\frac{dy}{dx} = \frac{v}{u} = 2\vartheta_1 \frac{x}{uc} \tag{3.10}$$

If we put $u \doteq q_m \cos\alpha$, the x component of the vector mean of far upstream and far downstream velocities, corresponding to assumption (2) in thin airfoil theory, then

$$\frac{dy}{dx} \cong 2\vartheta_1 \frac{x}{q_m \cos\alpha \cdot c} \tag{3.11}$$

and thus the airfoil is approximately parabolic. From the given parabolic shape of the airfoil, ϑ_1 is determined and the expression for the exit angle can be deduced. This particular choice of the x component of velocity is the analog of the correct x component for an isolated airfoil. It is a reasonable choice for s large; however, for s approaching zero, the leaving direction is not parallel to

the trailing edge as it should be. To remedy this, Rannie chose for the x component of velocity the exact value at the trailing edge, so that the flow angle at the trailing edge coincides with the airfoil slope at that point. Such a choice guarantees that the leaving angle from the cascade is consistent with the cascade geometry at all solidities.

In section 8 of this part, we will see that for any camber or airfoil shape, the present method is also consistent.

4. A Remark on the Slightly Cambered Cascade of Low Solidity.

In section 2 of this part, it was shown that for the limiting case of spacing-chord ratio $s \to \infty$, the usual assumptions of thin airfoil theory are valid. In this section, consider the case of large but finite s. For large s, $q_n - y_0' f_n$ in section 2 reduces to

$$q_n - y_0' f_n = \left[-\frac{1}{2\pi} A_{n1} - \frac{\pi}{6(sc)^2} \cos 2\beta \cdot \left(\frac{c}{2}\right)^2 A_{n3} - \frac{1}{2sc}\left(\frac{c}{2}\right) \cos\beta \cdot B_n \right]$$

where terms of order ϵ are justifiably neglected, as in assumption (1) of section 2. The boundary condition becomes

$$\sum_{n=0}^{\infty} \left[-\frac{1}{2\pi} A_{n1} - \frac{\pi}{6(sc)^2} \cos 2\beta \cdot \left(\frac{c}{2}\right)^2 A_{n3} - \frac{1}{2sc}\left(\frac{c}{2}\right) \cos\beta \cdot B_n \right] a_n = y_0' - \tan\alpha \qquad (3.12)$$

This boundary condition, although somewhat in disguise, is the same as assumption (2) of section 2. If we neglect the x component of the induced velocity,

$$\frac{v_0 + V_\infty}{\cancel{u_0} + U_\infty} = y_0'$$

and substitute the expression for v_0 obtained in (2.29) for zero thickness $b_n = 0$, we get

$$\sum_{n=0}^{\infty} a_n g_n = y_0' - \tan\alpha$$

It can be recognized easily that the expression in the bracket on the left hand side of equation (3. 12) is g_n itself, the higher order term $y_0' f_n$ being neglected.

Now, for $S \gg 1$, the range of inner expansion occupies the entire chord. This implies

$$\delta_1 \longrightarrow \theta \ , \quad \delta_2 \longrightarrow \pi - \theta$$

and A_{nm} and B_n in Appendix 2 are reduced to the following forms.

$$A_{n1} = \pi \cos n\theta, \quad A_{03} = \pi\left(\cos\theta + \frac{1}{2}\right) \ , \quad B_n = 0 \quad (n \geq 0)$$

$$A_{13} = \frac{\pi}{2}\cos\theta$$

$$A_{23} = -\frac{\pi}{4}$$

$$A_{n3} = 0 \qquad (n \geq 3)$$

The vanishing of the B_n's for any n corresponds to the disappearance of the outer expansion range. Substituting these expressions into (3. 12) and writing explicitly, we get

$$\left[-\frac{1}{2} - \frac{\pi^2}{24S^2}\cos 2\beta\left(\cos\theta + \frac{1}{2}\right)\right] a_0 + \left[-\frac{1}{2}\cos\theta - \frac{\pi^2}{48S^2}\cos 2\beta \cdot \cos\theta\right] a_1$$

$$+\left[-\frac{1}{2}\cos 2\theta + \frac{\pi^2}{96S^2}\cdot\cos 2\beta\right] a_2 - \sum_{n=3}^{\infty} \frac{1}{2}\cos n\theta \cdot a_n = y_0' - \tan\alpha$$

Rearrange the left hand side of this equation as

$$\left[\left(-\frac{1}{2} - \frac{\pi^2}{48S^2}\cos 2\beta\right) a_0 + \frac{\pi^2}{96S^2}\cos 2\beta \cdot a_2\right] + \left(-\frac{\pi^2}{24S^2}\cos 2\beta \cdot a_0 - \frac{1}{2}a_1\right.$$

$$\left. - \frac{\pi^2}{48S^2}\cos 2\beta \cdot a_1\right)\cos\theta - \frac{1}{2}a_2\cos 2\theta - \sum_{n=3}^{\infty} \frac{1}{2}\cos n\theta \cdot a_n = y_0' - \tan\alpha$$

Expand the right hand side of the equation in Fourier series as

$$\gamma_0' - \tan\alpha = -\frac{1}{2}\tilde{a}_0 - \frac{1}{2}\sum_{n=1}^{\infty} \tilde{a}_n \cdot \cos n\theta$$

where

$$\tilde{a}_0 = -\frac{2}{\pi}\int_0^{\pi} (\gamma_0' - \tan\alpha)\, d\theta \quad , \quad \tilde{a}_n = -\frac{4}{\pi}\int_0^{\pi} \gamma_0' \cos n\theta\, d\theta \qquad n \geq 1$$

The $\tilde{a}_n$'s denote the vorticity for the isolated airfoil of $S \longrightarrow \infty$. Equating the coefficients of cosine on both sides of the equation and re-arranging, we get

$$\tilde{a}_0 = a_0\left[1 + \frac{\pi^2}{24S^2}\cos 2\beta\right] - a_2 \frac{\pi^2}{48S^2}\cos 2\beta$$

$$\tilde{a}_1 = a_0 \frac{\pi^2}{12S^2}\cos 2\beta + a_1\left[1 + \frac{\pi^2}{24S^2}\cos 2\beta\right] \quad , \quad \tilde{a}_n = a_n \ (n \geq 1)$$

The result is that a particular case of the present method is the same as those obtained in ref. 1, p. 156, where, due to the different form of the original vorticity distribution such as

$$\gamma = U_\infty \left(a_0 \tan\frac{\theta}{2} + \sum_{n=1}^{\infty} \frac{1}{2} a_n \sin n\theta\right) ,$$

the demonimator in the second term in $\tilde{a}_0$ appears to be $24S^2$ instead of $48S^2$, and in the first term of $\tilde{a}_1$, $24S^2$ instead of $12S^2$. From these expressions, for the case of $S \gg 1$, the vorticity can be evaluated as a correction to the one corresponding to the isolated airfoil.

5. Moderately Cambered Cascades.

In this section, let us consider the moderately cambered cascade. As a yardstick to make comparison with the present method, we refer to the direct numerical solution of the exact integral equation by

the use of the digital computer. In ref. 6, Jakob gives a program for the cascade problem. In his method, the vortices, the magnitude of which is equal to the surface velocity, are distributed on the surface of the airfoil. This distribution on the surface is a more accurate description of the flow outside the airfoil contour than one in which both sources and vortices are located upon the camber line, as in the present method. The tangential flow condition yields an integral equation with the surface velocity as an unknown.

Direct numerical solution of the integral equation is carried out by dividing the airfoil surface into a number of elements and assuming the vorticity is constant along any element. Physically, this means the approximation of chordwise continuous vorticity distribution by a number of discrete vortices. The integral is then replaced by a sum taken over the entire chord, and the strength of each discrete vortex can be determined as a solution of simultaneous linear equations. The most crucial step is to take care of the singularities in the kernel of the integral, for the computer cannot handle such singular behavior properly. This is done by studying the property of the principal integral analytically. With the aid of a high-speed computer, the number of such discrete vortices can be increased to as many as we like, resulting in higher accuracy. Jakob's programming allows one to distribute up to a total number of 100 discrete vortices. In working out the results by use of the computer to make comparison with the present method, this maximum number of vortices was employed. The choice of position on the airfoil surface where such vortices are placed is described in Jakob's report. In short, they are clustered

more closely near the leading and trailing edges where the curvature of the airfoil contour, and hence change of vorticity strength, is greatest. Even though there is no direct convenient way to check Jakob's programming with the known exact solution, such as flat plate, due to the difficulties associated with the leading edge infinity, this method can be regarded as highly reliable, and for 100 points, almost exact.

As an additional remark, in Jakob's programming, the upstream inlet angles are given in terms of α_u rather than α. Thus, in making comparison with the present method where the upstream inlet angles are given in terms of α, α_u is changed to by using the circulation obtained by the computer.

As an example of a moderately cambered cascade, the NACA 8410 type airfoil shown in Figure 8 was studied. This airfoil has the following geometrical characteristics:

max. camber/chord = 8 per cent,

position of max. camber/chord = 40 per cent from the leading edge,

max. thickness/chord = 10 per cent.

The camber line consists of two parabolic arcs having a continuous slope at the point of maximum camber. The thickness distribution is given by

$$t = \pm 0.5(0.2969\sqrt{\eta} - 0.1260\eta - 0.3516\eta^2 + 0.2843\eta^3 - 0.1015\eta^4) \qquad (3.13)$$

where η is the ratio of the distance along the chord measured from the leading edge.

In this case, the series in the first bracket of f_η in equation

Figure 8. NACA 8410 Airfoil.

(2.27) and g_n in equation (2.28) become an infinite series, and the problem of where to truncate the series must be considered. In general, the convergence property of this series is as follows: the series becomes less convergent as the maximum camber of the airfoil becomes large or as the solidity decreases, i.e., as spacing-chord ratio increases. In the present example of maximum camber of 8 per cent, $S = 1.0$, the fifth term becomes negligibly small, and even in the case of a highly cambered airfoil of the next section, where the maximum camber is 25 per cent, the sixth term is negligible. Of course, these do not serve as a rigorous justification for truncation of the series at a particular term. Figures 9 and 10 show the comparison of the present method with the computer solution for the cascade in a compressor arrangement with stagger angle $\beta = 45°$, spacing-chord ratio $S = 1.0$, and for two different angles of attack. In both cases, the agreement between the present method and the computer results is good. The discrepancies are small even at the points near the leading edge, where the present method, being collocated at only three discrete points, cannot be expected to give good results. For the overall characteristics, such as circulation and exit angle, the agreement is quite satisfactory. At this point, a comment about the practical solution for the singularities' strength is needed. These singularity strengths are obtained as the solutions of simultaneous linear equations. For three-point collocation in its exact form, two sets of simultaneous equations, which are independent of each other, given by equations (2.38) and (2.39), must be solved. For practical purposes, iterative solutions reduce the numerical labor considerably:

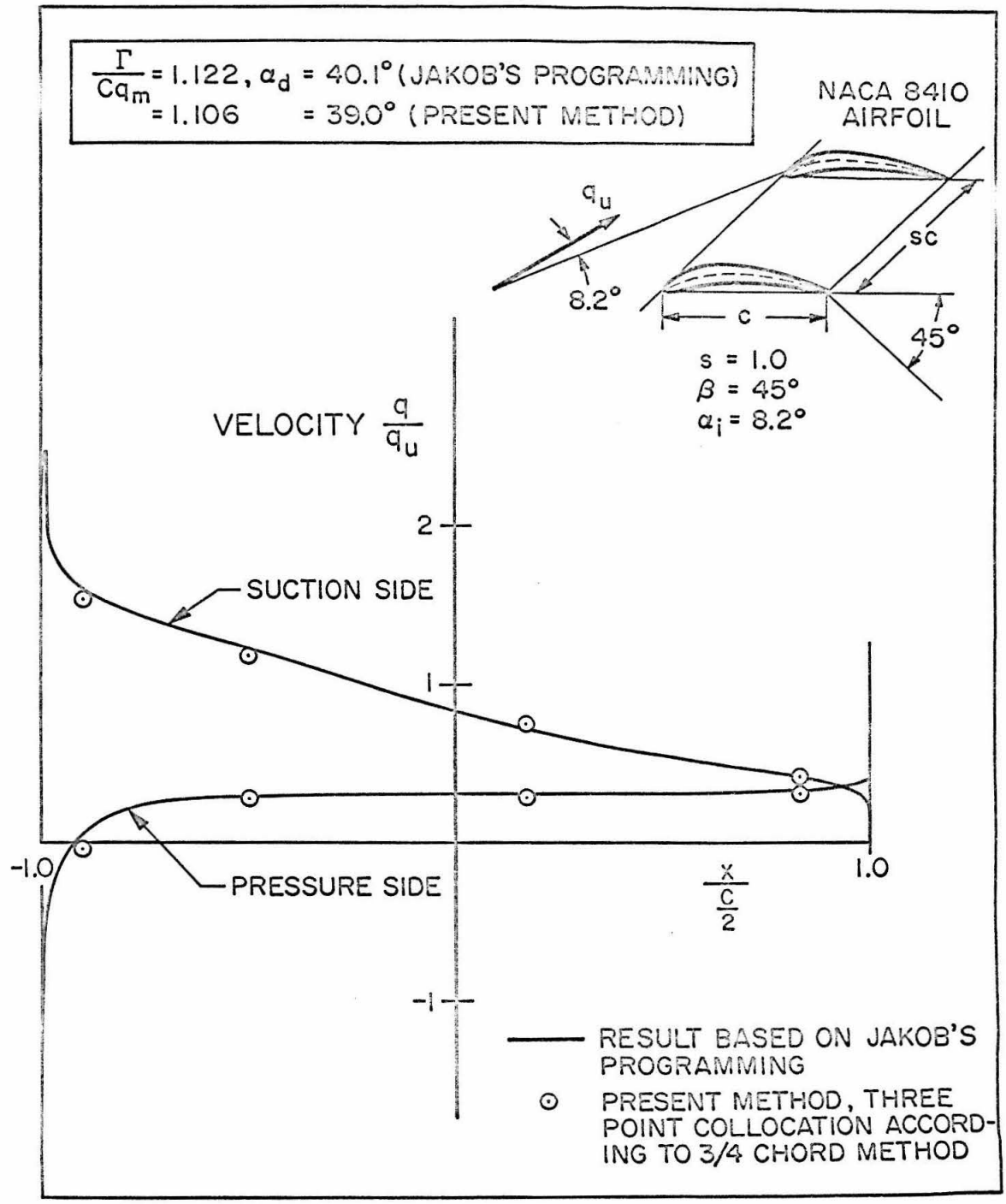

Figure 9. Velocity distribution for compressor cascade, $\alpha_i = 8.2^o$.

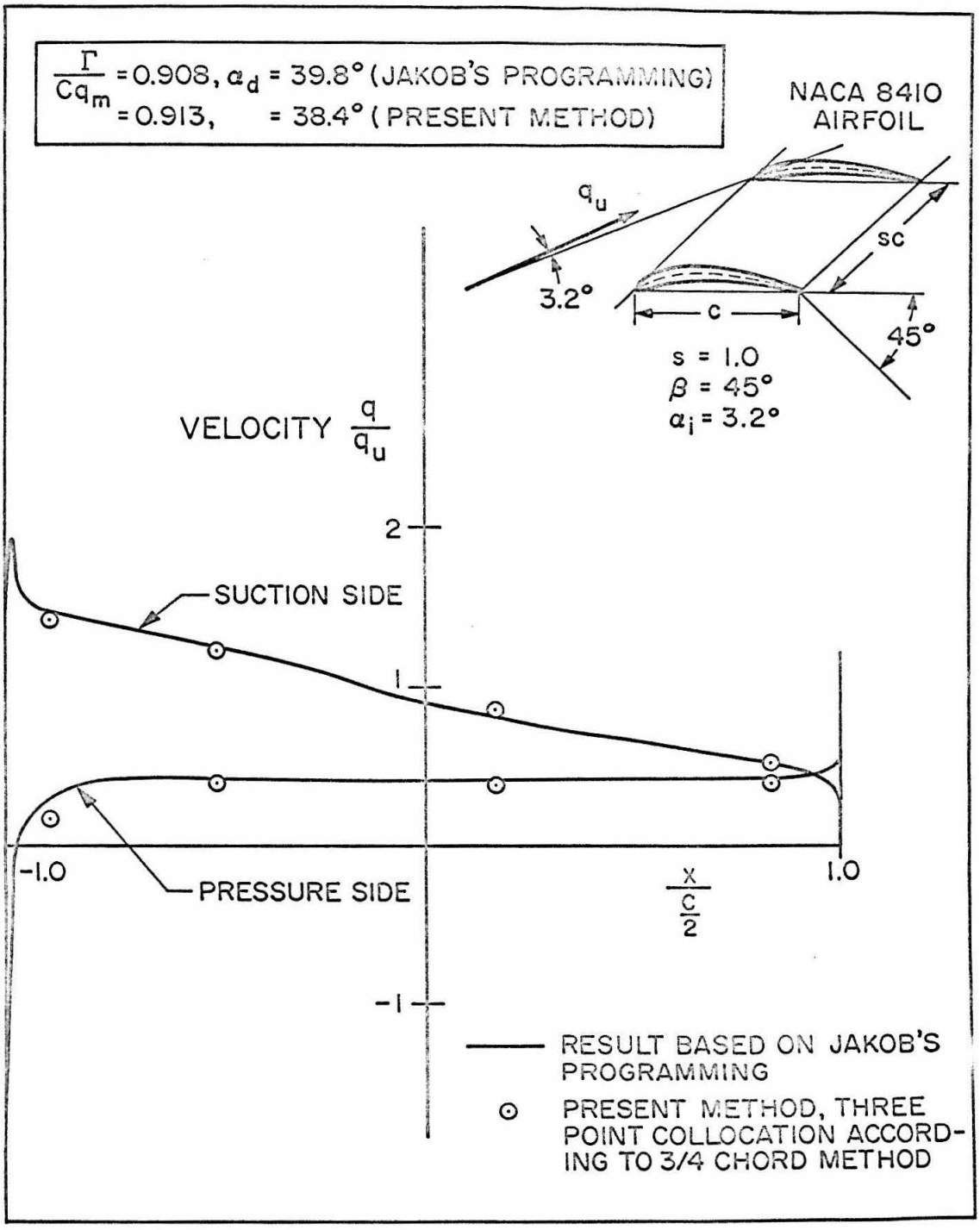

Figure 10. Velocity distribution for compressor cascade, $\alpha_i = 3.2^\circ$.

first, the vorticity strengths are determined by neglecting the thickness, and then, with this vorticity strength, the source strength is determined, and this source strength modifies the vorticity. For a thickness of about 10 per cent as treated here, this iteration is sufficient.

Figures 11 and 12 show the results for the turbine arrangement at two different angles of attack. The solidity is unity and the stagger angle is -30 degrees. In these cases, although discrepancies are somewhat larger than the former ones, the agreement between the present method and the computer results is reasonably good. Also, the agreement for the overall factors is good. Therefore, it is concluded that various assumptions made in the analysis of Part II, such as the range of expansion and the choice of control points, are justified for the moderately cambered cascade.

According to the present method, the velocity becomes infinitely large at the leading edge, even for the airfoil with finite radius of curvature at the point. At attempt was made to improve the calculation, and although it was not pursued because the amount of numerical work required seemed inconsistent with the spirit of the present method, a brief description is given below.

To illustrate the idea, consider the simplest case of an isolated, uncambered airfoil, as shown in the figure on the left. To obtain a finite velocity at the leading edge, the distribution of sources and vortices begins at a distance $\frac{\rho}{2}$ from the

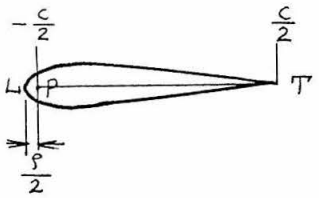

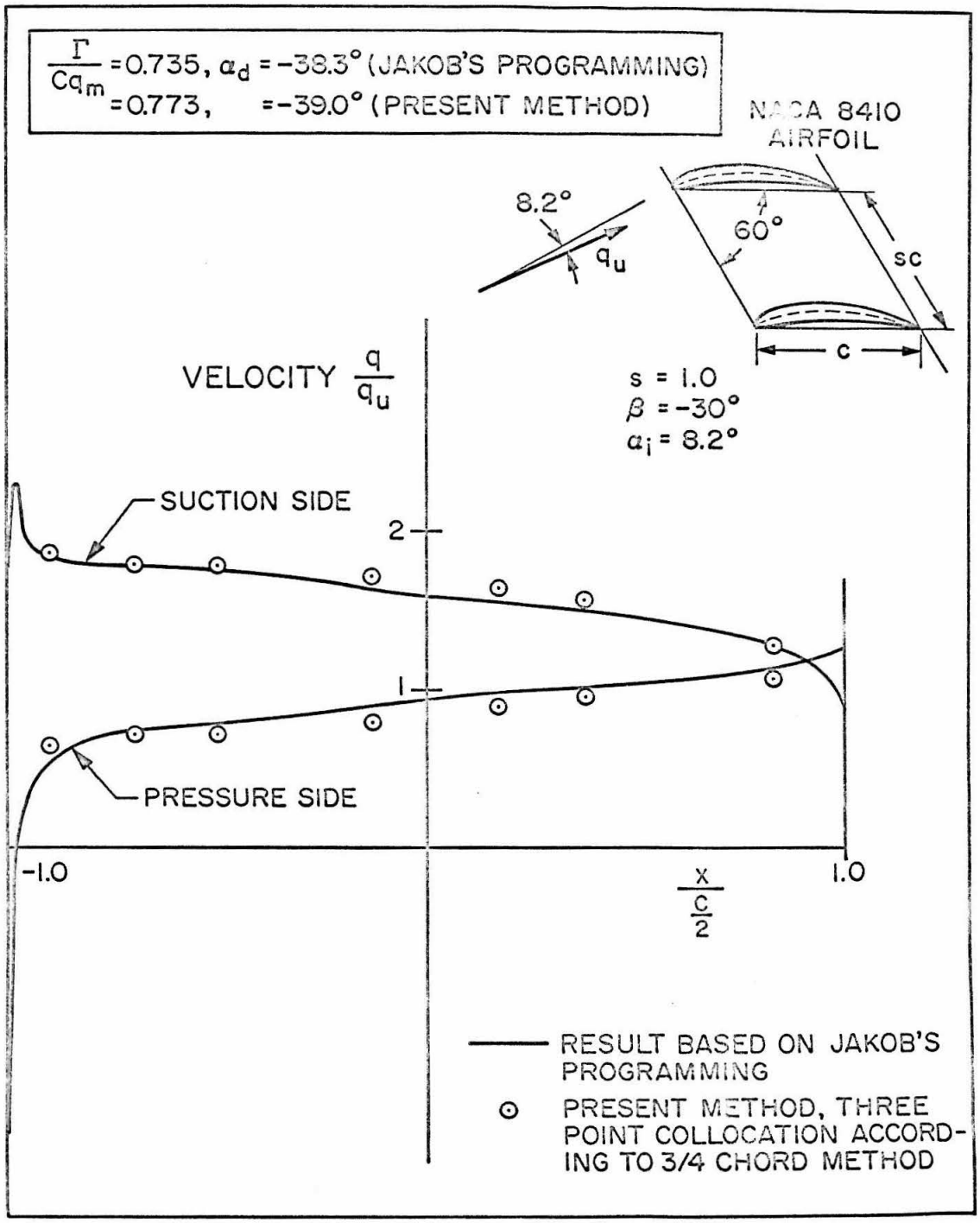

Figure 11. Velocity distribution for turbine cascade, $\alpha_i = 8.2^o$.

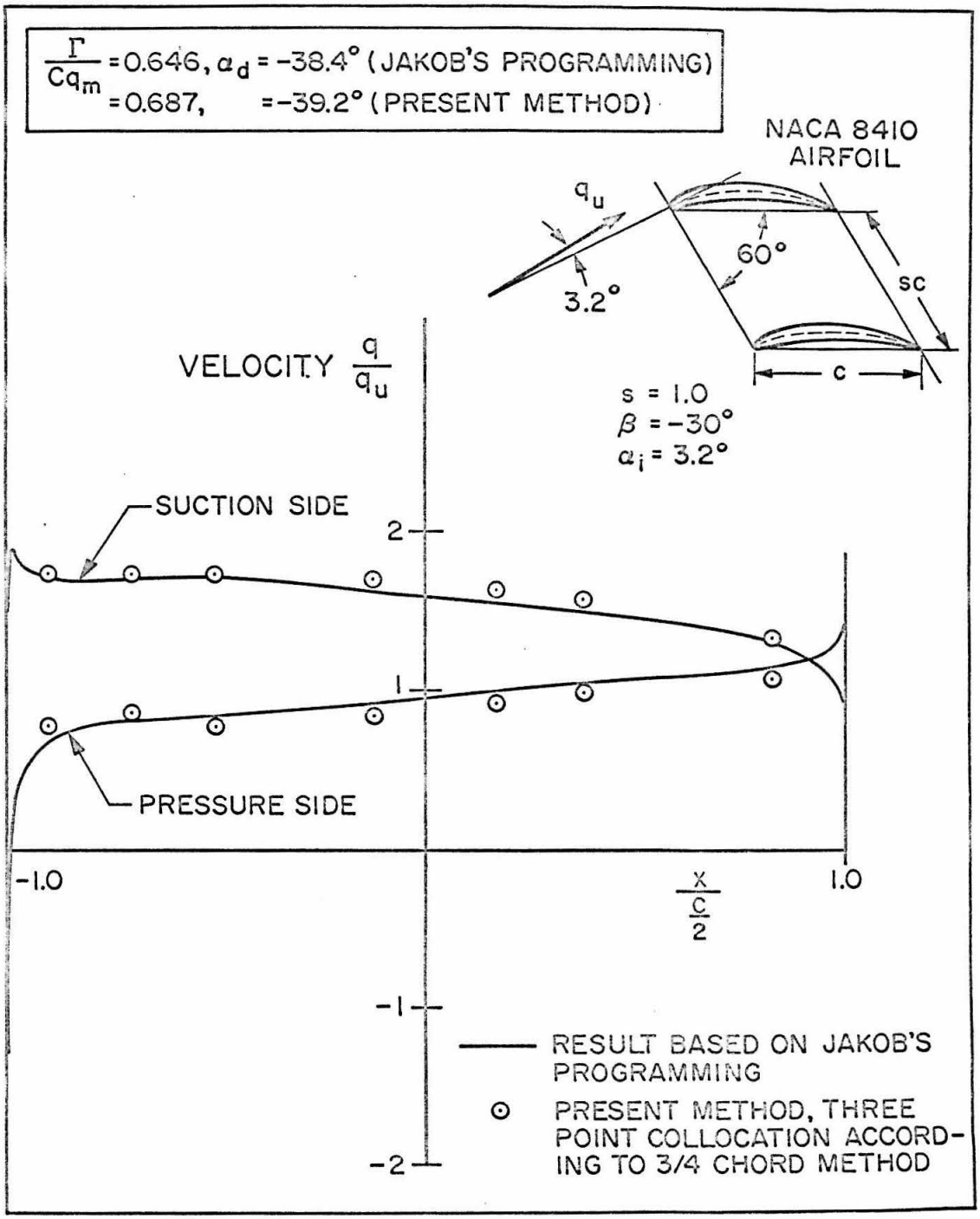

Figure 12. Velocity distribution for turbine cascade, $\alpha_i = 3.2^o$.

leading edge where ρ is the radius of curvature of the leading edge. For such a distribution of vortices and sources on a straight line, the velocity field for the flow past the airfoil is given by a simple expression. Using this, the velocity can be obtained on the airfoil surface instead of on the chord line, once the strengths of sources and vortices are known, and the velocity at the leading edge becomes finite. The airfoil surface is identified with the streamline through the stagnation point; the position of the latter is readily determined. By successive approximations, the strengths of sources and vortices to give any airfoil shape can be determined.

Combining this idea with the tangent slope method, a cambered airfoil can also be treated. By the tangent slope method, the vorticity distribution can be displaced from the camber line to a straight line, and the above procedure is then applied to obtain the velocity on the airfoil surface. Of course, in the cambered airfoil, the correction term to the tangent slope term, explained in section 2, Part II, must be added. Again, the strengths of sources and vortices are determined from the flow tangency condition on the airfoil surface, as the solutions of simultaneous linear equations. The unfortunate aspect of this method is that, to take the effect of airfoil shape into consideration, four collocation points near the leading edge, in addition to the usual collocation points distributed over the chord, were not sufficient to represent the contour of the nose of an airfoil. The increase of the number of collocation points results in a larger amount of numerical work.

6. The Case of a Highly Cambered Cascade.

Figure 13 shows the outline of an example of a highly cambered airfoil. The geometrical characteristics of this airfoil are essentially the same as an NACA four-digit type airfoil. The major specifications are as follows:

maximum camber/chord = 25 per cent,

position of maximum camber/chord = 40 per cent from the leading edge,

maximum thickness/chord = 10 per cent.

The camber line consists of two parabolic arcs having a continuous slope at the point of maximum camber, i.e.,

$$\frac{y_0(x)}{c} = \frac{f}{c}\frac{1}{\eta_1^2}(2\eta_1\eta - \eta^2) \qquad 0 \leqq \eta \leqq \eta_1,$$

$$\frac{y_0(x)}{c} = \frac{f}{c}\frac{1}{(1-\eta_1)^2}\left[(1-2\eta_1) + 2\eta_1\eta - \eta^2\right] \qquad \eta_1 \leqq \eta \leqq 1$$

where

$$\frac{f}{c} = 0.25, \quad \eta_1 = 0.4$$

and η is defined in the preceding section. The thickness distribution is given by equation (3.13). The results for this airfoil in a turbine arrangement with stagger angle $\beta = -30°$ and solidity unity are shown in Figure 14. Here, the discrepancy between the present method and the computer results is appreciably large for the velocity distribution at all points along the chord. The main cause for this discrepancy is considered to be due to the neglect of higher harmonics. From three-point collocation, the first three terms of source and vorticity distribution are a_0, a_1, a_2, b_0, $b_1 = -2b_0$, b_2, and b_3. The contribution from the other higher harmonics is neglected. Now, as the camber of the airfoil increases, the higher

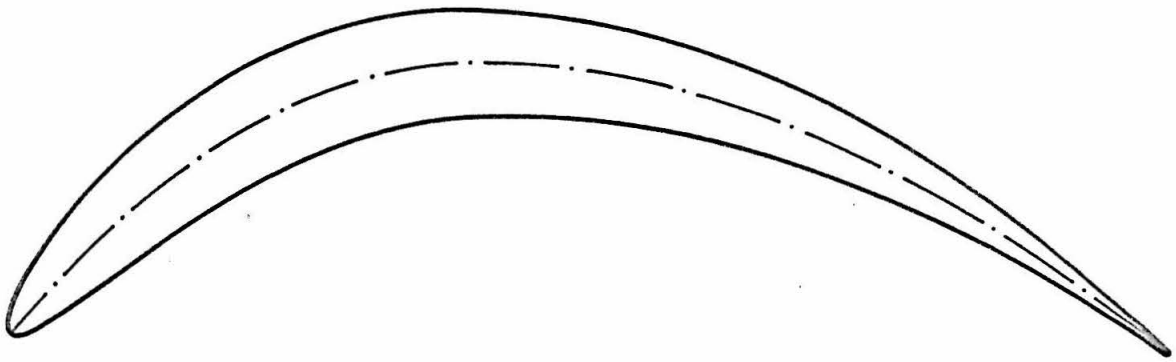

Figure 13. Airfoil with 25 per cent camber.

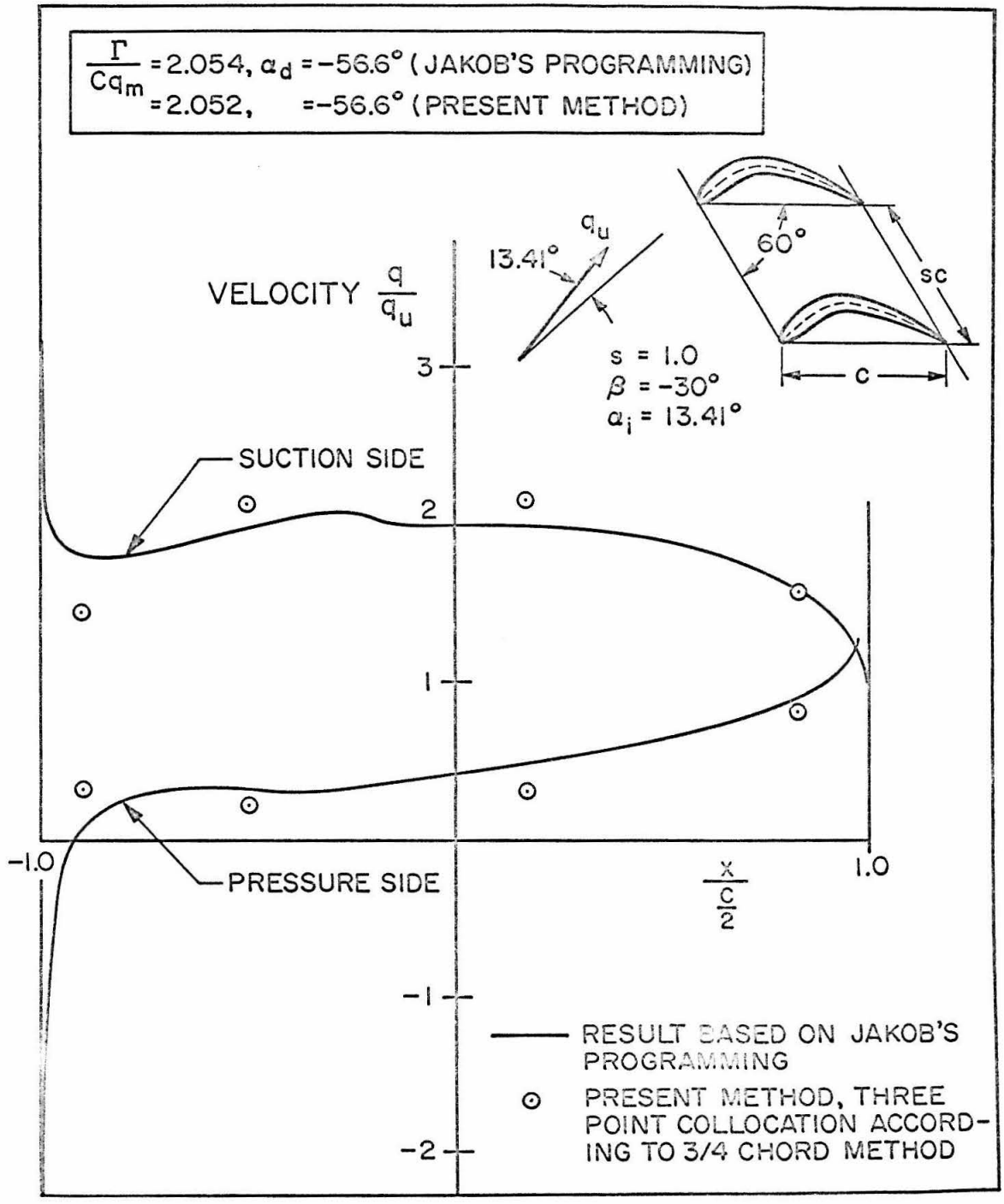

Figure 14. Velocity distribution for a cascade of 25 per cent camber airfoils.

harmonics in the vorticity distribution become important. To illustrate this point, the values of the a_n terms for the various cambers are listed in Table 1. From this table, it is observed that the magnitude of a_1 and a_2 increases as the camber of the airfoil becomes

TABLE 1.

	a_0	a_1	a_2
zero camber (Figure 5)	1.4932 tan α	-0.6422 tan α	0.0428 tan α
8 per cent camber (Figures 11 and 12)	1.6400 tan α -0.0585	-0.3170 tan α +0.6740	-0.0511 tan α -0.1595
25 per cent camber (Figure 14)	1.9496 tan α -0.0190	-0.0561 tan α +2.1523	0.1858 tan α -0.2501

larger, and much higher harmonics, which are ignored in the three-point collocation scheme, gain importance for the study of detailed velocity distribution. The accuracy of velocity distribution can be increased by increasing the number of control points, but for practical purposes, we would like to keep the number of collocation points as small as possible. The influence of the neglect of a_4 and higher order terms in three-point collocation would be felt most at the preceding term a_3 and less on the first and second terms a_0 , a_1 . Now the overall characteristics, such as circulation and exit angles, depend upon only the a_0 and a_1 terms, as shown in section 10, Part II. Thus, even if the higher harmonics are neglected in the vorticity distribution by the adoption of three-point collocation, we expect that the gross factors might be obtained more accurately. That this is indeed so can be seen from the values of circulation Γ and

exit angle α_2 in Figure 14. (The almost complete agreement of these values with the computer results is considered to be accidental.) Although these values are for one angle of attack only, it is seen in Figure 15 that the agreement continues for other incidence angles. Figure 16 shows the case of the same airfoil, but with the different spacing-chord ratio of 0.5. Here again, the present method can predict the exit angle with the range of one degree as compared to the computer results.

Judging from these results, it is concluded in this section that the present method, although it does not provide the local velocity distribution with good accuracy, does furnish the overall characteristic reasonably well.

7. Functional Relationship of the Exit Angle to Other Parameters for a Highly Cambered Cascade: Parabolic Airfoil with 25 Per Cent Camber.

In section 3 of this part, an example of the relation of the exit angle to other parameters was worked out for a slightly cambered cascade. In this section, let us obtain a similar formula applicable to a highly cascade. In this case, it is better to prescribe the factors expressing airfoil shape as numbers, instead of K_0 and K_1 as done in section 3, so as to get simplified formulas.

As an example, consider the parabolic airfoil cascade of solidity $s = 1.0$. Let the maximum camber be 25 per cent of chord; then the camber line equation becomes

$$\frac{y_0}{c} = -0.25\left[\left(\frac{\frac{x}{c}}{\frac{1}{2}}\right)^2 - 1\right]$$

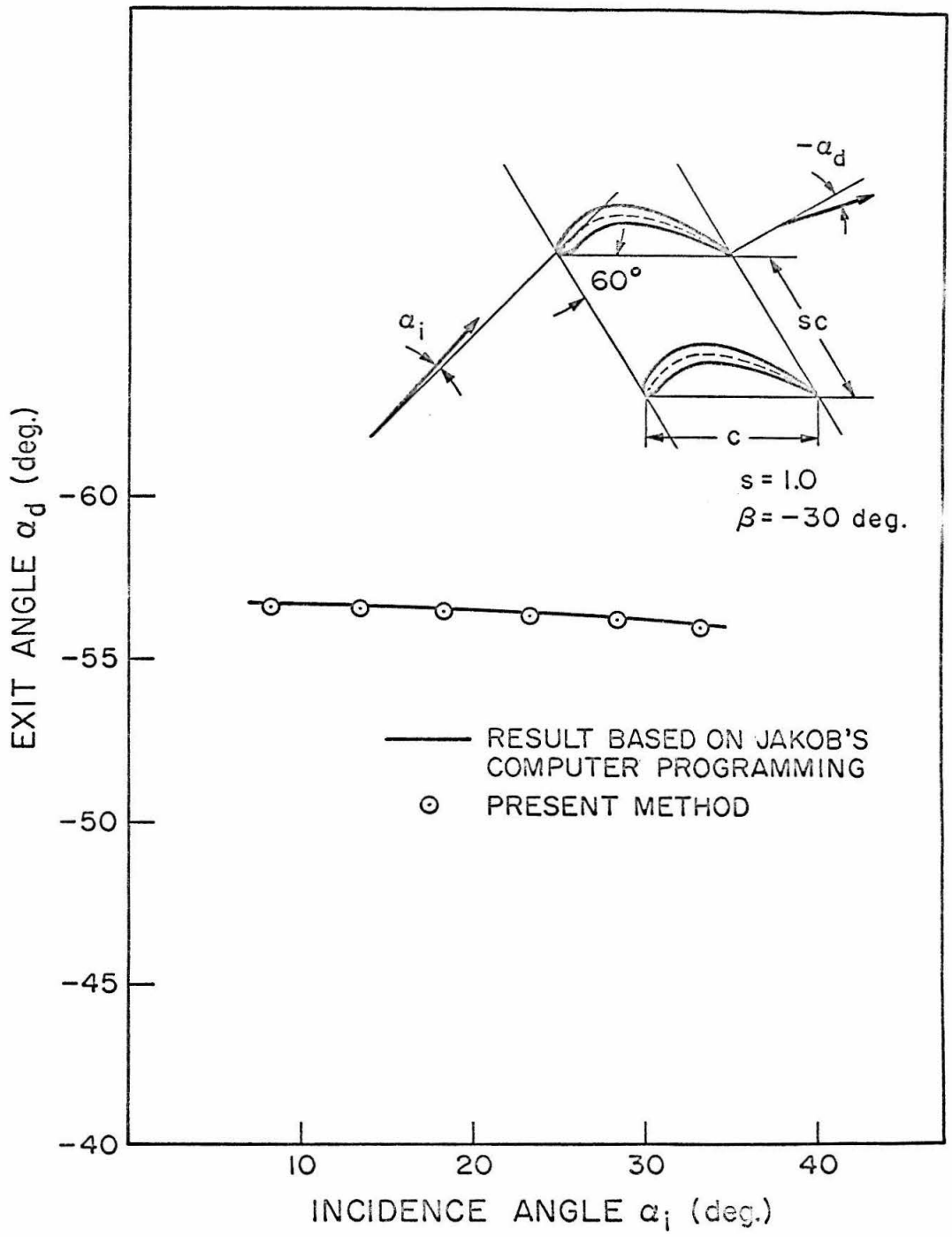

Figure 15. Exit angle versus incidence angle, S = 1.0.

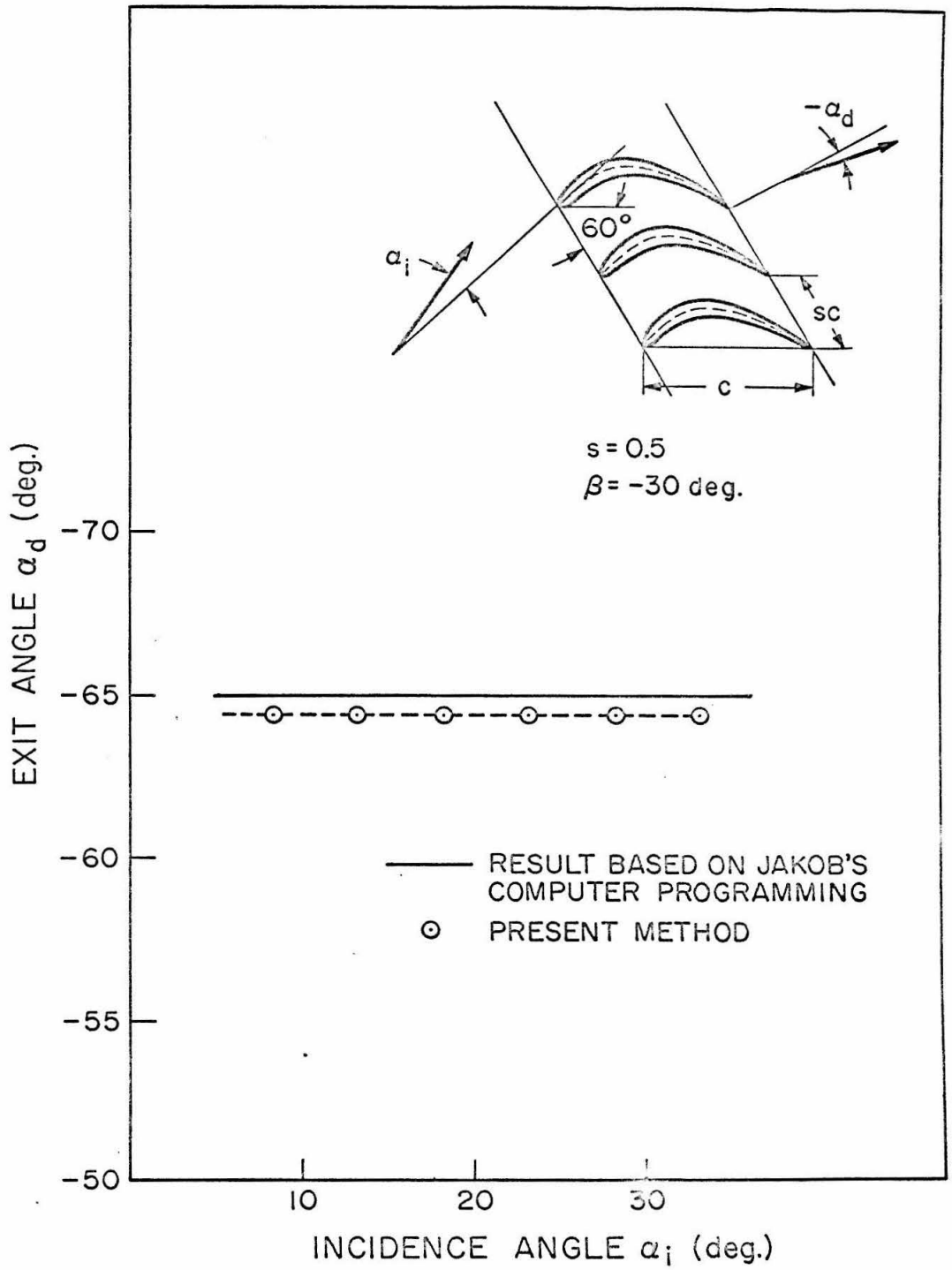

Figure 16. Exit angle versus incidence angle, S = 0.5.

Consider the zero thickness airfoil. Based upon the three-point collocation chosen according to the three-quarter method, the exit angle α_d can be expressed by the following formula:

$$\tan\alpha_d = \tan(\alpha+\beta) - \frac{\pi}{4}\sec(\alpha+\beta)\frac{1}{R_0(\beta)}\left[R_1(\beta)\cos\alpha + R_2(\beta)\sin\alpha\right]$$

where

$$R_n(\beta) \equiv C_0^{(n)} + \sum_{m=1}^{\infty} C_m^{(n)}\cdot\cos m\beta + \sum_{m=1}^{\infty} S_m^{(n)}\cdot\sin m\beta$$

The coefficients $C_m^{(n)}$, $S_m^{(n)}$, etc., are tabulated in Table 2. Thus, for a given solidity of $S = 1.0$, and given parabolic airfoil shape, this formula enables us to compute the exit angle α_d in terms of attack angle and stagger angle. Any other airfoil shape or solidity can be treated in a similar way.

TABLE 2.

$C_m^{(n)}$ and $S_m^{(n)}$ for a Parabolic Cascade of 0.25 Per Cent Camber, Solidity = 1.0.

$C_0^{(0)} = -1.1395698$	$C_0^{(1)} = -0.7098496$	$C_0^{(2)} = -3.6833350$
$C_1^{(0)} = -0.9620596$	$C_1^{(1)} = -0.0636729$	$C_1^{(2)} = 1.4659480$
$C_2^{(0)} = -0.4429371$	$C_2^{(1)} = -0.2155733$	$C_2^{(2)} = -1.0608070$
$C_3^{(0)} = -0.1602979$	$C_3^{(1)} = -0.0009919$	$C_3^{(2)} = 0.0779449$
$C_4^{(0)} = -0.0328556$	$C_4^{(1)} = -0.0082174$	$C_4^{(2)} = -0.0355160$
$C_5^{(0)} = -0.0064075$	$C_5^{(1)} = 0.0$	$C_5^{(2)} = 0.0$
$C_6^{(0)} = -0.0010934$	$C_6^{(1)} = 0.0$	$C_6^{(2)} = 0.0$
$S_1^{(0)} = -0.2327600$	$S_1^{(1)} = -0.0540893$	$S_1^{(2)} = 0.3774247$
$S_2^{(0)} = -0.0719335$	$S_2^{(1)} = 0.0870694$	$S_2^{(2)} = -0.0089040$
$S_3^{(0)} = -0.0250258$	$S_3^{(1)} = -0.0099241$	$S_3^{(2)} = 0.0107248$
$S_4^{(0)} = -0.0117860$	$S_4^{(1)} = 0.0069052$	$S_4^{(2)} = -0.0030035$

TABLE 2 (cont'd.)

$S_5^{(0)} = -0.0010946$	$S_5^{(1)} = 0.0$	$S_5^{(2)} = 0.0$
$S_6^{(0)} = -0.0003375$	$S_6^{(1)} = 0.0$	$S_6^{(2)} = 0.0$

8. A Remark on the Limiting Case of a High Solidity Cascade: the Basis for Channel Theory.

In section 2 of this part, the limiting case of the low solidity cascade, i.e., high spacing-chord ratio, was discussed. It was found there that the present method reduces to the familiar thin airfoil theory for the isolated airfoil. Also, in section 4, a perturbation to this limiting case is described.

It is of interest to investigate the other limiting case of high solidity, i.e., the closely spaced cascade, by applying the present method. It is noted that the present section is different from the preceding ones in the respect that no restriction will be imposed on the magnitude of camber.

Let the spacing-chord ratio be small, say, $s \ll 1$, and consider again the airfoil with zero thickness. The flow tangency condition becomes

$$\sum_{n=1}^{\infty} a_n (g_n - \gamma_0' f_n) = \gamma_0' - \tan\alpha \qquad (3.14)$$

In the case of closely spaced airfoils, the flow exit angle is expected to be almost parallel to the slope at the trailing edge. Hence, let us satisfy (3.14) at the trailing edge and see what conclusion we can draw from this, i.e.,

$$\sum_{n=1}^{\infty} a_n \left(g_n\Big|_{\frac{x}{c/2}=1} - y_o' f_n\Big|_{\frac{x}{c/2}=1} \right) = y_o'\Big|_{\frac{x}{c/2}=1} - \tan\alpha \qquad (3.15)$$

Now for closely spaced airfoils, the range of inner expansion is small, and particularly at the trailing edge the right side of the inner expansion is zero, i.e.,

$$\delta_1 = 0 \qquad (3.16)$$

while from section 7, Part II, the left side of the range is given by

$$\begin{aligned} 1 - 1\cdot 0440 S &= \cos\delta_2 \\ &= 1 - \frac{\delta_2^2}{2!} + \frac{\delta_2^4}{4!} - \cdots \\ \delta_2 &= \sqrt{2\cdot 0880 S}\,(1 + O(S)) \end{aligned} \qquad (3.17)$$

Using (3.16) and (3.17), the A_{nm}'s which appear in g_n and f_n are found to be as follows:

$$\begin{aligned} A_{n1} &= O(\delta_2) = O(S^{\frac{1}{2}}), \\ A_{n2} &= O(\delta_2^3) = O(S^{\frac{3}{2}}), \\ A_{nm} &= O(\delta_2^5) = O(S^{\frac{5}{2}}) \qquad n \geq 3 \end{aligned}$$

For example, from Appendix 2,

$$A_{o1}\Big|_{\theta=o} = \left[\delta_1 + \delta_2 - \frac{1-\cos\theta}{\sin\theta} \log \left| \frac{\sin(\theta + \frac{1}{2}\delta_2)\sin\frac{1}{2}\delta_1}{\sin(\theta - \frac{1}{2}\delta_1)\sin\frac{1}{2}\delta_2} \right| \right]_{\theta=o} - \delta_2$$

$$A_{o2}\Big|_{\theta=o} = \left[(\delta_1 + \delta_2) - (\sin(\theta + \delta_2) - \sin(\theta - \delta_1)) \right]_{\theta=o} = \delta_2 - \sin\delta_2 = \frac{\delta_2^3}{3!} + \cdots$$

$$A_{03}\Big|_{\theta=0} = \Big[(\delta_1+\delta_2)\Big(\cos\theta+\frac{1}{2}\Big) - \big(\sin(\theta+\delta_2)-\sin(\theta-\delta_1)\big)\big(1+\cos\theta\big) + \frac{1}{4}\big(\sin 2(\theta+\delta_2)-\sin 2(\theta-\delta_1)\big)\Big]_{\theta=0}$$

$$= \frac{3}{2}\delta_2 - 2\sin\delta_2 + \frac{1}{4}\sin 2\delta_2$$

$$= \frac{3}{2}\delta_2 - 2\Big[\delta_2 - \frac{\delta_2^3}{3!} + \frac{\delta_2^5}{5!} + \cdots\Big] + \frac{1}{4}\Big[2\delta_2 - \frac{(2\delta_2)^3}{3!} + \frac{(2\delta_2)^5}{5!} - \cdots\Big]$$

$$= \frac{6}{5!}\delta_2^5$$

Also

$$B_0 = \pi + O(S^{\frac{3}{2}}),\quad B_1 = \frac{\pi}{2} + O(S^{\frac{3}{2}}),\quad B_n = O(S^{\frac{3}{2}})\ (n \geq 2)$$

Substituting these into expressions for q_n and f_n, obtained in section 7, Part II, equation (3.15) can be written explicitly as

$$a_0\Big\{\underbrace{\frac{1}{2\pi}\Big[-A_{01}+O(S^{\frac{3}{2}})\Big]}_{O(\sqrt{S})} - \underbrace{\frac{\pi}{6(SC)^2}\Big[(\cos 2\beta - 2y_0'\sin 2\beta - y_0'^2\cos 2\beta)\Big(\frac{C}{2}\Big)^2 A_{03}+\cdots\Big]}_{O(\sqrt{S})} - \underbrace{\frac{1}{2SC}\Big(\frac{C}{2}\Big)(\cos\beta - y_0'\sin\beta)\Big(\underline{\underline{\pi}}+O(S^{\frac{3}{2}})\Big)}_{O(\frac{1}{S})}\Big\}$$

$$+ a_1\Big\{\underbrace{\frac{1}{2\pi}\Big[-A_{11}+O(S^{\frac{3}{2}})\Big]}_{O(\sqrt{S})} - \underbrace{\frac{\pi}{6(SC)^2}\Big[(\cos 2\beta - 2y_0'\sin 2\beta - y_0'^2\cos 2\beta)\Big(\frac{C}{2}\Big)^2 A_{13}+\cdots\Big]}_{O(\sqrt{S})} - \underbrace{\frac{1}{2SC}\Big(\frac{C}{2}\Big)(\cos\beta - y_0'\sin\beta)\Big(\underline{\underline{\frac{\pi}{2}}}+O(S^{\frac{3}{2}})\Big)}_{O(\frac{1}{S})}\Big\}$$

$$+ \sum_{n=2}^{\infty} a_n\Big\{\underbrace{\frac{1}{2\pi}\Big[-A_{n1}+O(S^{\frac{3}{2}})\Big]}_{O(\sqrt{S})} - \underbrace{\frac{\pi}{6(SC)^2}\Big[(\cos 2\beta - 2y_0'\sin 2\beta - y_0'^2\cos 2\beta)\Big(\frac{C}{2}\Big)^2 A_{n3}+\cdots\Big]}_{O(\sqrt{S})} - \underbrace{\frac{1}{2SC}\Big(\frac{C}{2}\Big)(\cos\beta - y_0'\sin\beta)B_n}_{O(\sqrt{S})}\Big\} = y_0' - \tan\alpha,$$

$$y_0' \equiv y_0'\Big|_{\frac{X}{\frac{C}{2}}=1}$$

(3.18)

The leading terms in the above equation are those underlined, and the other terms in the bracket { } are all of the order of $\sqrt{s}$. Originally, the underlined terms came from the outer expansion integral, which is predominant in the closely spaced cascade, while the inner expansion integrals are of the lower order of $\sqrt{s}$, reflecting the narrow range of the inner expansion. Neglecting the terms of the order of $\sqrt{s}$, (3.18) becomes

$$-\frac{\pi}{2sc}\left(\frac{c}{2}\right)\left(\cos\beta - y_o'\cdot\sin\beta\right)\left(a_o + \frac{1}{2}a_1\right) = y_o' - \tan\alpha \quad , \quad y_o' \equiv y_o'\Big|_{\frac{x}{\frac{c}{2}}=1}$$

From the expression of circulation given in section 10, Part II,

$$\frac{\Gamma}{2sc q_m} = \frac{-\cos\alpha\cdot y_o' + \sin\alpha}{\cos\beta - y_o'\cdot\sin\beta} \quad , \quad y_o' \equiv y_o'\Big|_{\frac{x}{\frac{c}{2}}=1}$$

and the expression for the exit angle becomes

$$\tan\alpha_d = \frac{\sin(\alpha+\beta) - \frac{\Gamma}{2sc q_m}}{\cos(\alpha+\beta)}$$

$$= \frac{\sin(\alpha+\beta) + \frac{y_o'\cdot\cos\beta - \sin\alpha}{\cos\beta - y_o'\cdot\sin\beta}}{\cos(\alpha+\beta)} \quad , \quad y_o' \equiv y_o'\Big|_{\frac{x}{\frac{c}{2}}=1}$$

Although this exit angle α_d appears to be dependent upon the attack angle α in this expression, it can be shown that actually it is independent of α in the following way:

$$\tan\alpha_d = \frac{\sin(\alpha+\beta)(\cos\beta - y_0'\cdot\sin\beta) + (y_0'\cdot\cos\alpha - \sin\alpha)}{\cos(\alpha+\beta)(\cos\beta - y_0'\cdot\sin\beta)}$$

$$= \frac{(\sin\alpha\cdot\cos^2\beta + \cos\alpha\cdot\sin\beta\cdot\cos\beta - \sin\alpha) + y_0'(-\sin\alpha\cdot\sin\beta\cdot\cos\beta - \cos\alpha\cdot\sin^2\beta + \cos\alpha)}{\cos(\alpha+\beta)(\cos\beta - y_0'\cdot\sin\beta)}$$

$$= \frac{(-\sin\alpha\cdot\sin^2\beta + \cos\alpha\cdot\sin\beta\cdot\cos\beta) + y_0'(-\sin\alpha\cdot\sin\beta\cdot\cos\beta + \cos\alpha\cdot\cos^2\beta)}{\cos(\alpha+\beta)(\cos\beta - y_0'\cdot\sin\beta)}$$

$$= \frac{\sin\beta(-\sin\alpha\cdot\sin\beta + \cos\alpha\cdot\cos\beta) + y_0'\cdot\cos\beta(-\sin\alpha\cdot\sin\beta + \cos\alpha\cdot\cos\beta)}{\cos(\alpha+\beta)(\cos\beta - y_0'\cdot\sin\beta)}$$

$$= \frac{\cancel{\cos(\alpha+\beta)}(\sin\beta + y_0'\cdot\cos\beta)}{\cancel{\cos(\alpha+\beta)}(\cos\beta - y_0'\cdot\cos\beta)}$$

$$= \frac{\sin\beta + y_0'\cdot\cos\beta}{\cos\beta - y_0'\cdot\sin\beta}$$

(3.19)

Thus, α_d is found to be independent of attack angle α. This relation has a very simple physical meaning. Rewriting (3.19) as

$$\tan\alpha_d = \frac{\tan\beta + y_0'}{1 - y_0'\cdot\tan\beta} = \frac{\tan\beta + \tan\theta}{1 - \tan\theta\cdot\tan\beta} = \tan(\beta+\theta),$$

$$\theta \cong \arctan y_0'\Big|_{\frac{x}{\frac{c}{2}}=1},$$

$$\therefore\ \alpha_d = \beta + \arctan y_0'\Big|_{\frac{x}{\frac{c}{2}}=1} \qquad (3.20)$$

Referring to the figure on the left, this relation means that the exit angle α_d is parallel to the slope at the trailing edge, or the deviation angle is zero, irrespective of the direction of the inlet flow.

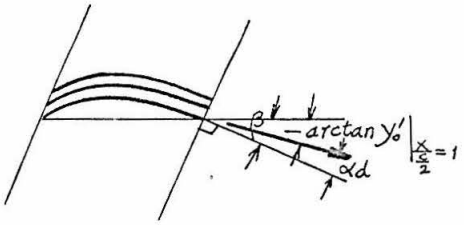

This is the basis of the channel flow theory for the closely spaced cascade (refs. 17 and 18). It is of interest to note that if we take the

effect of higher order terms in equation (3. 18), which is of the order of $\sqrt{s}$, the deviation angle would be found to be of the order of $\sqrt{s}$. This behavior is consistent with Constant's Rule (ref. 21), which was obtained from examination of cascade experiments.

REFERENCES

1. Robinson, A., and Laurmann, J. A., Wing Theory, Cambridge at the University Press (1956).

2. Garrick, I. E., "On the plane potential flow past a lattice of arbitrary airfoils," NACA Report No. 788 (1944).

3. Theodorsen, Th., "Theory of wing sections of arbitrary shape," NACA Report No. 411 (1932).

4. Schlichting, H., "Berechnung der reibungslosen inkompressiblen Strömung für ein vorgegebens ebens Schaufelgitter," VDI Forschungsheft, 477 (1955).

5. Mellor, G. L., "An analysis of axial compressor cascade performance. Part 1," ASME Paper No. 58-A-83 (1959).

6. Jakob, K. W., "Some programs for incompressible aerodynamic flow calculations," Technical Report No. 122, Computing Center, California Institute of Technology (1964).

7. Smith, A. M. O., and Pierce, J., "Exact solution of Neumann problem. Calculation of non-circulatory plane and axially symmetric flows about or within arbitrary boundaries," Douglas Aircraft Company Report No. ES 26988 (1958).

8. Giesing, J. P., "Extension of the Douglas Neumann program to problems of lifting, infinite cascade," Douglas Aircraft Company Report No. LB 31653 (1964).

9. Bromwich, T. J. I'A., An Introduction to the Theory of Infinite Series, MacMillan Company (1926).

10. Dwight, H. B., Tables of Integrals and Other Mathematical Data, MacMillan Company (1934).

11. Karman, Th. v., Aerodynamic Theory, Ed. by W. F. Durand, Springer Verlag (1934).

12. Allen, H., "General theory of airfoil sections having arbitrary shape or pressure distribution," NACA Report No. 833 (1945).

13. Birnbaum, W., "Die tragende Wirbelfläche als Hilfsmittel zur Behandlung des ebenen Problems der Tragflügeltheorie," Z. angew. Math. u. Mech. 3 (1923).

14. Glauert, H., Elements of Airfoil and Airscrew Theory, Cambridge University Press (1947).

15. Wieghardt, K., "Chordwise distribution of a simple rectangular wing," NACA TM No. 963 (1940).

16. Byrd, P. F., "Ergänzung zu dem Aufsatz von N. Scholtz, Beiträge zu Theorie der tragenden Fläche," Ing. Arc. 19 (1951).

17. Rannie, W. D., Jet Propulsion, Ed. H. S. Tsien, Air Technical Service Command (1946).

18. Bowen, J. T., Sabersky, R. H., and Rannie, W. D., "Theoretical and Experimental Investigation of Axial Flow Compressors," Mechanical Engineering Laboratory, California Institute of Technology (1949).

19. Klingemann, G., "Verfahren zur Bereschnung der Theoretischen Kennlinien von Turbomaschinen," Ing. Arch. 6 (1940).

20. Rannie, W. D., private communication.

21. Howell, A. R., "The present basis of axial flow compressor design, Part 1," Aero. Research Council, R and M. 2095 (1942).

APPENDIX 1.

The Relation Between the Strengths of Sources and Vortices and Induced Velocity Just Off the Camber Line in a Cascade.

In the following, it will be proved for the cascade that induced velocities just above and below the camber line are equal to one-half of the strengths of sources and vortices.

From (2. 17), the induced velocity at an arbitrary point z can be expressed as

$$u - iv = \frac{1}{2sc} e^{i\beta} \int_{-\frac{c}{2}}^{\frac{c}{2}} (m'(x_1) + i\gamma'(x_1)) \coth\left[\frac{\pi(z-z_1)}{sc} e^{i\beta}\right] dx_1$$

Divide the range of integration into three parts, i. e.,

$$u - iv = \frac{1}{2sc} e^{i\beta} \left[\int_{x-\delta}^{x+\delta} + \int_{x+\delta}^{\frac{c}{2}} + \int_{-\frac{c}{2}}^{x-\delta} \right] \qquad (I-1)$$

where δ is a constant.

Now $z - z_1$ can be written as

$$\begin{aligned} z - z_1 &= x - x_1 + i(y - y_0(x)) \\ &= x - x_1 + i(y_0(x) - y_0(x_1)) + i(y - y_0(x)) \end{aligned}$$

where y_0 denotes the position of camber line. Choose y in such a way as

$$y - y_0(x) = h = \text{constant},$$

and expanding $y_0(x)$ around x in a Taylor series, one obtains

$$z - z_1 = ih + (x - x_1) + iy_0'(x)(x - x_1) - \frac{1}{2} iy_0''(x)(x - x_1)^2 + \cdots$$

Changing the independent variable from x to ϵ defined by

$$x - x_1 = \epsilon h$$

then

$$z - z_1 = h\left[i + \epsilon(1 + i\gamma_0'(x)) - \frac{1}{2} i\gamma_0''(x)\epsilon^2 h + \cdots \right]$$

and

$$x_1 = x - \epsilon h \quad , \quad dx_1 = -h\, d\epsilon$$

Substituting these into the first integral in (I-1), we get

$$u(x) - i\vartheta(x) = \frac{-1}{2sc} e^{i\beta} \int_{\frac{\delta}{h}}^{-\frac{\delta}{h}} \left[m'(x-\epsilon h) + i\gamma'(x-\epsilon h) \right] \cdot \coth\left[\frac{\pi}{sc} h \left\{ i + \epsilon(1 + i\gamma_0'(x)) - \frac{1}{h} i\gamma_0'' \cdot \epsilon h^2 + \cdots \right\} e^{i\beta} \right] h\, d\epsilon$$
$$+ \frac{1}{2sc} e^{i\beta} \left[\int_{x+\delta}^{\frac{c}{2}} + \int_{-\frac{c}{2}}^{x-\delta} \left(m'(x_1) + i\gamma'(x_1) \right) \coth\left[\frac{\pi(z_0 - z_1 + ih)}{sc} e^{i\beta} \right] dx_1 \right.$$

for small h

$$u(x) - i\vartheta(x) = \frac{1}{2sc} e^{i\beta} \int_{\frac{\delta}{h}}^{-\frac{\delta}{h}} \left[m'(x-\epsilon h) + i\gamma'(x-\epsilon h) \right] \cdot (-h)$$
$$\times \left\{ \frac{\bar{e}^{i\beta}}{\frac{\pi}{sc} h \left[i + \epsilon(1 + i\gamma_0') - \frac{1}{2} i\gamma_0'' \epsilon^2 h + \cdots \right]} + \frac{1}{3} \frac{\pi}{sc} h \left[i + \epsilon(1 + i\gamma_0') + \cdots \right] \right\} d\epsilon$$
$$+ \frac{1}{2sc} e^{i\beta} \left[\int_{x+\delta}^{\frac{c}{2}} + \int_{-\frac{c}{2}}^{x-\delta} \left(m'(x_1) + i\gamma'(x_1) \right) \coth\left[\frac{\pi(z_0 - z_1 + ih)}{sc} e^{i\beta} \right] dx_1 \right.$$

Let $h \to +0$, keeping δ a positive constant

$$u_+(x) - i\vartheta_+(x) = \frac{1}{2\pi} \left[m'(x_1) + i\gamma'(x_1) \right] \int_{-\infty}^{\infty} \frac{d\epsilon}{i + \epsilon(1 + i\gamma_0')}$$
$$+ \frac{1}{2sc} e^{i\beta} \left[\int_{x+\delta}^{\frac{c}{2}} + \int_{\frac{c}{2}}^{x-\delta} \left(m'(x_1) + i\gamma'(x_1) \right) \coth\left[\frac{\pi(z_0 - z_1) e^{i\beta}}{sc} \right] dx_1 \right.$$

Next, let $\delta \to 0$

$$u_+(x) - i v_+(x) = \frac{1}{2\pi}\left[m'(x_1) + i\gamma'(x_1)\right]\int_{-\infty}^{\infty} \frac{d\epsilon}{i + \epsilon(1 + i y_0')}$$

$$+ \frac{1}{2sc} e^{i\beta} \int_{-\frac{c}{2}}^{\frac{c}{2}} \left(m'(x_1) + i\gamma'(x_1)\right) \cdot \coth\left[\frac{\pi(z_0 - z_1)}{sc} e^{i\beta}\right] dx_1$$

The second integral on the right hand side of this equation is identified as the induced velocity on the camber line, and from now on we drop this term with the understanding that the velocities are measured with this induced velocity as a base.

$$u_+(x) - i v_+(x) = \frac{1}{2\pi}\left[m'(x) + i\gamma'(x)\right]\int_{-\infty}^{\infty} \frac{d\epsilon}{i + \epsilon(1 + i y_0')}$$

$$= \frac{1}{2\pi}\left[m'(x) + i\gamma'(x)\right] \frac{1}{1 + i y_0'} \log\left[i + \epsilon(1 + i y_0')\right]\Big|_{\epsilon = -\infty}^{\epsilon = +\infty} \qquad \text{(I-2)}$$

using $\log(-1) = -\pi i$

$$u_+(x) - i v_+(x) = -\frac{i}{2} \frac{m'(x) + i\gamma'(x)}{1 + i y_0'} \qquad \text{(I-3)}$$

The choice of $-\pi i$ instead of πi in equation (I-2) comes from the reason that, by choosing a negative value, (I-3) can be reduced to the familiar expression $u_+(x) = \frac{1}{2}\gamma'(x)$, for the particular case $m'(x) = 0$ and $y_0' \equiv 0$. Writing (I-3) as

$$u_+(x) - i v_+(x) = -\frac{i}{2} \frac{\left[m'(x) + i\gamma'(x)\right](1 - i y_0')}{1 + y_0'^2}$$

$$= \frac{1}{2} \frac{-m'(x) y_0' + \gamma'(x)}{1 + y_0'^2} + \frac{1}{2} \frac{-m'(x) - \gamma'(x) y_0'}{1 + y_0'^2} i$$

$$\therefore\ u_+(x) = \frac{1}{2} \frac{\gamma'(x) - m'(x) y_0'}{1 + y_0'^2} = \frac{1}{2} \frac{\gamma(x) - m(x) y_0'}{\sqrt{1 + y_0'^2}}$$

$$v_+(x) = \frac{1}{2} \frac{m'(x) + \gamma'(x) y_0'}{1 + y_0'^2} = \frac{1}{2} \frac{m(x) + \gamma(x) y_0'}{\sqrt{1 + y_0'^2}}$$

In the above, changes from modified singularities to true singularities are made. Converting these expressions to the velocities tangential and normal to the camber line, we get

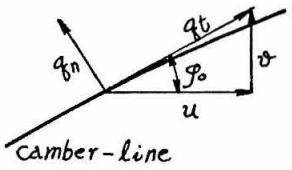

$$q_{t,+}(x) = u_+ \cdot \cos\varphi_0 + v_+ \cdot \sin\varphi_0$$
$$= \frac{\gamma(x) - m(x)\cdot y_0'}{2(1+y_0'^2)} + \frac{m(x)\cdot y_0' + \gamma(x)\cdot y_0'^2}{2(1+y_0'^2)} = \frac{1}{2}\gamma(x),$$

$$q_{n,+}(x) = -u_+ \cdot \sin\varphi_0 + v_+ \cdot \cos\varphi_0$$
$$= -\frac{\gamma(x)\cdot y_0' - m(x)\cdot y_0'^2}{2(1+y_0'^2)} + \frac{m(x) + \gamma(x)\cdot y_0'^2}{2(1+y_0'^2)} = \frac{1}{2}m(x)$$

Similarly,

$$q_{t,-}(x) = -\frac{1}{2}\gamma(x),$$
$$q_{n,-}(x) = -\frac{1}{2}m(x)$$

Thus

$$\gamma(x) = q_{t,+}(x) - q_{t,-}(x),$$
$$m(x) = q_{n,+}(x) - q_{n,-}(x)$$

APPENDIX 2.

Derivations of A_{nm} and B_n.

From (2.24) and (2.25), A_{nm} and B_n are defined as

$$\int_i \gamma'(x_1)(x - x_1)^{m-2} dx_1 = U_\infty \left(\frac{c}{2}\right)^{m-1} \sum_{n=0}^{\infty} a_n \cdot A_{nm} \qquad \text{(II-1)}$$

$$\int_0 \gamma'(x_1)\, dx_1 = U_\infty \left(\frac{c}{2}\right) \sum_{n=0}^{\infty} a_n \cdot B_n \qquad \text{(II-2)}$$

Substitute the following expression

$$\gamma'(x_1) = U_\infty \left(a_0 \tan\frac{\phi}{2} + \sum_{n=1}^{\infty} a_n \sin n\phi \right)$$

into the above equation (II-1) and express the range of integration explicitly as

$$\int_{\theta-\delta_1}^{\theta+\delta_2} \left(a_0 \tan\frac{\phi}{2} + \sum_{n=1}^{\infty} a_n \sin n\phi \right)(\cos\theta - \cos\phi)^{m-2} \cdot \sin\phi \cdot d\phi = \sum_{n=0}^{\infty} a_n \cdot A_{nm}$$

Equating the coefficients of a_n, one obtains

$$A_{0m} = \int_{\theta-\delta_1}^{\theta+\delta_2} (1 - \cos\phi)(\cos\theta - \cos\phi)^{m-2} d\phi \qquad \text{(II-3)}$$

$$A_{nm} = \frac{1}{2} \int_{\theta-\delta_1}^{\theta+\delta_2} \left[\cos(n-1)\phi - \cos(n+1)\phi \right](\cos\theta - \cos\phi)^{m-2} d\phi \qquad \text{(II-4)}$$
$$n \geq 1$$

Similarly, from (II-2),

$$B_0 = \int_{\theta+\delta_2}^{\pi} (1 - \cos\phi)\, d\phi + \int_0^{\theta-\delta_1} \qquad \text{(II-5)}$$

$$B_n = \frac{1}{2}\left\{\int_{\theta+\delta_2}^{\pi}\left[\cos(n-1)\phi - \cos(n+1)\phi\right]d\phi + \int_{0}^{\theta-\delta_1}\right\}, \quad n \geq 1 \qquad \text{(II-6)}$$

First, the A_{nm} are obtained, and then the B_n are derived.

I. A_{nm}

(1) $m = 1$; A_{n1}

$$A_{01} = \int_{\theta-\delta_1}^{\theta+\delta_2} \frac{1-\cos\phi}{\cos\theta - \cos\phi}\cdot d\phi$$

$$A_{n1} = \frac{1}{2}\int_{\theta-\delta_1}^{\theta+\delta_2} \frac{\cos(n-1)\phi - \cos(n+1)\phi}{\cos\theta - \cos\phi}\cdot d\phi \quad , \quad n \geq 1$$

These integrals can be obtained once we evaluate $\int_{\theta-\delta_1}^{\theta+\delta_2} \frac{\cos n\phi}{\cos\phi - \cos\theta}\,d\phi \equiv I_n$.

$$I_0 = \int_{\theta-\delta_1}^{\theta+\delta_2} \frac{1}{\cos\phi - \cos\theta}d\phi = \left[\frac{1}{\sin\theta}\log\left|\frac{\sin\frac{1}{2}(\theta+\phi)}{\sin\frac{1}{2}(\theta-\phi)}\right|\right]_{\theta-\delta_1}^{\theta+\delta_2}$$

$$= \lim_{\epsilon\to 0}\left\{\frac{1}{\sin\theta}\left[\log\left|\frac{\sin\frac{1}{2}(\theta+\phi)}{\sin\frac{1}{2}(\theta-\phi)}\right|\right]_{\phi=\theta+\epsilon}^{\phi=\theta+\delta_2} + \frac{1}{\sin\theta}\left[\log\left|\frac{\sin\frac{1}{2}(\theta+\phi)}{\sin\frac{1}{2}(\theta-\phi)}\right|\right]_{\phi=\theta-\delta_1}^{\phi=\theta-\epsilon}\right\}$$

$$= \lim_{\epsilon\to 0}\left\{\frac{1}{\sin\theta}\log\left|\frac{\sin(\theta+\frac{1}{2}\delta_2)\cdot\sin\frac{1}{2}\delta_1}{\sin(\theta-\frac{1}{2}\delta_1)\cdot\sin\frac{1}{2}\delta_2}\right| + \frac{1}{\sin\theta}\log\left|\frac{\sin(\theta-\frac{1}{2}\epsilon)}{\sin(\theta+\frac{1}{2}\epsilon)}\right|\right\}$$

$$= \frac{1}{\sin\theta}\log\left|\frac{\sin(\theta+\frac{1}{2}\delta_2)\cdot\sin\frac{1}{2}\delta_1}{\sin(\theta-\frac{1}{2}\delta_1)\cdot\sin\frac{1}{2}\delta_2}\right|$$

$$I_1 = \int_{\theta-\delta_1}^{\theta+\delta_2} \frac{\cos\phi \cdot d\phi}{\cos\phi - \cos\theta} = \Big[\phi\Big]_{\theta-\delta_1}^{\theta+\delta_2} + \cos\theta \cdot I_0$$

$$= (\delta_1 + \delta_2) + \frac{\cos\theta}{\sin\theta} \cdot \log\left| \frac{\sin(\theta + \frac{1}{2}\delta_2)\cdot \sin\frac{1}{2}\delta_1}{\sin(\theta - \frac{1}{2}\delta_1)\cdot \sin\frac{1}{2}\delta_2} \right|$$

As particular cases, let $\delta_2 = \pi - \theta$ and $\delta_1 = \theta$ in I_0 and I_1 ; then $I_0 = 0$ and $I_1 = \pi$, and these are well-known Glauert integrals (ref. 14). In general,

$$I_{n+1} + I_{n-1} = \int \frac{\cos(n+1)\phi + \cos(n-1)\phi}{\cos\phi - \cos\theta} d\phi = \frac{2}{n} \sin n\phi \Big|_{\theta-\delta_1}^{\theta+\delta_2} + 2\cos\theta \cdot I_n$$

$$= \frac{2}{n}\Big[\sin n(\theta+\delta_2) - \sin n(\theta-\delta_1) \Big] + 2\cos\theta \cdot I_n$$

and from this recurrence formula, I_n for arbitrary n can be obtained. The A_{n1} 's can be written as

$$A_{01} = I_1 - I_0 ,$$

$$A_{n1} = \frac{1}{2}\left(I_{n+1} - I_{n-1} \right) \qquad n \geq 1$$

The final expressions for the A_{n1} are as follows:

$$A_{01} = (\delta_1 + \delta_2) - \frac{1-\cos\theta}{\sin\theta} \cdot \log\left| \frac{\sin(\theta + \frac{1}{2}\delta_2)\sin\frac{1}{2}\delta_1}{\sin(\theta - \frac{1}{2}\delta_1)\sin\frac{1}{2}\delta_2} \right| ,$$

$$A_{11} = \frac{1}{2}\left(I_2 - I_0 \right)$$

$$= (\delta_1 + \delta_2)\cdot\cos\theta + \Big[\sin(\theta+\delta_2) - \sin(\theta-\delta_1) \Big]$$

$$- \frac{1}{\sin\theta}\Big[1 - \cos\theta \cdot \cos\theta \Big] \log\left| \frac{\sin(\theta + \frac{1}{2}\delta_2)\sin\frac{1}{2}\delta_1}{\sin(\theta - \frac{1}{2}\delta_1)\sin\frac{1}{2}\delta_2} \right|$$

$$A_{21} = \frac{1}{2}(I_3 - I_1)$$

$$= (\delta_1+\delta_2)\cos 2\theta + 2\cos\theta\cdot\left[\sin(\theta+\delta_2) - \sin(\theta-\delta_1)\right]$$

$$+ \frac{1}{2}\cdot\left[\sin 2(\theta+\delta_2) - \sin 2(\theta-\delta_1)\right]$$

$$- \frac{1}{\sin\theta}\left[\cos\theta - \cos\theta\cdot\cos 2\theta\right]\cdot \log\left|\frac{\sin(\theta+\frac{1}{2}\delta_2)\cdot\sin\frac{1}{2}\delta_1}{\sin(\theta-\frac{1}{2}\delta_1)\cdot\sin\frac{1}{2}\delta_2}\right|$$

$$A_{31} = \frac{1}{2}(I_4 - I_2)$$

$$= (\delta_1+\delta_2)\cos 3\theta + 2\cos 2\theta\cdot\left[\sin(\theta+\delta_2) - \sin(\theta-\delta_1)\right]$$

$$+ \cos\theta\cdot\left[\sin 2(\theta+\delta_2) - \sin 2(\theta-\delta_1)\right] + \frac{1}{3}\left[\sin 3(\theta+\delta_2) - \sin 3(\theta-\delta_1)\right]$$

$$- \frac{1}{\sin\theta}\left[\cos 2\theta - \cos\theta\cdot\cos 3\theta\right]\cdot \log\left|\frac{\sin(\theta+\frac{1}{2}\delta_2)\cdot\sin\frac{1}{2}\delta_1}{\sin(\theta-\frac{1}{2}\delta_1)\cdot\sin\frac{1}{2}\delta_2}\right|$$

- - - - - - - -

$$A_{n1} = \frac{1}{2}(I_{n+1} - I_{n-1})$$

$$= (\delta_1+\delta_2)\cos n\theta + 2\cos(n-1)\theta\cdot\left[\sin(\theta+\delta_2) - \sin(\theta-\delta_1)\right]$$

$$+ \frac{2}{2}\cos(n-2)\theta\cdot\left[\sin 2(\theta+\delta_2) - \sin 2(\theta-\delta_1)\right]$$

$$+ \frac{2}{3}\cos(n-3)\theta\left[\sin 3(\theta+\delta_2) - \sin 3(\theta-\delta_1)\right]$$

$$+ \text{- - - - - -}$$

$$+ \frac{2}{n-1}\cos\theta\left[\sin(n-1)(\theta+\delta_2) - \sin(n-1)(\theta-\delta_1)\right]$$

$$+ \frac{1}{n}\left[\sin n(\theta+\delta_2) - \sin n(\theta-\delta_1)\right]$$

$$- \frac{1}{\sin\theta}\left[\cos(n-1)\theta - \cos\theta\cdot\cos n\theta\right]\cdot \log\left|\frac{\sin(\theta+\frac{1}{2}\delta_2)\sin\frac{1}{2}\delta_1}{\sin(\theta-\frac{1}{2}\delta_1)\sin\frac{1}{2}\delta_2}\right| \qquad n \geq 1$$

$m \geq 2$; A_{nm}

Integrals (II-3) and (II-4) can be obtained once J_m's and $K_{n,m}$'s defined by

$$J_m \equiv \int_{\theta-\delta_1}^{\theta+\delta_2} (1-\cos\phi)\cos^{m-2}\phi \cdot d\phi \quad , \quad K_{n,m} \equiv \frac{1}{2}\int_{\theta-\delta_1}^{\theta+\delta_2} \left[\cos(n-1)\phi - \cos(n+1)\phi\right]\cos^{m-2}\phi \, d\phi$$

are integrated.

$$m=2; \quad J_2 = \int_{\theta-\delta_1}^{\theta+\delta_2} (1-\cos\phi)\,d\phi = (\delta_1+\delta_2) - \left[\sin(\theta+\delta_2) - \sin(\theta-\delta_1)\right],$$

$$K_{n,2} = \frac{1}{2}\int_{\theta-\delta_1}^{\theta+\delta_2} \left[\cos(n-1)\phi - \cos(n+1)\phi\right] d\phi$$

$$= \begin{cases} \frac{1}{2}(\delta_1+\delta_2) - \frac{1}{4}\left[\sin 2(\theta+\delta_2) - \sin 2(\theta-\delta_1)\right], & n=1 \\ \frac{1}{2}\,\dfrac{\sin(n-1)(\theta+\delta_2) - \sin(n-1)(\theta-\delta_1)}{n-1} & \\ -\frac{1}{2}\,\dfrac{\sin(n+1)(\theta+\delta_2) - \sin(n+1)(\theta-\delta_1)}{n+1} & , \; n \neq 1 \end{cases}$$

$$m=3; \quad J_3 = \int_{\theta-\delta_1}^{\theta+\delta_2} (1-\cos\phi)\cos\phi \cdot d\phi$$

$$= -\frac{1}{2}(\delta_1+\delta_2) + \left[\sin(\theta+\delta_2) - \sin(\theta-\delta_1)\right] - \frac{1}{4}\left[\sin 2(\theta+\delta_2) - \sin 2(\theta-\delta_1)\right]$$

$$K_{n,3} = \frac{1}{2}\int_{\theta-\delta_1}^{\theta+\delta_2} \left[\cos(n-1)\phi - \cos(n+1)\phi\right]\cos\phi \, d\phi$$

$$= \begin{cases} \frac{1}{4}\,\dfrac{\sin(n-2)(\theta+\delta_2) - \sin(n-2)(\theta-\delta_1)}{n-2} & \\ -\frac{1}{4}\,\dfrac{\sin(n+2)(\theta+\delta_2) - \sin(n+2)(\theta-\delta_1)}{n+2} & , \; n \neq 2 \end{cases}$$

$$= \begin{cases} \frac{1}{4}(\delta_1+\delta_2) - \frac{1}{16}\left[\sin 4(\theta+\delta_2) - \sin 4(\theta-\delta_1)\right] & , \; n=2 \end{cases}$$

$m = 4$;

$$J_4 = \int_{\theta-\delta_1}^{\theta+\delta_2} (1-\cos\phi)\cos^2\phi\, d\phi$$

$$= \frac{1}{2}(\delta_1+\delta_2) - \frac{3}{4}\left[\sin(\theta+\delta_2) - \sin(\theta-\delta_1)\right]$$

$$+ \frac{1}{4}\left[\sin 2(\theta+\delta_2) - \sin 2(\theta-\delta_1)\right] - \frac{1}{12}\left[\sin 3(\theta+\delta_2) - \sin 3(\theta-\delta_1)\right]$$

$$K_{n,4} = \frac{1}{2}\int_{\theta-\delta_1}^{\theta+\delta_2} \left[\cos(n-1)\phi - \cos(n+1)\phi\right]\cos^2\phi\, d\phi$$

$$= \begin{cases} \frac{1}{8}\,\frac{\sin(n-3)(\theta+\delta_2) - \sin(n-3)(\theta-\delta_1)}{n-3} \\ + \frac{1}{8}\,\frac{\sin(n-1)(\theta+\delta_2) - \sin(n-1)(\theta-\delta_1)}{n-1} \\ - \frac{1}{8}\,\frac{\sin(n+1)(\theta+\delta_2) - \sin(n+1)(\theta-\delta_1)}{n+1} \\ - \frac{1}{8}\,\frac{\sin(n+3)(\theta+\delta_2) - \sin(n+3)(\theta-\delta_1)}{n+3} & , n \neq 1, 3, \\ \frac{1}{8}(\delta_1+\delta_2) - \frac{1}{32}\left[\sin 4(\theta+\delta_2) - \sin 4(\theta-\delta_1)\right] & , n = 1, \\ \frac{1}{8}(\delta_1+\delta_2) + \frac{1}{16}\left[\sin 2(\theta+\delta_2) - \sin 2(\theta-\delta_1)\right] \\ - \frac{1}{32}\left[\sin 4(\theta+\delta_2) - \sin 4(\theta-\delta_1)\right] \\ - \frac{1}{48}\left[\sin 6(\theta+\delta_2) - \sin 6(\theta-\delta_1)\right] & , n = 3 \end{cases}$$

$m=5;\quad J_5 = \int_{\theta-\delta_1}^{\theta+\delta_2} (1-\cos\phi)\cos^3\phi\, d\phi$

$$= -\frac{3}{8}(\delta_1+\delta_2) + \frac{3}{4}\left[\sin(\theta+\delta_2)-\sin(\theta-\delta_1)\right] - \frac{1}{4}\left[\sin 2(\theta+\delta_2)-\sin 2(\theta-\delta_1)\right]$$
$$+ \frac{1}{12}\left[\sin 3(\theta+\delta_2)-\sin 3(\theta-\delta_1)\right] - \frac{1}{32}\left[\sin 4(\theta+\delta_2)-\sin 4(\theta-\delta_1)\right]$$

$$K_{n,5} = \frac{1}{2}\int_{\theta-\delta_1}^{\theta+\delta_2} \left[\cos(n-1)\phi - \cos(n+1)\phi\right]\cdot\cos^3\phi\, d\phi$$

$$= \begin{cases} \frac{1}{16}\frac{\sin(n-4)(\theta+\delta_2)-\sin(n-4)(\theta-\delta_1)}{n-4} \\ +\frac{1}{8}\frac{\sin(n-2)(\theta+\delta_2)-\sin(n-2)(\theta-\delta_1)}{n-2} \\ -\frac{1}{8}\frac{\sin(n+2)(\theta+\delta_2)-\sin(n+2)(\theta-\delta_1)}{n+2} \\ -\frac{1}{16}\frac{\sin(n+4)(\theta+\delta_2)-\sin(n+4)(\theta-\delta_1)}{n+4} & , n\neq 2,4 \\ \frac{1}{8}(\delta_1+\delta_2)+\frac{1}{32}\left[\sin 2(\theta+\delta_2)-\sin 2(\theta-\delta_1)\right] \\ -\frac{1}{32}\left[\sin 4(\theta+\delta_2)-\sin 4(\theta-\delta_1)\right] \\ -\frac{1}{96}\left[\sin 6(\theta+\delta_2)-\sin 6(\theta-\delta_1)\right] & , n=2 \\ \frac{1}{16}(\delta_1+\delta_2)+\frac{1}{16}\left[\sin 2(\theta+\delta_2)-\sin 2(\theta-\delta_1)\right] \\ -\frac{1}{48}\left[\sin 6(\theta+\delta_2)-\sin 6(\theta-\delta_1)\right] \\ -\frac{1}{128}\left[\sin 8(\theta+\delta_2)-\sin 8(\theta-\delta_1)\right] & , n=4 \end{cases}$$

Using these, the A_{nm}'s are obtained easily in the following way.

(2) $m = 2$; A_{n2}

$$A_{02} = \int_{\theta-\delta_1}^{\theta+\delta_2} (1-\cos\phi)\,d\phi = J_2 = (\delta_1+\delta_2) - \left[\sin(\theta+\delta_2) - \sin(\theta-\delta_1)\right]$$

$$A_{n2} = \frac{1}{2}\int_{\theta-\delta_1}^{\theta+\delta_2} \left[\cos(n-1)\phi - \cos(n+1)\phi\right] d\phi = K_{n,2}$$

$$= \begin{cases} \frac{1}{2}(\delta_1+\delta_2) - \frac{1}{4}\left[\sin 2(\theta+\delta_2) - \sin 2(\theta-\delta_1)\right] & , \ n=1 \\ \frac{1}{2}\,\frac{\sin(n-1)(\theta+\delta_2) - \sin(n-1)(\theta-\delta_1)}{n-1} & \\ -\frac{1}{2}\,\frac{\sin(n+1)(\theta+\delta_2) - \sin(n-1)(\theta-\delta_1)}{n+1} & , \ n\neq 1 \end{cases}$$

(3) $m = 3$; A_{n3}

$$A_{03} = \int_{\theta-\delta_1}^{\theta+\delta_2} (1-\cos\phi)(\cos\theta-\cos\phi)\,d\phi = \cos\theta\cdot J_2 - J_3$$

$$= (\delta_1+\delta_2)\left(\cos\theta+\frac{1}{2}\right) - \left[\sin(\theta+\delta_2) - \sin(\theta-\delta_1)\right](1+\cos\theta) + \frac{1}{4}\left[\sin 2(\theta+\delta_2) - \sin 2(\theta-\delta_1)\right]$$

$$A_{n3} = \frac{1}{2}\int_{\theta-\delta_1}^{\theta+\delta_2} \left[\cos(n-1)\phi - \cos(n+1)\phi\right](\cos\theta-\cos\phi)\,d\phi = \cos\theta\cdot K_{n,2} - K_{n,3}$$

$$= \begin{cases} (\delta_1+\delta_2)\frac{\cos\theta}{2} - \frac{1}{4}\left[\sin(\theta+\delta_2) - \sin(\theta-\delta_1)\right] - \frac{1}{4}\left[\sin 2(\theta+\delta_2) - \sin 2(\theta-\delta_1)\right]\cdot\cos\theta & \\ \quad + \frac{1}{12}\left[\sin 3(\theta+\delta_2) - \sin 3(\theta-\delta_1)\right] & , \ n=1, \\ -\frac{1}{4}(\delta_1+\delta_2) + \frac{1}{12}\left[\sin(\theta+\delta_2) - \sin(\theta-\delta_1)\right]\cos\theta & \\ -\frac{1}{6}\left[\sin 3(\theta+\delta_2) - \sin 3(\theta-\delta_1)\right]\cos\theta + \frac{1}{16}\left[\sin 4(\theta+\delta_2) - \sin 4(\theta-\delta_1)\right] & , \ n=2 \\ -\frac{1}{4}\,\frac{\sin(n-2)(\theta+\delta_2) - \sin(n-2)(\theta-\delta_1)}{n-2} & \\ +\frac{1}{2}\,\frac{\sin(n-1)(\theta+\delta_2) - \sin(n-1)(\theta-\delta_1)}{n-1}\cdot\cos\theta & \\ -\frac{1}{2}\,\frac{\sin(n+1)(\theta+\delta_2) - \sin(n+1)(\theta-\delta_1)}{n+1}\cdot\cos\theta & \\ +\frac{1}{4}\,\frac{\sin(n+1)(\theta+\delta_2) - \sin(n+2)(\theta-\delta_1)}{n+2} & , \ n+1, 2 \end{cases}$$

(4) $\underline{m=4\ ;\ A_{n4}}$

$$A_{04} = \int_{\theta-\delta_1}^{\theta+\delta_2} (1-\cos\phi)(\cos\theta-\cos\phi)^2 d\phi = (\cos\theta)^2 \cdot J_2 - 2\cos\theta \cdot J_3 + J_4$$

$$= (\delta_1+\delta_2)\left(\frac{1}{2}+\cos\theta+\cos^2\theta\right) - \left(\frac{3}{4}+2\cos\theta+\cos^2\theta\right)\left[\sin(\theta+\delta_2)-\sin(\theta-\delta_1)\right]$$
$$+\left(\frac{1}{4}+\frac{1}{2}\cos\theta\right)\left[\sin 2(\theta+\delta_2)-\sin 2(\theta-\delta_1)\right]$$
$$-\frac{1}{12}\left[\sin 3(\theta+\delta_2)-\sin 3(\theta-\delta_1)\right],$$

$$A_{n4} = \frac{1}{2}\int_{\theta-\delta_1}^{\theta+\delta_2} \left[\cos(n-1)\phi - \cos(n+1)\phi\right](\cos\theta-\cos\phi)^2 d\phi$$

$$= (\cos\theta)^2 \cdot K_{n,2} - 2\cos\theta \cdot K_{n,3} + K_{n,4}$$

$$= \begin{cases} (\delta_1+\delta_2)\left(\frac{1}{8}+\frac{1}{2}\cos^2\theta\right) - \frac{\cos\theta}{2}\left[\sin(\theta+\delta_2)-\sin(\theta-\delta_1)\right] \\ -\frac{\cos^2\theta}{4}\left[\sin 2(\theta+\delta_2)-\sin 2(\theta-\delta_1)\right] + \frac{1}{6}\cos\theta\left[\sin 3(\theta+\delta_2)-\sin 3(\theta-\delta_1)\right] \\ -\frac{1}{32}\left[\sin 4(\theta+\delta_2)-\sin 4(\theta-\delta_1)\right] \qquad , \ n=1, \end{cases}$$

$$= \begin{cases} -\frac{1}{2}(\delta_1+\delta_2)\cos\theta + \left(\frac{1}{4}+\frac{1}{2}\cos^2\theta\right)\left[\sin(\theta+\delta_2)-\sin(\theta-\delta_1)\right] \\ -\left(\frac{1}{24}+\frac{1}{6}\cos^2\theta\right)\left[\sin 3(\theta+\delta_2)-\sin 3(\theta-\delta_1)\right] \\ +\frac{\cos\theta}{8}\left[\sin 4(\theta+\delta_2)-\sin 4(\theta-\delta_1)\right] - \frac{1}{40}\left[\sin 5(\theta+\delta_2)-\sin 5(\theta-\delta_1)\right] \ , \ n=2, \end{cases}$$

$$= \begin{cases} \frac{1}{8}(\delta_1+\delta_2) - \frac{\cos\theta}{2}\left[\sin(\theta+\delta_2)-\sin(\theta-\delta_1)\right] \\ +\left(\frac{1}{16}+\frac{\cos^2\theta}{4}\right)\left[\sin 2(\theta+\delta_2)-\sin 2(\theta-\delta_1)\right] \\ -\left(\frac{1}{32}+\frac{\cos^2\theta}{8}\right)\left[\sin 4(\theta+\delta_2)-\sin 4(\theta-\delta_1)\right] + \frac{\cos\theta}{10}\left[\sin 5(\theta+\delta_2)-\sin 5(\theta-\delta_1)\right] \\ -\frac{1}{48}\left[\sin 6(\theta+\delta_2)-\sin 6(\theta-\delta_1)\right], \qquad n=3, \end{cases}$$

$$= \begin{cases} \frac{1}{8}\cdot\frac{\sin(n-3)(\theta+\delta_2)-\sin(n-3)(\theta-\delta_1)}{n-3} - \frac{\cos\theta}{2}\cdot\frac{\sin(n-2)(\theta+\delta_2)-\sin(n-2)(\theta-\delta_1)}{n-2} \\ +\left(\frac{1}{8}+\frac{\cos^2\theta}{2}\right)\frac{\sin(n-1)(\theta+\delta_2)-\sin(n-1)(\theta-\delta_1)}{n-1} \\ -\left(\frac{1}{8}+\frac{\cos^2\theta}{2}\right)\frac{\sin(n+1)(\theta+\delta_2)-\sin(n+1)(\theta-\delta_1)}{n+1} \\ +\frac{\cos\theta}{2}\cdot\frac{\sin(n+2)(\theta+\delta_2)-\sin(n+2)(\theta-\delta_1)}{n+2} \\ -\frac{1}{8}\cdot\frac{\sin(n+3)(\theta+\delta_2)-\sin(n+3)(\theta-\delta_2)}{n+3} \qquad , \ n\neq 1,\ 2,\ 3 \end{cases}$$

(5) $m = 5$; $An5$

$$A_{05} = \int_{\theta-\delta_1}^{\theta+\delta_2} (1-\cos\phi)(\cos\theta-\cos\phi)^3 d\phi$$

$$= (\cos\theta)^3 J_2 - 3(\cos\theta)^2 J_3 + 3\cos\theta J_4 - J_5$$

$$= (\delta_1+\delta_2)\left((\cos\theta)^3 + \frac{3}{2}(\cos\theta)^2 + \frac{3}{2}\cos\theta + \frac{3}{8}\right)$$
$$-\left[(\cos\theta)^3 + 3(\cos\theta)^2 + \frac{9}{4}\cos\theta + \frac{3}{4}\right]\left(\sin(\theta+\delta_2) - \sin(\theta-\delta_1)\right)$$
$$+\left[\frac{3}{4}(\cos\theta)^2 + \frac{3}{4}\cos\theta + \frac{1}{4}\right]\left(\sin 2(\theta+\delta_2) - \sin 2(\theta-\delta_1)\right)$$
$$-\left(\frac{1}{4}\cos\theta + \frac{1}{12}\right)\left(\sin 3(\theta+\delta_2) - \sin 3(\theta-\delta_1)\right) + \frac{1}{32}\left(\sin 4(\theta+\delta_2) - \sin 4(\theta-\delta_1)\right)$$

$$An5 = \begin{cases} (\delta_1+\delta_2)\left(\frac{1}{2}(\cos\theta)^3 + \frac{3}{8}\cos\theta\right) - \left(\frac{3}{4}(\cos\theta)^2 + \frac{1}{8}\right)\left(\sin(\theta+\delta_2) - \sin(\theta-\delta_1)\right) \\ -\frac{1}{4}(\cos\theta)^3\left(\sin 2(\theta+\delta_2) - \sin 2(\theta-\delta_1)\right) \\ +\left(\frac{1}{4}(\cos\theta)^2 + \frac{1}{48}\right)\left(\sin 3(\theta+\delta_2) - \sin 3(\theta-\delta_1)\right) \\ -\frac{3}{32}(\cos\theta)\left(\sin 4(\theta+\delta_2) - \sin 4(\theta-\delta_1)\right) + \frac{1}{80}\left(\sin 5(\theta+\delta_2) - \sin 5(\theta-\delta_1)\right), \quad n=1, \\ -(\delta_1+\delta_2)\left(\frac{3}{4}(\cos\theta)^2 + \frac{1}{8}\right) + \left(\frac{1}{2}(\cos\theta)^3 + \frac{3}{4}\cos\theta\right)\left(\sin(\theta+\delta_2) - \sin(\theta-\delta_1)\right) \\ -\frac{1}{32}\left(\sin 2(\theta+\delta_2) - \sin 2(\theta-\delta_1)\right) - \left(\frac{1}{6}(\cos\theta)^3 + \frac{1}{8}\cos\theta\right)\left(\sin 3(\theta+\delta_2) - \sin 3(\theta-\delta_1)\right) \\ +\left(\frac{3}{16}(\cos\theta)^2 + \frac{1}{32}\right)\left(\sin 4(\theta+\delta_2) - \sin 4(\theta-\delta_1)\right) \\ -\frac{3}{40}\cos\theta\left(\sin 5(\theta+\delta_2) - \sin 5(\theta-\delta_1)\right) + \frac{1}{96}\left(\sin 6(\theta+\delta_2) - \sin 6(\theta-\delta_1)\right), \quad n=2, \\ \frac{3}{8}(\delta_1+\delta_2)\cos\theta - \left(\frac{3}{4}(\cos\theta)^2 + \frac{3}{16}\right)\left(\sin(\theta+\delta_2) - \sin(\theta-\delta_1)\right) \\ +\left(\frac{1}{4}(\cos\theta)^3 + \frac{3}{16}\cos\theta\right)\left(\sin 2(\theta+\delta_2) - \sin 2(\theta-\delta_1)\right) \\ -\left(\frac{1}{8}(\cos\theta)^3 + \frac{3}{32}\cos\theta\right)\left(\sin 4(\theta+\delta_2) - \sin 4(\theta-\delta_1)\right) \\ +\left(\frac{3}{20}(\cos\theta)^2 + \frac{1}{40}\right)\left(\sin 5(\theta+\delta_2) - \sin 5(\theta-\delta_1)\right) \\ -\frac{3}{48}\cos\theta\cdot\left(\sin 6(\theta+\delta_2) - \sin 6(\theta-\delta_1)\right) + \frac{1}{112}\left(\sin 7(\theta+\delta_2) - \sin 7(\theta-\delta_1)\right), \\ n=3, \end{cases}$$

$$
\begin{cases}
-\frac{1}{16}(\delta_1+\delta_2)+\frac{3}{8}\cos\theta\,(\sin(\theta+\delta_2)-\sin(\theta-\delta_1)) \\
-\left(\frac{3}{8}(\cos\theta)^2+\frac{1}{16}\right)(\sin 2(\theta+\delta_2)-\sin 2(\theta-\delta_1)) \\
+\left(\frac{1}{6}(\cos\theta)^3+\frac{1}{8}\cos\theta\right)(\sin 3(\theta+\delta_2)-\sin 3(\theta-\delta_1)) \\
-\left(\frac{1}{10}(\cos\theta)^3+\frac{3}{40}\cos\theta\right)(\sin 5(\theta+\delta_2)-\sin 5(\theta-\delta_1)) \\
+\left(\frac{1}{8}(\cos\theta)^2+\frac{1}{48}\right)(\sin 6(\theta+\delta_2)-\sin 6(\theta-\delta_1)) \\
-\frac{3}{56}\cos\theta\,(\sin 7(\theta+\delta_2)-\sin 7(\theta-\delta_1))+\frac{1}{128}(\sin 8(\theta+\delta_2)-\sin 8(\theta-\delta_1)), & n=4, \\
-\frac{1}{16}\,\frac{\sin(n-4)(\theta+\delta_2)-\sin(n-4)(\theta-\delta_1)}{n-4} \\
+\frac{3\cos\theta}{8}\cdot\frac{1}{n-3}\left[\sin(n-3)(\theta+\delta_2)-\sin(n-3)(\theta-\delta_1)\right] \\
-\left(\frac{3}{4}(\cos\theta)^2+\frac{1}{8}\right)\frac{1}{n-2}\left[\sin(n-2)(\theta+\delta_2)-\sin(n-2)(\theta-\delta_1)\right] \\
+\left(\frac{1}{2}(\cos\theta)^3+\frac{3}{8}\cos\theta\right)\frac{1}{n-1}\left[\sin(n-1)(\theta+\delta_2)-\sin(n-1)(\theta-\delta_1)\right] \\
-\left(\frac{1}{2}(\cos\theta)^3+\frac{3}{8}\cos\theta\right)\frac{1}{n+1}\left[\sin(n+1)(\theta+\delta_2)-\sin(n+1)(\theta-\delta_1)\right] \\
+\left(\frac{1}{8}+\frac{3}{4}(\cos\theta)^2\right)\frac{1}{n+2}\left[\sin(n+2)(\theta+\delta_2)-\sin(n+2)(\theta-\delta_1)\right] \\
-\frac{3}{8}\cos\theta\cdot\frac{1}{n+3}\left[\sin(n+3)(\theta+\delta_2)-\sin(n+3)(\theta-\delta_1)\right] \\
+\frac{1}{16}\,\frac{1}{n+4}\left[\sin(n+4)(\theta+\delta_2)-\sin(n+4)(\theta-\delta_1)\right], & n=1,2,3,4
\end{cases}
$$

In a similar way, the expressions for other higher coefficients can be derived.

II. B_n

$$B_0 = \int_0^{\pi} (1-\cos\phi)\,d\phi - \int_{\theta-\delta_1}^{\theta+\delta_2}$$

$$= \pi - A_{02},$$

$$B_n = \frac{1}{2}\left\{\int_0^{\pi}\left[\cos(n-1)\phi - \cos(n+1)\phi\right]d\phi - \int_{\theta-\delta}^{\theta+\delta_2}\right\}$$

$$= \begin{cases} \frac{1}{2}\pi - A_{12} & , n=1 \\ -A_{n2} & , n\neq 1 \end{cases}$$

APPENDIX 3.

Tables of A_{nm}.

S	X	A01	A02	A03	A04	A05
0.5	0.99990	1.07236	0.19412	0.06185	0.02329	0.00951
0.5	0.95000	1.04569	0.22474	0.06739	0.02518	0.01024
0.5	0.90000	1.01992	0.25735	0.07237	0.02707	0.01096
0.5	0.85000	0.99514	0.29193	0.07670	0.02903	0.01167
0.5	0.80000	0.97137	0.32850	0.08028	0.03114	0.01236
0.5	0.75000	0.94867	0.36711	0.08305	0.03349	0.01301
0.5	0.70000	0.92708	0.40781	0.08494	0.03617	0.01358
0.5	0.65000	0.90670	0.45067	0.08585	0.03930	0.01402
0.5	0.60000	0.88764	0.49576	0.08574	0.04300	0.01427
0.5	0.55000	0.87001	0.54318	0.08453	0.04740	0.01425
0.5	0.50000	0.85397	0.59303	0.08216	0.05264	0.01385
0.5	0.45000	0.84388	0.64323	0.07975	0.05824	0.01329
0.5	0.40000	0.84629	0.69017	0.07945	0.06308	0.01319
0.5	0.35000	0.85608	0.73653	0.08012	0.06774	0.01328
0.5	0.30000	0.87197	0.78321	0.08150	0.07239	0.01350
0.5	0.25000	0.89358	0.83077	0.08352	0.07710	0.01383
0.5	0.20000	0.92094	0.87967	0.08615	0.08195	0.01427
0.5	0.15000	0.95436	0.93038	0.08943	0.08699	0.01482
0.5	0.10000	0.99445	0.98336	0.09342	0.09229	0.01550
0.5	0.05000	1.04205	1.03914	0.09821	0.09791	0.01632
0.5	0.	1.09838	1.09838	0.10395	0.10395	0.01731
0.5	-0.05000	1.16508	1.16183	0.11085	0.11051	0.01850
0.5	-0.10000	1.24442	1.23051	0.11918	0.11774	0.01995
0.5	-0.15000	1.33952	1.30574	0.12937	0.12583	0.02174
0.5	-0.20000	1.45489	1.38936	0.14203	0.13507	0.02399
0.5	-0.25000	1.59720	1.48411	0.15814	0.14591	0.02689
0.5	-0.30000	1.77710	1.59432	0.17935	0.15912	0.03077
0.5	-0.35000	2.01312	1.72770	0.20880	0.17614	0.03631
0.5	-0.40000	2.34366	1.90083	0.25371	0.20037	0.04509
0.5	-0.45000	2.88662	2.16804	0.33949	0.24412	0.06310
0.5	-0.50000	3.80925	2.59255	0.48888	0.31505	0.09241
0.5	-0.55000	3.86013	2.54240	0.38668	0.25763	0.05672
0.5	-0.60000	3.91301	2.48966	0.28839	0.20955	0.02929
0.5	-0.65000	3.96804	2.43421	0.19423	0.17034	0.00880
0.5	-0.70000	4.02545	2.37587	0.10442	0.13955	-0.00605
0.5	-0.75000	4.08549	2.31443	0.01922	0.11666	-0.01643
0.5	-0.80000	4.14844	2.24966	-0.06108	0.10115	-0.02346
0.5	-0.85000	4.21466	2.18128	-0.13618	0.09243	-0.02817
0.5	-0.90000	4.28458	2.10896	-0.20570	0.08986	-0.03149
0.5	-0.92000	4.31370	2.07884	-0.23186	0.09041	-0.03261
0.5	-0.94000	4.34354	2.04799	-0.25703	0.09179	-0.03368
0.5	-0.95000	4.35874	2.03229	-0.26923	0.09277	-0.03421
0.5	-0.96000	4.37413	2.01639	-0.28118	0.09394	-0.03475
0.5	-0.98000	4.40553	1.98400	-0.30427	0.09683	-0.03587
0.5	-0.99990	4.43644	1.95094	-0.32617	0.10037	-0.03705
0.5	-0.50000	3.80925	2.59255	0.48888	0.31505	0.09241
0.5	0.16670	0.94249	0.91321	0.08826	0.08528	0.01462
0.5	0.83330	0.98709	0.30392	0.07798	0.02972	0.01191
0.5	-0.62500	3.94024	2.46229	0.24078	0.18886	0.01826
0.5	-0.12500	1.28976	1.26720	0.12401	0.12166	0.02080
0.5	0.37500	0.85037	0.71336	0.07969	0.06542	0.01321
0.5	0.87500	1.00741	0.27439	0.07462	0.02804	0.01132

S	X	A11	A12	A13	A14	A15
0.5	0.99990	1.95050	0.32637	0.10040	0.03706	0.01495
0.5	0.95000	1.81435	0.37085	0.10623	0.03885	0.01559
0.5	0.90000	1.68050	0.41660	0.11043	0.04047	0.01614
0.5	0.85000	1.54908	0.46337	0.11285	0.04204	0.01661
0.5	0.80000	1.41997	0.51102	0.11337	0.04369	0.01696
0.5	0.75000	1.29306	0.55938	0.11186	0.04559	0.01715
0.5	0.70000	1.16823	0.60834	0.10822	0.04791	0.01710
0.5	0.65000	1.04540	0.65774	0.10236	0.05082	0.01673
0.5	0.60000	0.92446	0.70747	0.09419	0.05453	0.01592
0.5	0.55000	0.80534	0.75740	0.08363	0.05922	0.01450
0.5	0.50000	0.68793	0.80739	0.07060	0.06511	0.01230
0.5	0.45000	0.58040	0.85293	0.05740	0.07116	0.00978
0.5	0.40000	0.49463	0.88679	0.04815	0.07513	0.00813
0.5	0.35000	0.41917	0.91420	0.04042	0.07818	0.00679
0.5	0.30000	0.35035	0.93667	0.03357	0.08061	0.00562
0.5	0.25000	0.28621	0.95494	0.02730	0.08254	0.00456
0.5	0.20000	0.22545	0.96946	0.02144	0.08407	0.00358
0.5	0.15000	0.16714	0.98050	0.01586	0.08521	0.00264
0.5	0.10000	0.11053	0.98827	0.01047	0.08601	0.00174
0.5	0.05000	0.05501	0.99289	0.00521	0.08649	0.00087
0.5	0.	-0.00000	0.99442	-0.00000	0.08665	-0.00000
0.5	-0.05000	-0.05500	0.99289	-0.00521	0.08649	-0.00087
0.5	-0.10000	-0.11053	0.98827	-0.01047	0.08601	-0.00174
0.5	-0.15000	-0.16714	0.98050	-0.01586	0.08521	-0.00264
0.5	-0.20000	-0.22545	0.96946	-0.02144	0.08407	-0.00358
0.5	-0.25000	-0.28621	0.95494	-0.02730	0.08254	-0.00456
0.5	-0.30000	-0.35035	0.93667	-0.03357	0.08061	-0.00562
0.5	-0.35000	-0.41917	0.91420	-0.04042	0.07818	-0.00679
0.5	-0.40000	-0.49463	0.88679	-0.04815	0.07513	-0.00813
0.5	-0.45000	-0.58040	0.85293	-0.05740	0.07116	-0.00978
0.5	-0.50000	-0.68793	0.80739	-0.07060	0.06511	-0.01230
0.5	-0.55000	-0.80534	0.75740	-0.08363	0.05922	-0.01450
0.5	-0.60000	-0.92446	0.70747	-0.09419	0.05453	-0.01592
0.5	-0.65000	-1.04540	0.65774	-0.10236	0.05082	-0.01673
0.5	-0.70000	-1.16823	0.60834	-0.10822	0.04791	-0.01710
0.5	-0.75000	-1.29306	0.55938	-0.11186	0.04559	-0.01715
0.5	-0.80000	-1.41997	0.51102	-0.11337	0.04369	-0.01696
0.5	-0.85000	-1.54908	0.46337	-0.11285	0.04204	-0.01661
0.5	-0.90000	-1.68050	0.41660	-0.11043	0.04047	-0.01614
0.5	-0.92000	-1.73374	0.39817	-0.10896	0.03984	-0.01593
0.5	-0.94000	-1.78738	0.37991	-0.10721	0.03919	-0.01571
0.5	-0.95000	-1.81435	0.37085	-0.10623	0.03885	-0.01559
0.5	-0.96000	-1.84142	0.36183	-0.10519	0.03851	-0.01547
0.5	-0.98000	-1.89589	0.34395	-0.10291	0.03780	-0.01521
0.5	-0.99990	-1.95050	0.32637	-0.10040	0.03706	-0.01495
0.5	-0.50000	-0.68793	0.80739	-0.07060	0.06511	-0.01230
0.5	0.16670	0.18639	0.97718	0.01770	0.08487	0.00295
0.5	0.83330	1.50571	0.47920	0.11324	0.04257	0.01674
0.5	-0.62500	-0.98470	0.68258	-0.09857	0.05256	-0.01639
0.5	-0.12500	-0.13867	0.98479	-0.01315	0.08566	-0.00219
0.5	0.37500	0.45591	0.90118	0.04415	0.07674	0.00743
0.5	0.87500	1.61450	0.43987	0.11187	0.04125	0.01639

S	X	A21	A22	A23	A24	A25
0.5	0.99990	3.24787	0.45186	0.12667	0.04421	0.01718
0.5	0.95000	2.70558	0.49214	0.12413	0.04264	0.01640
0.5	0.90000	2.19170	0.52901	0.11783	0.04056	0.01540
0.5	0.85000	1.70669	0.56203	0.10778	0.03824	0.01419
0.5	0.80000	1.24992	0.59089	0.09400	0.03599	0.01273
0.5	0.75000	0.82082	0.61536	0.07660	0.03410	0.01096
0.5	0.70000	0.41885	0.63523	0.05569	0.03287	0.00877
0.5	0.65000	0.04353	0.65035	0.03142	0.03261	0.00602
0.5	0.60000	-0.30559	0.66059	0.00397	0.03360	0.00253
0.5	0.55000	-0.62892	0.66588	-0.02645	0.03614	-0.00192
0.5	0.50000	-0.92686	0.66618	-0.05961	0.04051	-0.00761
0.5	0.45000	-1.18350	0.65284	-0.09066	0.04449	-0.01349
0.5	0.40000	-1.37788	0.61314	-0.11174	0.04384	-0.01725
0.5	0.35000	-1.53498	0.55910	-0.12806	0.04114	-0.02009
0.5	0.30000	-1.66313	0.49486	-0.14107	0.03712	-0.02233
0.5	0.25000	-1.76678	0.42287	-0.15144	0.03215	-0.02410
0.5	0.20000	-1.84873	0.34490	-0.15955	0.02647	-0.02548
0.5	0.15000	-1.91086	0.26243	-0.16567	0.02028	-0.02652
0.5	0.10000	-1.95444	0.17671	-0.16993	0.01371	-0.02724
0.5	0.05000	-1.98028	0.08887	-0.17246	0.00691	-0.02767
0.5	0.	-1.98885	0.00000	-0.17329	0.00000	-0.02781
0.5	-0.05000	-1.98028	-0.08887	-0.17246	-0.00691	-0.02767
0.5	-0.10000	-1.95444	-0.17671	-0.16993	-0.01371	-0.02724
0.5	-0.15000	-1.91086	-0.26243	-0.16567	-0.02028	-0.02652
0.5	-0.20000	-1.84873	-0.34490	-0.15955	-0.02647	-0.02548
0.5	-0.25000	-1.76678	-0.42286	-0.15144	-0.03215	-0.02410
0.5	-0.30000	-1.66313	-0.49486	-0.14107	-0.03712	-0.02233
0.5	-0.35000	-1.53498	-0.55910	-0.12806	-0.04114	-0.02009
0.5	-0.40000	-1.37788	-0.61314	-0.11174	-0.04384	-0.01725
0.5	-0.45000	-1.18350	-0.65284	-0.09066	-0.04449	-0.01349
0.5	-0.50000	-0.92686	-0.66618	-0.05961	-0.04051	-0.00761
0.5	-0.55000	-0.62893	-0.66588	-0.02645	-0.03614	-0.00192
0.5	-0.60000	-0.30559	-0.66059	0.00397	-0.03360	0.00253
0.5	-0.65000	0.04353	-0.65035	0.03142	-0.03261	0.00602
0.5	-0.70000	0.41885	-0.63523	0.05569	-0.03287	0.00877
0.5	-0.75000	0.82081	-0.61536	0.07660	-0.03410	0.01096
0.5	-0.80000	1.24992	-0.59089	0.09400	-0.03599	0.01273
0.5	-0.85000	1.70669	-0.56203	0.10778	-0.03824	0.01419
0.5	-0.90000	2.19170	-0.52901	0.11783	-0.04056	0.01540
0.5	-0.92000	2.39375	-0.51471	0.12081	-0.04144	0.01583
0.5	-0.94000	2.60046	-0.49981	0.12318	-0.04226	0.01622
0.5	-0.95000	2.70558	-0.49214	0.12413	-0.04264	0.01640
0.5	-0.96000	2.81187	-0.48434	0.12494	-0.04301	0.01658
0.5	-0.98000	3.02803	-0.46832	0.12611	-0.04367	0.01690
0.5	-0.99990	3.24787	-0.45186	0.12667	-0.04421	0.01718
0.5	-0.50000	-0.92686	-0.66618	-0.05961	-0.04051	-0.00761
0.5	0.16670	-1.89223	0.29040	-0.16384	0.02239	-0.02621
0.5	0.83330	1.55102	0.57214	0.10359	0.03747	0.01373
0.5	-0.62500	-0.13428	-0.65608	0.01808	-0.03293	0.00438
0.5	-0.12500	-1.93491	-0.21990	-0.16802	-0.01703	-0.02692
0.5	0.37500	-1.46043	0.58759	-0.12038	0.04269	-0.01876
0.5	0.87500	1.94563	0.54602	0.11327	0.03941	0.01482

S	X	A31	A32	A33	A34	A35
0.5	0.99990	3.64088	0.32392	0.06449	0.01700	0.00519
0.5	0.95000	2.34196	0.31596	0.04433	0.00937	0.00208
0.5	0.90000	1.20654	0.29995	0.02055	0.00173	-0.00103
0.5	0.85000	0.22824	0.27652	-0.00613	-0.00539	-0.00408
0.5	0.80000	-0.60188	0.24641	-0.03494	-0.01156	-0.00707
0.5	0.75000	-1.29256	0.21046	-0.06515	-0.01636	-0.01007
0.5	0.70000	-1.85231	0.16961	-0.09599	-0.01943	-0.01317
0.5	0.65000	-2.28951	0.12487	-0.12673	-0.02048	-0.01652
0.5	0.60000	-2.61235	0.07729	-0.15662	-0.01927	-0.02027
0.5	0.55000	-2.82892	0.02797	-0.18501	-0.01561	-0.02464
0.5	0.50000	-2.94715	-0.02198	-0.21123	-0.00939	-0.02984
0.5	0.45000	-2.95123	-0.08405	-0.22798	-0.00413	-0.03418
0.5	0.40000	-2.82321	-0.17280	-0.22523	-0.00555	-0.03448
0.5	0.35000	-2.61187	-0.26670	-0.21235	-0.00919	-0.03288
0.5	0.30000	-2.33796	-0.35761	-0.19245	-0.01367	-0.03001
0.5	0.25000	-2.01533	-0.44063	-0.16732	-0.01827	-0.02621
0.5	0.20000	-1.65475	-0.51238	-0.13820	-0.02251	-0.02172
0.5	0.15000	-1.26526	-0.57044	-0.10611	-0.02609	-0.01671
0.5	0.10000	-0.85484	-0.61306	-0.07189	-0.02879	-0.01134
0.5	0.05000	-0.43078	-0.63909	-0.03628	-0.03047	-0.00573
0.5	0.	-0.00000	-0.64784	-0.00000	-0.03103	0.00000
0.5	-0.05000	0.43078	-0.63909	0.03628	-0.03047	0.00573
0.5	-0.10000	0.85484	-0.61306	0.07189	-0.02879	0.01134
0.5	-0.15000	1.26526	-0.57044	0.10611	-0.02609	0.01671
0.5	-0.20000	1.65475	-0.51238	0.13820	-0.02251	0.02172
0.5	-0.25000	2.01533	-0.44063	0.16732	-0.01827	0.02621
0.5	-0.30000	2.33796	-0.35761	0.19245	-0.01367	0.03001
0.5	-0.35000	2.61187	-0.26670	0.21235	-0.00919	0.03288
0.5	-0.40000	2.82321	-0.17280	0.22523	-0.00555	0.03448
0.5	-0.45000	2.95123	-0.08405	0.22798	-0.00413	0.03418
0.5	-0.50000	2.94715	-0.02198	0.21123	-0.00939	0.02984
0.5	-0.55000	2.82892	0.02797	0.18501	-0.01561	0.02464
0.5	-0.60000	2.61235	0.07729	0.15662	-0.01927	0.02027
0.5	-0.65000	2.28951	0.12487	0.12673	-0.02048	0.01652
0.5	-0.70000	1.85231	0.16961	0.09600	-0.01943	0.01317
0.5	-0.75000	1.29256	0.21046	0.06515	-0.01636	0.01007
0.5	-0.80000	0.60188	0.24641	0.03494	-0.01156	0.00707
0.5	-0.85000	-0.22824	0.27652	0.00613	-0.00539	0.00408
0.5	-0.90000	-1.20654	0.29995	-0.02055	0.00173	0.00103
0.5	-0.92000	-1.64135	0.30728	-0.03045	0.00475	-0.00021
0.5	-0.94000	-2.10187	0.31338	-0.03984	0.00782	-0.00145
0.5	-0.95000	-2.34196	0.31596	-0.04433	0.00937	-0.00208
0.5	-0.96000	-2.58869	0.31821	-0.04868	0.01091	-0.00270
0.5	-0.98000	-3.10242	0.32174	-0.05692	0.01399	-0.00395
0.5	-0.99990	-3.64088	0.32392	-0.06449	0.01700	-0.00519
0.5	-0.50000	2.94715	-0.02198	0.21123	-0.00939	0.02984
0.5	0.16670	-1.39806	-0.55269	-0.11711	-0.02499	-0.01843
0.5	0.83330	-0.06506	0.26717	-0.01555	-0.00758	-0.00508
0.5	-0.62500	2.46472	0.10137	0.14182	-0.02017	0.01833
0.5	-0.12500	1.06220	-0.59376	0.08922	-0.02756	0.01406
0.5	0.37500	-2.72641	-0.21973	-0.21981	-0.00720	-0.03387
0.5	0.87500	0.69832	0.28912	0.00753	-0.00192	-0.00256

S	X	A41	A42	A43	A44	A45
0.5	0.99990	3.38532	C.06694	-0.03171	-0.02060	-C.01027
0.5	0.95000	1.11222	C.01951	-0.05863	-0.02901	-C.01328
0.5	0.90000	-0.61983	-C.03019	-0.08432	-0.03539	-0.01549
0.5	0.85000	-1.87173	-C.07969	-0.10740	-0.03926	-0.01690
0.5	0.80000	-2.70575	-C.12675	-0.12679	-0.04034	-0.01759
0.5	0.75000	-3.18057	-C.16937	-0.14161	-0.03849	-C.01770
0.5	0.70000	-3.35131	-C.20579	-0.15122	-0.03373	-C.01743
0.5	0.65000	-3.26963	-C.23456	-0.15520	-0.02620	-0.01700
0.5	0.60000	-2.98382	-C.25459	-0.15338	-0.01618	-C.01664
0.5	0.55000	-2.53883	-C.26510	-0.14583	-0.00403	-0.01659
0.5	0.50000	-1.97633	-C.26570	-0.13284	0.00978	-0.01709
0.5	0.45000	-1.30450	-C.27252	-0.10625	0.02015	-0.01589
0.5	0.40000	-0.53508	-C.30093	-0.05734	0.02068	-0.00959
0.5	0.35000	0.24009	-C.32110	-0.00220	0.01818	-0.00175
0.5	0.30000	0.97558	-0.32453	0.05294	0.01469	0.00638
0.5	0.25000	1.64038	-C.30855	0.10431	0.01114	0.01411
0.5	0.20000	2.21160	-C.27345	0.14930	0.00796	0.02096
0.5	0.15000	2.67216	-C.22134	0.18602	0.00532	0.02659
0.5	0.10000	3.00960	-C.15555	0.21314	0.00320	0.03076
0.5	0.05000	3.21538	-C.08022	0.22976	0.00149	0.03333
0.5	0.	3.28452	-C.00000	0.23536	-0.00000	0.03420
0.5	-0.05000	3.21538	C.08022	0.22976	-0.00149	0.03333
0.5	-0.10000	3.00960	C.15555	0.21314	-0.00320	0.03076
0.5	-0.15000	2.67216	C.22134	0.18602	-0.00532	0.02659
0.5	-0.20000	2.21160	C.27345	0.14930	-0.00796	0.02096
0.5	-0.25000	1.64038	C.30855	0.10431	-0.01114	0.01411
0.5	-0.30000	0.97558	C.32453	0.05294	-0.01469	0.00638
0.5	-0.35000	0.24009	C.32110	-0.00220	-0.01818	-0.00175
0.5	-0.40000	-0.53508	C.30093	-0.05734	-0.02068	-0.00959
0.5	-0.45000	-1.30450	C.27252	-0.10625	-0.02015	-0.01589
0.5	-0.50000	-1.97633	C.26570	-0.13284	-0.00978	-0.01709
0.5	-0.55000	-2.53883	C.26510	-0.14583	0.00403	-0.01659
0.5	-0.60000	-2.98382	C.25459	-0.15338	0.01618	-0.01664
0.5	-0.65000	-3.26963	C.23456	-0.15520	0.02620	-0.01700
0.5	-0.70000	-3.35131	C.20579	-0.15122	0.03373	-0.01743
0.5	-0.75000	-3.18057	C.16937	-0.14161	0.03849	-0.01770
0.5	-0.80000	-2.70575	C.12675	-0.12679	0.04034	-0.01759
0.5	-0.85000	-1.87173	C.07969	-0.10740	0.03926	-0.01690
0.5	-0.90000	-0.61983	C.03019	-0.08432	0.03539	-0.01549
0.5	-0.92000	0.01176	C.01020	-0.07429	0.03311	-0.01471
0.5	-0.94000	0.72428	-C.00967	-0.06392	0.03046	-0.01379
0.5	-0.95000	1.11222	-C.01951	-0.05863	0.02901	-0.01328
0.5	-0.96000	1.52199	-C.02927	-0.05330	0.02747	-0.01274
0.5	-0.98000	2.40924	-C.04844	-0.04251	0.02416	-0.01156
0.5	-0.99990	3.38532	-C.06694	-0.03171	0.02060	-0.01027
0.5	-0.50000	-1.97633	C.26570	-0.13284	-0.00978	-0.01709
0.5	0.16670	2.53150	-C.24045	0.17477	0.00614	0.02486
0.5	0.83330	-2.19379	-C.09578	-0.11434	-0.03994	-0.01721
0.5	-0.62500	-3.14936	C.24573	-0.15501	0.02148	-0.01679
0.5	-0.12500	2.85689	C.18991	0.20085	-0.00420	0.02887
0.5	0.37500	-0.14491	-C.31278	-0.03007	0.01964	-0.00577
0.5	0.87500	-1.30182	-C.05511	-0.09626	-0.03766	-0.01629

S	X	A01	A02	A03	A04	A05
0.7	0.99990	1.29820	0.33522	0.15083	0.07991	0.04587
0.7	0.95000	1.28484	0.37412	0.16157	0.08509	0.04870
0.7	0.90000	1.27267	0.41519	0.17186	0.09035	0.05157
0.7	0.85000	1.26181	0.45844	0.18163	0.09577	0.05449
0.7	0.80000	1.25237	0.50393	0.19083	0.10144	0.05746
0.7	0.75000	1.24448	0.55177	0.19941	0.10747	0.06047
0.7	0.70000	1.23829	0.60207	0.20733	0.11399	0.06350
0.7	0.65000	1.23397	0.65495	0.21456	0.12113	0.06651
0.7	0.60000	1.23175	0.71056	0.22107	0.12904	0.06946
0.7	0.55000	1.23188	0.76907	0.22685	0.13789	0.07229
0.7	0.50000	1.23467	0.83069	0.23190	0.14785	0.07492
0.7	0.45000	1.24048	0.89565	0.23623	0.15913	0.07727
0.7	0.40000	1.24976	0.96424	0.23988	0.17195	0.07923
0.7	0.35000	1.26305	1.03679	0.24289	0.18656	0.08068
0.7	0.30000	1.28103	1.11372	0.24536	0.20322	0.08150
0.7	0.25000	1.30624	1.19426	0.24837	0.22158	0.08205
0.7	0.20000	1.34608	1.27416	0.25588	0.23907	0.08447
0.7	0.15000	1.39813	1.35669	0.26665	0.25704	0.08814
0.7	0.10000	1.46286	1.44374	0.28062	0.27620	0.09301
0.7	0.05000	1.54212	1.53709	0.29831	0.29714	0.09926
0.7	0.	1.63897	1.63897	0.32064	0.32064	0.10728
0.7	-0.05000	1.75824	1.75246	0.34920	0.34783	0.11770
0.7	-0.10000	1.90784	1.88248	0.38674	0.38055	0.13169
0.7	-0.15000	2.10192	2.03779	0.43857	0.42239	0.15157
0.7	-0.20000	2.37116	2.23807	0.51735	0.48187	0.18309
0.7	-0.25000	2.82572	2.55783	0.67391	0.59431	0.25081
0.7	-0.30000	3.38142	2.91862	0.84056	0.70415	0.31021
0.7	-0.35000	3.41197	2.88611	0.71919	0.60882	0.22457
0.7	-0.40000	3.44370	2.85164	0.60093	0.52443	0.15316
0.7	-0.45000	3.47661	2.81518	0.48590	0.45065	0.09439
0.7	-0.50000	3.51075	2.77669	0.37422	0.38711	0.04670
0.7	-0.55000	3.54613	2.73611	0.26605	0.33346	0.00862
0.7	-0.60000	3.58281	2.69337	0.16153	0.28929	-0.02129
0.7	-0.65000	3.62085	2.64841	0.06084	0.25419	-0.04439
0.7	-0.70000	3.66032	2.60112	-0.03585	0.22772	-0.06197
0.7	-0.75000	3.70133	2.55140	-0.12834	0.20941	-0.07525
0.7	-0.80000	3.74397	2.49914	-0.21642	0.19877	-0.08538
0.7	-0.85000	3.78839	2.44417	-0.29985	0.19527	-0.09339
0.7	-0.90000	3.83473	2.38635	-0.37837	0.19834	-0.10027
0.7	-0.92000	3.85384	2.36238	-0.40834	0.20128	-0.10290
0.7	-0.94000	3.87330	2.33790	-0.43745	0.20513	-0.10553
0.7	-0.95000	3.88317	2.32547	-0.45169	0.20738	-0.10687
0.7	-0.96000	3.89313	2.31291	-0.46570	0.20984	-0.10822
0.7	-0.98000	3.91333	2.28739	-0.49305	0.21539	-0.11101
0.7	-0.99990	3.93265	2.26144	-0.51935	0.22168	-0.11393
0.7	-0.50000	3.51075	2.77669	0.37422	0.38711	0.04670
0.7	0.16670	1.37939	1.32870	0.26271	0.25094	0.08679
0.7	0.83330	1.25850	0.47338	0.18477	0.09763	0.05548
0.7	-0.62500	3.60165	2.67118	0.11070	0.27063	-0.03361
0.7	-0.12500	1.99802	1.95615	0.41036	0.39999	0.14067
0.7	0.37500	1.25586	0.99999	0.24146	0.17901	0.08003
0.7	0.87500	1.26707	0.43654	0.17681	0.09304	0.05302

S	X	A11	A12	A13	A14	A15
0.7	0.99990	2.26105	0.51958	0.22174	0.11395	0.06411
0.7	0.95000	2.13131	0.56796	0.22996	0.11724	0.06569
0.7	0.90000	2.00288	0.61700	0.23618	0.12010	0.06702
0.7	0.85000	1.87592	0.66647	0.24025	0.12268	0.06812
0.7	0.80000	1.75034	0.71625	0.24206	0.12513	0.06896
0.7	0.75000	1.62607	0.76619	0.24150	0.12761	0.06950
0.7	0.70000	1.50302	0.81619	0.23847	0.13029	0.06967
0.7	0.65000	1.38111	0.86610	0.23289	0.13336	0.06938
0.7	0.60000	1.26025	0.91582	0.22467	0.13701	0.06852
0.7	0.55000	1.14035	0.96520	0.21374	0.14144	0.06692
0.7	0.50000	1.02132	1.01413	0.20000	0.14685	0.06441
0.7	0.45000	0.90305	1.06246	0.18341	0.15347	0.06076
0.7	0.40000	0.78542	1.11006	0.16388	0.16150	0.05573
0.7	0.35000	0.66833	1.15678	0.14134	0.17117	0.04904
0.7	0.30000	0.55163	1.20247	0.11575	0.18269	0.04036
0.7	0.25000	0.43854	1.24446	0.08887	0.19492	0.03034
0.7	0.20000	0.34114	1.27310	0.06799	0.20241	0.02298
0.7	0.15000	0.25116	1.29354	0.04960	0.20746	0.01668
0.7	0.10000	0.16542	1.30749	0.03249	0.21081	0.01089
0.7	0.05000	0.08213	1.31564	0.01608	0.21273	0.00538
0.7	0.	-0.00000	1.31832	-0.00000	0.21337	-0.00000
0.7	-0.05000	-0.08213	1.31564	-0.01608	0.21273	-0.00538
0.7	-0.10000	-0.16542	1.30749	-0.03249	0.21081	-0.01089
0.7	-0.15000	-0.25116	1.29354	-0.04960	0.20746	-0.01668
0.7	-0.20000	-0.34114	1.27310	-0.06799	0.20241	-0.02298
0.7	-0.25000	-0.43854	1.24446	-0.08887	0.19492	-0.03034
0.7	-0.30000	-0.55162	1.20247	-0.11575	0.18269	-0.04036
0.7	-0.35000	-0.66833	1.15678	-0.14134	0.17117	-0.04904
0.7	-0.40000	-0.78542	1.11006	-0.16388	0.16150	-0.05573
0.7	-0.45000	-0.90305	1.06246	-0.18341	0.15347	-0.06076
0.7	-0.50000	-1.02132	1.01413	-0.20000	0.14685	-0.06441
0.7	-0.55000	-1.14035	0.96520	-0.21374	0.14144	-0.06692
0.7	-0.60000	-1.26025	0.91582	-0.22467	0.13701	-0.06852
0.7	-0.65000	-1.38111	0.86610	-0.23289	0.13336	-0.06938
0.7	-0.70000	-1.50302	0.81619	-0.23847	0.13029	-0.06967
0.7	-0.75000	-1.62607	0.76619	-0.24150	0.12761	-0.06950
0.7	-0.80000	-1.75034	0.71625	-0.24206	0.12513	-0.06896
0.7	-0.85000	-1.87592	0.66647	-0.24025	0.12268	-0.06812
0.7	-0.90000	-2.00288	0.61700	-0.23618	0.12010	-0.06702
0.7	-0.92000	-2.05407	0.59733	-0.23395	0.11900	-0.06652
0.7	-0.94000	-2.10551	0.57773	-0.23137	0.11784	-0.06597
0.7	-0.95000	-2.13131	0.56796	-0.22996	0.11724	-0.06569
0.7	-0.96000	-2.15719	0.55821	-0.22847	0.11662	-0.06539
0.7	-0.98000	-2.20912	0.53880	-0.22525	0.11532	-0.06477
0.7	-0.99990	-2.26105	0.51958	-0.22174	0.11395	-0.06411
0.7	-0.50000	-1.02132	1.01413	-0.20000	0.14685	-0.06441
0.7	0.16670	0.28063	1.28749	0.05556	0.20598	0.01871
0.7	0.83330	1.83382	0.68307	0.24111	0.12351	0.06843
0.7	-0.62500	-1.32056	0.89099	-0.22912	0.13510	-0.06903
0.7	-0.12500	-0.20788	1.30127	-0.04093	0.20932	-0.01374
0.7	0.37500	0.72682	1.13354	0.15299	0.16612	0.05262
0.7	0.87500	1.93922	0.64169	0.23849	0.12142	0.06760

S	X	A21	A22	A23	A24	A25
0.7	0.99990	3.48249	0.59558	0.21552	0.09966	0.05209
0.7	0.95000	2.91358	0.61920	0.20246	0.09138	0.04700
0.7	0.90000	2.37118	0.63824	0.18492	0.08214	0.04141
0.7	0.85000	1.85611	0.65251	0.16306	0.07233	0.03539
0.7	0.80000	1.36805	0.66188	0.13703	0.06229	0.02895
0.7	0.75000	0.90672	0.66630	0.10703	0.05242	0.02207
0.7	0.70000	0.47186	0.66572	0.07328	0.04306	0.01469
0.7	0.65000	0.06324	0.66015	0.03605	0.03459	0.00671
0.7	0.60000	-0.31933	0.64963	-0.00440	0.02737	-0.00202
0.7	0.55000	-0.67601	0.63425	-0.04776	0.02174	-0.01169
0.7	0.50000	-1.00693	0.61412	-0.09370	0.01804	-0.02250
0.7	0.45000	-1.31217	0.58940	-0.14188	0.01660	-0.03472
0.7	0.40000	-1.59177	0.56029	-0.19190	0.01773	-0.04862
0.7	0.35000	-1.84572	0.52705	-0.24340	0.02174	-0.06451
0.7	0.30000	-2.07396	0.48998	-0.29593	0.02890	-0.08274
0.7	0.25000	-2.26966	0.44448	-0.34541	0.03679	-0.10166
0.7	0.20000	-2.40975	0.37325	-0.37762	0.03500	-0.11336
0.7	0.15000	-2.51174	0.28886	-0.40003	0.02888	-0.12130
0.7	0.10000	-2.58189	0.19652	-0.41512	0.02038	-0.12658
0.7	0.05000	-2.62306	0.09940	-0.42386	0.01051	-0.12962
0.7	0.	-2.63664	0.00000	-0.42673	0.00000	-0.13061
0.7	-0.05000	-2.62306	-0.09940	-0.42386	-0.01051	-0.12962
0.7	-0.10000	-2.58189	-0.19652	-0.41512	-0.02038	-0.12658
0.7	-0.15000	-2.51174	-0.28886	-0.40003	-0.02888	-0.12130
0.7	-0.20000	-2.40975	-0.37325	-0.37762	-0.03500	-0.11336
0.7	-0.25000	-2.26966	-0.44448	-0.34541	-0.03679	-0.10166
0.7	-0.30000	-2.07396	-0.48998	-0.29593	-0.02890	-0.08274
0.7	-0.35000	-1.84572	-0.52705	-0.24340	-0.02174	-0.06451
0.7	-0.40000	-1.59177	-0.56029	-0.19190	-0.01773	-0.04862
0.7	-0.45000	-1.31217	-0.58940	-0.14188	-0.01660	-0.03472
0.7	-0.50000	-1.00693	-0.61412	-0.09370	-0.01804	-0.02250
0.7	-0.55000	-0.67601	-0.63425	-0.04776	-0.02174	-0.01169
0.7	-0.60000	-0.31933	-0.64963	-0.00440	-0.02737	-0.00202
0.7	-0.65000	0.06324	-0.66015	0.03605	-0.03459	0.00671
0.7	-0.70000	0.47186	-0.66572	0.07328	-0.04306	0.01469
0.7	-0.75000	0.90672	-0.66630	0.10703	-0.05242	0.02207
0.7	-0.80000	1.36805	-0.66188	0.13703	-0.06229	0.02895
0.7	-0.85000	1.85611	-0.65251	0.16306	-0.07233	0.03539
0.7	-0.90000	2.37118	-0.63824	0.18492	-0.08214	0.04141
0.7	-0.92000	2.58484	-0.63119	0.19246	-0.08593	0.04370
0.7	-0.94000	2.80289	-0.62338	0.19930	-0.08959	0.04592
0.7	-0.95000	2.91358	-0.61920	0.20246	-0.09138	0.04700
0.7	-0.96000	3.02537	-0.61483	0.20543	-0.09312	0.04806
0.7	-0.98000	3.25228	-0.60554	0.21085	-0.09649	0.05013
0.7	-0.99990	3.48249	-0.59558	0.21552	-0.09966	0.05209
0.7	-0.50000	-1.00693	-0.61412	-0.09370	-0.01804	-0.02250
0.7	0.16670	-2.48142	0.31812	-0.39344	0.03125	-0.11898
0.7	0.83330	1.69011	0.65619	0.15482	0.06898	0.03328
0.7	-0.62500	-0.13129	-0.65551	0.01621	-0.03080	0.00245
0.7	-0.12500	-2.55057	-0.24346	-0.40841	-0.02485	-0.12424
0.7	0.37500	-1.72196	0.54417	-0.21749	0.01936	-0.05630
0.7	0.87500	2.11025	0.64598	0.17452	0.07728	0.03845

S	X	A31	A32	A33	A34	A35
0.7	0.99990	3.51209	0.24041	0.00996	-0.01885	-0.01852
0.7	0.95000	2.16609	0.20360	-0.02804	-0.03762	-0.02865
0.7	0.90000	0.98876	0.16199	-0.06761	-0.05507	-0.03792
0.7	0.85000	-0.02554	0.11668	-0.10771	-0.07050	-0.04616
0.7	0.80000	-0.88522	0.06871	-0.14740	-0.08336	-0.05330
0.7	0.75000	-1.59858	0.01920	-0.18579	-0.09313	-0.05935
0.7	0.70000	-2.17386	-0.03075	-0.22200	-0.09939	-0.06436
0.7	0.65000	-2.61920	-0.08000	-0.25522	-0.10181	-0.06844
0.7	0.60000	-2.94272	-0.12745	-0.28470	-0.10012	-0.07176
0.7	0.55000	-3.15247	-0.17200	-0.30975	-0.09415	-0.07453
0.7	0.50000	-3.25648	-0.21260	-0.32979	-0.08381	-0.07697
0.7	0.45000	-3.26279	-0.24825	-0.34430	-0.06909	-0.07936
0.7	0.40000	-3.17943	-0.27801	-0.35286	-0.05008	-0.08199
0.7	0.35000	-3.01445	-0.30105	-0.35519	-0.02693	-0.08515
0.7	0.30000	-2.77596	-0.31662	-0.35110	0.00013	-0.08917
0.7	0.25000	-2.46233	-0.33140	-0.33515	0.02678	-0.09144
0.7	0.20000	-2.05154	-0.36857	-0.28904	0.03831	-0.08114
0.7	0.15000	-1.58241	-0.40682	-0.22737	0.04381	-0.06477
0.7	0.10000	-1.07484	-0.43795	-0.15627	0.04642	-0.04489
0.7	0.05000	-0.54323	-0.45797	-0.07948	0.04755	-0.02293
0.7	0.	-0.00000	-0.46486	-0.00000	0.04786	-0.00000
0.7	-0.05000	0.54323	-0.45797	0.07948	0.04755	0.02293
0.7	-0.10000	1.07483	-0.43795	0.15626	0.04642	0.04489
0.7	-0.15000	1.58241	-0.40682	0.22737	0.04381	0.06477
0.7	-0.20000	2.05154	-0.36857	0.28904	0.03831	0.08114
0.7	-0.25000	2.46233	-0.33140	0.33515	0.02678	0.09144
0.7	-0.30000	2.77596	-0.31662	0.35110	0.00013	0.08917
0.7	-0.35000	3.01444	-0.30105	0.35519	-0.02693	0.08515
0.7	-0.40000	3.17943	-0.27801	0.35286	-0.05008	0.08199
0.7	-0.45000	3.26279	-0.24825	0.34430	-0.06909	0.07936
0.7	-0.50000	3.25649	-0.21260	0.32979	-0.08381	0.07697
0.7	-0.55000	3.15247	-0.17200	0.30975	-0.09415	0.07453
0.7	-0.60000	2.94272	-0.12745	0.28470	-0.10012	0.07176
0.7	-0.65000	2.61920	-0.08000	0.25522	-0.10181	0.06844
0.7	-0.70000	2.17386	-0.03075	0.22200	-0.09939	0.06436
0.7	-0.75000	1.59858	0.01920	0.18579	-0.09313	0.05935
0.7	-0.80000	0.88522	0.06871	0.14740	-0.08336	0.05330
0.7	-0.85000	0.02555	0.11668	0.10771	-0.07050	0.04616
0.7	-0.90000	-0.98876	0.16199	0.06761	-0.05507	0.03792
0.7	-0.92000	-1.43965	0.17914	0.05167	-0.04829	0.03433
0.7	-0.94000	-1.91717	0.19562	0.03587	-0.04124	0.03058
0.7	-0.95000	-2.16609	0.20360	0.02804	-0.03762	0.02865
0.7	-0.96000	-2.42187	0.21138	0.02028	-0.03395	0.02669
0.7	-0.98000	-2.95428	0.22636	0.00496	-0.02645	0.02266
0.7	-0.99990	-3.51209	0.24041	-0.00996	-0.01885	0.01852
0.7	-0.50000	3.25649	-0.21260	0.32979	-0.08381	0.07697
0.7	0.16670	-1.74418	-0.39456	-0.24924	0.04239	-0.07072
0.7	0.83330	-0.32946	0.10090	-0.12105	-0.07511	-0.04867
0.7	-0.62500	2.79568	-0.10402	0.27047	-0.10149	0.07019
0.7	-0.12500	1.33246	-0.42358	0.19273	0.04536	0.05517
0.7	0.37500	-3.10663	-0.29042	-0.35482	-0.03901	-0.08348
0.7	0.87500	0.46176	0.13973	-0.08765	-0.06307	-0.04217

S	X	A41	A42	A43	A44	A45
0.7	0.99990	3.06016	-0.13472	-0.15792	-0.10030	-0.06105
0.7	0.95000	0.79480	-0.17627	-0.18050	-0.10555	-0.06179
0.7	0.90000	-0.91540	-0.21144	-0.19648	-0.10543	-0.05962
0.7	0.85000	-2.13288	-0.23875	-0.20515	-0.09987	-0.05482
0.7	0.80000	-2.92183	-0.25714	-0.20615	-0.08906	-0.04776
0.7	0.75000	-3.34299	-0.26593	-0.19946	-0.07341	-0.03895
0.7	0.70000	-3.45376	-0.26477	-0.18530	-0.05349	-0.02893
0.7	0.65000	-3.30819	-0.25372	-0.16422	-0.03006	-0.01831
0.7	0.60000	-2.95703	-0.23318	-0.13700	-0.00398	-0.00772
0.7	0.55000	-2.44770	-0.20394	-0.10467	0.02375	0.00222
0.7	0.50000	-1.82435	-0.16714	-0.06847	0.05209	0.01090
0.7	0.45000	-1.12785	-0.12423	-0.02981	0.07994	0.01773
0.7	0.40000	-0.39575	-0.07697	0.00977	0.10618	0.02219
0.7	0.35000	0.33771	-0.02740	0.04861	0.12972	0.02380
0.7	0.30000	1.04162	0.02224	0.08502	0.14952	0.02218
0.7	0.25000	1.70129	0.06012	0.12427	0.15949	0.02083
0.7	0.20000	2.32628	0.05739	0.18538	0.14260	0.03222
0.7	0.15000	2.85065	0.04383	0.24421	0.11380	0.04567
0.7	0.10000	3.24283	0.02842	0.29102	0.07869	0.05713
0.7	0.05000	3.48469	0.01377	0.32082	0.04011	0.06467
0.7	0.	3.56636	0.00000	0.33102	0.00000	0.06728
0.7	-0.05000	3.48469	-0.01377	0.32082	-0.04011	0.06467
0.7	-0.10000	3.24283	-0.02842	0.29102	-0.07869	0.05713
0.7	-0.15000	2.85066	-0.04383	0.24421	-0.11380	0.04567
0.7	-0.20000	2.32628	-0.05739	0.18538	-0.14260	0.03222
0.7	-0.25000	1.70129	-0.06012	0.12427	-0.15949	0.02083
0.7	-0.30000	1.04163	-0.02224	0.08502	-0.14952	0.02218
0.7	-0.35000	0.33771	0.02740	0.04861	-0.12972	0.02380
0.7	-0.40000	-0.39575	0.07697	0.00977	-0.10618	0.02219
0.7	-0.45000	-1.12785	0.12423	-0.02981	-0.07994	0.01773
0.7	-0.50000	-1.82435	0.16714	-0.06847	-0.05209	0.01090
0.7	-0.55000	-2.44770	0.20394	-0.10467	-0.02375	0.00222
0.7	-0.60000	-2.95703	0.23318	-0.13700	0.00398	-0.00772
0.7	-0.65000	-3.30819	0.25372	-0.16422	0.03006	-0.01831
0.7	-0.70000	-3.45376	0.26477	-0.18530	0.05349	-0.02893
0.7	-0.75000	-3.34299	0.26593	-0.19946	0.07341	-0.03895
0.7	-0.80000	-2.92183	0.25714	-0.20615	0.08906	-0.04776
0.7	-0.85000	-2.13289	0.23875	-0.20515	0.09987	-0.05482
0.7	-0.90000	-0.91540	0.21144	-0.19648	0.10543	-0.05962
0.7	-0.92000	-0.29415	0.19825	-0.19094	0.10613	-0.06083
0.7	-0.94000	0.41014	0.18387	-0.18425	0.10596	-0.06158
0.7	-0.95000	0.79480	0.17627	-0.18050	0.10555	-0.06179
0.7	-0.96000	1.20185	0.16841	-0.17648	0.10492	-0.06188
0.7	-0.98000	2.08539	0.15196	-0.16766	0.10302	-0.06170
0.7	-0.99990	3.06016	0.13472	-0.15792	0.10030	-0.06105
0.7	-0.50000	-1.82435	0.16714	-0.06847	-0.05209	0.01090
0.7	0.16670	2.68903	0.04881	0.22556	0.12431	0.04126
0.7	0.83330	-2.44098	-0.24593	-0.20634	-0.09683	-0.05269
0.7	-0.62500	-3.15527	0.24459	-0.15132	0.01729	-0.01297
0.7	-0.12500	3.06462	-0.03611	0.26950	-0.09682	0.05180
0.7	0.37500	-0.02718	-0.05234	0.02939	0.11835	0.02338
0.7	0.87500	-1.58164	-0.22615	-0.20176	-0.10332	-0.05753

S	X	A01	A02	A03	A04	A05
1.0	0.99990	1.61480	0.61587	0.40221	0.30735	0.25364
1.0	0.95000	1.61792	0.66935	0.42599	0.32431	0.26722
1.0	0.90000	1.62301	0.72571	0.44996	0.34194	0.28139
1.0	0.85000	1.63027	0.78502	0.47412	0.36038	0.29621
1.0	0.80000	1.63997	0.84750	0.49855	0.37985	0.31180
1.0	0.75000	1.65240	0.91339	0.52333	0.40057	0.32826
1.0	0.70000	1.66791	0.98299	0.54860	0.42284	0.34572
1.0	0.65000	1.68694	1.05665	0.57453	0.44697	0.36433
1.0	0.60000	1.71001	1.13481	0.60136	0.47338	0.38427
1.0	0.55000	1.73777	1.21800	0.62941	0.50252	0.40577
1.0	0.50000	1.77103	1.30689	0.65911	0.53499	0.42915
1.0	0.45000	1.81084	1.40233	0.69106	0.57153	0.45482
1.0	0.40000	1.85855	1.50546	0.72606	0.61311	0.48339
1.0	0.35000	1.91600	1.61783	0.76533	0.66105	0.51577
1.0	0.30000	1.98579	1.74163	0.81064	0.71724	0.55338
1.0	0.25000	2.07175	1.88021	0.86485	0.78460	0.59860
1.0	0.20000	2.18010	2.03912	0.93286	0.86805	0.65571
1.0	0.15000	2.32229	2.22888	1.02444	0.97727	0.73365
1.0	0.10000	2.52534	2.47534	1.16447	1.13706	0.85645
1.0	0.05000	2.93247	2.92243	1.49819	1.49502	1.17363
1.0	0.	3.14159	3.14159	1.57080	1.57080	1.17810
1.0	-0.05000	3.14180	3.14137	1.41395	1.42133	0.95412
1.0	-0.10000	3.14750	3.13529	1.26336	1.28089	0.75849
1.0	-0.15000	3.15683	3.12506	1.11752	1.15072	0.58790
1.0	-0.20000	3.16854	3.11183	0.97539	1.03169	0.43940
1.0	-0.25000	3.18212	3.09607	0.83664	0.92394	0.31081
1.0	-0.30000	3.19730	3.07801	0.70113	0.82739	0.20015
1.0	-0.35000	3.21387	3.05780	0.56883	0.74189	0.10559
1.0	-0.40000	3.23171	3.03553	0.43973	0.66722	0.02537
1.0	-0.45000	3.25072	3.01128	0.31388	0.60313	-0.04218
1.0	-0.50000	3.27083	2.98507	0.19132	0.54934	-0.09867
1.0	-0.55000	3.29200	2.95694	0.07213	0.50553	-0.14564
1.0	-0.60000	3.31419	2.92687	-0.04359	0.47137	-0.18459
1.0	-0.65000	3.33738	2.89488	-0.15574	0.44649	-0.21691
1.0	-0.70000	3.36158	2.86093	-0.26420	0.43052	-0.24395
1.0	-0.75000	3.38678	2.82500	-0.36885	0.42304	-0.26698
1.0	-0.80000	3.41300	2.78705	-0.46953	0.42363	-0.28720
1.0	-0.85000	3.44026	2.74703	-0.56611	0.43183	-0.30572
1.0	-0.90000	3.46860	2.70487	-0.65840	0.44714	-0.32359
1.0	-0.92000	3.48024	2.68739	-0.69408	0.45514	-0.33076
1.0	-0.94000	3.49207	2.66955	-0.72903	0.46417	-0.33804
1.0	-0.95000	3.49805	2.66050	-0.74622	0.46905	-0.34174
1.0	-0.96000	3.50408	2.65135	-0.76324	0.47418	-0.34548
1.0	-0.98000	3.51627	2.63278	-0.79669	0.48514	-0.35312
1.0	-0.99990	3.52742	2.61393	-0.82921	0.49695	-0.36098
1.0	-0.50000	3.27083	2.98507	0.19132	0.54934	-0.09867
1.0	0.16670	2.26992	2.16102	0.99024	0.93695	0.70437
1.0	0.83330	1.63323	0.80552	0.48225	0.36676	0.30133
1.0	-0.62500	3.32566	2.91112	-0.10011	0.45779	-0.20149
1.0	-0.12500	3.15182	3.13059	1.18994	1.21443	0.67028
1.0	0.37500	1.88592	1.56037	0.74507	0.63618	0.49903
1.0	0.87500	1.62635	0.75498	0.46201	0.35105	0.28871

S	X	A11	A12	A13	A14	A15
1.0	0.99990	2.61358	0.82947	0.49703	0.36103	0.28808
1.0	0.95000	2.48560	0.87925	0.50636	0.36519	0.29035
1.0	0.90000	2.35801	0.92889	0.51298	0.36830	0.29181
1.0	0.85000	2.23099	0.97816	0.51674	0.37050	0.29246
1.0	0.80000	2.10445	1.02695	0.51754	0.37192	0.29227
1.0	0.75000	1.97831	1.07510	0.51526	0.37274	0.29120
1.0	0.70000	1.85246	1.12248	0.50978	0.37310	0.28917
1.0	0.65000	1.72680	1.16894	0.50100	0.37318	0.28607
1.0	0.60000	1.60120	1.21434	0.48880	0.37313	0.28175
1.0	0.55000	1.47554	1.25849	0.47307	0.37313	0.27602
1.0	0.50000	1.34966	1.30122	0.45368	0.37334	0.26866
1.0	0.45000	1.22338	1.34233	0.43050	0.37390	0.25940
1.0	0.40000	1.09650	1.38159	0.40338	0.37496	0.24791
1.0	0.35000	0.96878	1.41874	0.37215	0.37664	0.23382
1.0	0.30000	0.83990	1.45347	0.33660	0.37902	0.21668
1.0	0.25000	0.70948	1.48542	0.29646	0.38215	0.19595
1.0	0.20000	0.57701	1.51408	0.25138	0.38595	0.17096
1.0	0.15000	0.44175	1.53878	0.20083	0.39021	0.14086
1.0	0.10000	0.30254	1.55840	0.14386	0.39431	0.10434
1.0	0.05000	0.15666	1.57036	0.07808	0.39615	0.05860
1.0	0.	-0.00000	1.57080	0.00000	0.39270	0.00000
1.0	-0.05000	-0.15666	1.57036	-0.07808	0.39615	-0.05860
1.0	-0.10000	-0.30254	1.55840	-0.14386	0.39431	-0.10434
1.0	-0.15000	-0.44175	1.53878	-0.20083	0.39021	-0.14086
1.0	-0.20000	-0.57701	1.51408	-0.25138	0.38595	-0.17096
1.0	-0.25000	-0.70948	1.48542	-0.29646	0.38215	-0.19595
1.0	-0.30000	-0.83990	1.45347	-0.33660	0.37902	-0.21668
1.0	-0.35000	-0.96878	1.41874	-0.37215	0.37664	-0.23382
1.0	-0.40000	-1.09650	1.38159	-0.40338	0.37496	-0.24791
1.0	-0.45000	-1.22338	1.34233	-0.43050	0.37390	-0.25940
1.0	-0.50000	-1.34966	1.30122	-0.45368	0.37334	-0.26866
1.0	-0.55000	-1.47554	1.25849	-0.47307	0.37313	-0.27602
1.0	-0.60000	-1.60120	1.21434	-0.48880	0.37313	-0.28175
1.0	-0.65000	-1.72680	1.16894	-0.50100	0.37318	-0.28607
1.0	-0.70000	-1.85246	1.12248	-0.50978	0.37310	-0.28917
1.0	-0.75000	-1.97831	1.07510	-0.51526	0.37274	-0.29120
1.0	-0.80000	-2.10445	1.02695	-0.51754	0.37192	-0.29227
1.0	-0.85000	-2.23099	0.97816	-0.51674	0.37050	-0.29246
1.0	-0.90000	-2.35801	0.92889	-0.51298	0.36830	-0.29181
1.0	-0.92000	-2.40897	0.90907	-0.51067	0.36717	-0.29132
1.0	-0.94000	-2.46003	0.88920	-0.50791	0.36589	-0.29070
1.0	-0.95000	-2.48560	0.87925	-0.50636	0.36519	-0.29035
1.0	-0.96000	-2.51119	0.86929	-0.50471	0.36444	-0.28996
1.0	-0.98000	-2.56245	0.84934	-0.50107	0.36282	-0.28908
1.0	-0.99990	-2.61358	0.82947	-0.49703	0.36103	-0.28808
1.0	-0.50000	-1.34966	1.30122	-0.45368	0.37334	-0.26866
1.0	0.16670	0.48730	1.53102	0.21837	0.38876	0.15155
1.0	0.83330	2.18868	0.99452	0.51735	0.37105	0.29249
1.0	-0.62500	-1.66400	1.19178	-0.49533	0.37316	-0.28407
1.0	-0.12500	-0.37274	1.54932	-0.17323	0.39235	-0.12351
1.0	0.37500	1.03277	1.40044	0.38829	0.37572	0.24122
1.0	0.87500	2.29443	0.95358	0.51523	0.36950	0.29223

S	X	A21	A22	A23	A24	A25
1.0	0.99990	3.56768	0.66472	0.27190	0.14582	0.09006
1.0	0.95000	2.96413	0.65785	0.23171	0.11316	0.06284
1.0	0.90000	2.38664	0.64604	0.18676	0.07933	0.03495
1.0	0.85000	1.83635	0.62939	0.13747	0.04493	0.00668
1.0	0.80000	1.31323	0.60803	0.08422	0.01054	-0.02178
1.0	0.75000	0.81727	0.58213	0.02741	-0.02330	-0.05028
1.0	0.70000	0.34848	0.55191	-0.03251	-0.05601	-0.07871
1.0	0.65000	-0.09305	0.51763	-0.09506	-0.08701	-0.10696
1.0	0.60000	-0.50723	0.47960	-0.15971	-0.11574	-0.13500
1.0	0.55000	-0.89389	0.43820	-0.22589	-0.14159	-0.16277
1.0	0.50000	-1.25278	0.39386	-0.29299	-0.16398	-0.19026
1.0	0.45000	-1.58361	0.34709	-0.36035	-0.18228	-0.21744
1.0	0.40000	-1.88597	0.29850	-0.42722	-0.19585	-0.24430
1.0	0.35000	-2.15933	0.24882	-0.49278	-0.20400	-0.27078
1.0	0.30000	-2.40301	0.19889	-0.55609	-0.20595	-0.29676
1.0	0.25000	-2.61609	0.14979	-0.61606	-0.20082	-0.32203
1.0	0.20000	-2.79735	0.10287	-0.67135	-0.18754	-0.34618
1.0	0.15000	-2.94503	0.05998	-0.72018	-0.16465	-0.36844
1.0	0.10000	-3.05630	0.02395	-0.75985	-0.12982	-0.38717
1.0	0.05000	-3.12505	0.00087	-0.78448	-0.07758	-0.39759
1.0	0.	-3.14159	-0.00000	-0.78540	-0.00000	-0.39270
1.0	-0.05000	-3.12505	-0.00087	-0.78448	0.07758	-0.39759
1.0	-0.10000	-3.05630	-0.02395	-0.75985	0.12982	-0.38717
1.0	-0.15000	-2.94503	-0.05998	-0.72018	0.16465	-0.36844
1.0	-0.20000	-2.79735	-0.10287	-0.67135	0.18754	-0.34618
1.0	-0.25000	-2.61609	-0.14979	-0.61606	0.20082	-0.32203
1.0	-0.30000	-2.40301	-0.19889	-0.55609	0.20595	-0.29676
1.0	-0.35000	-2.15933	-0.24882	-0.49278	0.20400	-0.27078
1.0	-0.40000	-1.88597	-0.29850	-0.42722	0.19585	-0.24430
1.0	-0.45000	-1.58361	-0.34709	-0.36035	0.18228	-0.21744
1.0	-0.50000	-1.25278	-0.39386	-0.29299	0.16398	-0.19026
1.0	-0.55000	-0.89389	-0.43820	-0.22589	0.14159	-0.16277
1.0	-0.60000	-0.50723	-0.47960	-0.15971	0.11574	-0.13500
1.0	-0.65000	-0.09305	-0.51763	-0.09506	0.08701	-0.10696
1.0	-0.70000	0.34848	-0.55191	-0.03251	0.05601	-0.07871
1.0	-0.75000	0.81727	-0.58213	0.02741	0.02330	-0.05028
1.0	-0.80000	1.31323	-0.60803	0.08422	-0.01054	-0.02178
1.0	-0.85000	1.83635	-0.62939	0.13747	-0.04493	0.00668
1.0	-0.90000	2.38664	-0.64604	0.18676	-0.07933	0.03495
1.0	-0.92000	2.61437	-0.65135	0.20528	-0.09296	0.04616
1.0	-0.94000	2.84645	-0.65588	0.22308	-0.10647	0.05730
1.0	-0.95000	2.96413	-0.65785	0.23171	-0.11316	0.06284
1.0	-0.96000	3.08290	-0.65962	0.24015	-0.11981	0.06835
1.0	-0.98000	3.32372	-0.66258	0.25645	-0.13296	0.07929
1.0	-0.99990	3.56768	-0.66472	0.27190	-0.14582	0.09006
1.0	-0.50000	-1.25278	-0.39386	-0.29299	0.16398	-0.19026
1.0	0.16670	-2.89958	0.07371	-0.70473	-0.17348	-0.36129
1.0	0.83330	1.65861	0.62277	0.12011	0.03342	-0.00281
1.0	-0.62500	-0.30357	-0.49906	-0.12715	0.10170	-0.12101
1.0	-0.12500	-3.00546	-0.04086	-0.74139	0.14893	-0.37841
1.0	0.37500	-2.02631	0.27375	-0.46022	-0.20065	-0.25760
1.0	0.87500	2.10810	0.63831	0.16264	0.06217	0.02085

S	X	A31	A32	A33	A34	A35
1.0	0.99990	3.19162	-0.04396	-0.24492	-0.24953	-0.22926
1.0	0.95000	1.83055	-0.09275	-0.29244	-0.27585	-0.24536
1.0	0.90000	0.64585	-0.13954	-0.33547	-0.29541	-0.25567
1.0	0.85000	-0.36797	-0.18314	-0.37291	-0.30747	-0.25997
1.0	0.80000	-1.21934	-0.22253	-0.40387	-0.31150	-0.25826
1.0	0.75000	-1.91667	-0.25671	-0.42755	-0.30712	-0.25065
1.0	0.70000	-2.46840	-0.28478	-0.44329	-0.29410	-0.23739
1.0	0.65000	-2.88302	-0.30591	-0.45055	-0.27237	-0.21884
1.0	0.60000	-3.16908	-0.31941	-0.44897	-0.24203	-0.19551
1.0	0.55000	-3.33520	-0.32470	-0.43836	-0.20335	-0.16803
1.0	0.50000	-3.39015	-0.32138	-0.41871	-0.15681	-0.13715
1.0	0.45000	-3.34281	-0.30925	-0.39024	-0.10307	-0.10377
1.0	0.40000	-3.20229	-0.28835	-0.35345	-0.04304	-0.06896
1.0	0.35000	-2.97794	-0.25901	-0.30910	0.02212	-0.03395
1.0	0.30000	-2.67948	-0.22196	-0.25836	0.09093	-0.00023
1.0	0.25000	-2.31710	-0.17839	-0.20285	0.16151	0.03041
1.0	0.20000	-1.90168	-0.13023	-0.14483	0.23140	0.05572
1.0	0.15000	-1.44522	-0.08043	-0.08758	0.29727	0.07266
1.0	0.10000	-0.96170	-0.03392	-0.03619	0.35407	0.07658
1.0	0.05000	-0.47091	-0.00130	-0.00136	0.39127	0.05741
1.0	0.	-0.00000	-0.	0.00000	0.39270	0.00000
1.0	-0.05000	0.47091	-0.00130	0.00136	0.39127	-0.05741
1.0	-0.10000	0.96170	-0.03392	0.03619	0.35407	-0.07658
1.0	-0.15000	1.44522	-0.08043	0.08758	0.29727	-0.07266
1.0	-0.20000	1.90168	-0.13023	0.14483	0.23140	-0.05572
1.0	-0.25000	2.31710	-0.17839	0.20285	0.16151	-0.03041
1.0	-0.30000	2.67948	-0.22196	0.25836	0.09093	0.00023
1.0	-0.35000	2.97794	-0.25901	0.30910	0.02212	0.03395
1.0	-0.40000	3.20229	-0.28835	0.35345	-0.04304	0.06896
1.0	-0.45000	3.34281	-0.30925	0.39024	-0.10307	0.10377
1.0	-0.50000	3.39015	-0.32138	0.41871	-0.15681	0.13715
1.0	-0.55000	3.33521	-0.32470	0.43836	-0.20335	0.16803
1.0	-0.60000	3.16908	-0.31941	0.44897	-0.24203	0.19551
1.0	-0.65000	2.88302	-0.30591	0.45055	-0.27237	0.21884
1.0	-0.70000	2.46840	-0.28478	0.44329	-0.29410	0.23739
1.0	-0.75000	1.91667	-0.25671	0.42755	-0.30712	0.25065
1.0	-0.80000	1.21934	-0.22253	0.40387	-0.31150	0.25826
1.0	-0.85000	0.36797	-0.18314	0.37291	-0.30747	0.25997
1.0	-0.90000	-0.64585	-0.13954	0.33547	-0.29541	0.25567
1.0	-0.92000	-1.09876	-0.12114	0.31887	-0.28845	0.25226
1.0	-0.94000	-1.57954	-0.10231	0.30145	-0.28033	0.24790
1.0	-0.95000	-1.83055	-0.09275	0.29244	-0.27585	0.24536
1.0	-0.96000	-2.08874	-0.08310	0.28325	-0.27110	0.24259
1.0	-0.98000	-2.62689	-0.06360	0.26435	-0.26079	0.23636
1.0	-0.99990	-3.19162	-0.04396	0.24492	-0.24953	0.22926
1.0	-0.50000	3.39015	-0.32138	0.41871	-0.15681	0.13715
1.0	0.16670	-1.60144	-0.09700	-0.10636	0.27597	0.06817
1.0	0.83330	-0.66998	-0.19682	-0.38401	-0.30973	-0.26007
1.0	-0.62500	3.04158	-0.31365	0.45088	-0.25826	0.20774
1.0	-0.12500	1.20583	-0.05633	0.06071	0.32724	-0.07665
1.0	0.37500	-3.10000	-0.27470	-0.33216	-0.01101	-0.05139
1.0	0.87500	0.11811	-0.16180	-0.35495	-0.30241	-0.25857

S	X	A41	A42	A43	A44	A45
1.0	0.99990	2.90285	-0.26279	-0.26265	-0.18631	-0.13198
1.0	0.95000	0.69941	-0.24919	-0.23564	-0.14655	-0.09150
1.0	0.90000	-0.94503	-0.22627	-0.19979	-0.09973	-0.04687
1.0	0.85000	-2.09562	-0.19491	-0.15649	-0.04768	-0.00008
1.0	0.80000	-2.81912	-0.15634	-0.10741	0.00759	0.04684
1.0	0.75000	-3.17885	-0.11210	-0.05449	0.06393	0.09182
1.0	0.70000	-3.23469	-0.06403	0.00011	0.11905	0.13277
1.0	0.65000	-3.04305	-0.01421	0.05408	0.17062	0.16767
1.0	0.60000	-2.65685	0.03506	0.10499	0.21633	0.19462
1.0	0.55000	-2.12545	0.08136	0.15039	0.25396	0.21191
1.0	0.50000	-1.49461	0.12218	0.18790	0.28147	0.21807
1.0	0.45000	-0.80642	0.15507	0.21526	0.29707	0.21195
1.0	0.40000	-0.09916	0.17771	0.23053	0.29934	0.19280
1.0	0.35000	0.59280	0.18808	0.23216	0.28739	0.16041
1.0	0.30000	1.23923	0.18466	0.21921	0.26097	0.11521
1.0	0.25000	1.81433	0.16671	0.19163	0.22075	0.05850
1.0	0.20000	2.29714	0.13471	0.15063	0.16866	-0.00725
1.0	0.15000	2.67232	0.09105	0.09937	0.10851	-0.07778
1.0	0.10000	2.93179	0.04165	0.04446	0.04748	-0.14564
1.0	0.05000	3.08057	0.00172	0.00180	0.00189	-0.19437
1.0	0.	3.14159	-0.00000	-0.00000	-0.00000	-0.19635
1.0	-0.05000	3.08057	-0.00172	0.00180	-0.00189	-0.19437
1.0	-0.10000	2.93179	-0.04165	0.04446	-0.04748	-0.14564
1.0	-0.15000	2.67232	-0.09105	0.09937	-0.10851	-0.07778
1.0	-0.20000	2.29714	-0.13471	0.15063	-0.16866	-0.00725
1.0	-0.25000	1.81433	-0.16671	0.19163	-0.22075	0.05850
1.0	-0.30000	1.23923	-0.18466	0.21921	-0.26097	0.11521
1.0	-0.35000	0.59280	-0.18808	0.23216	-0.28739	0.16041
1.0	-0.40000	-0.09916	-0.17771	0.23053	-0.29934	0.19280
1.0	-0.45000	-0.80642	-0.15507	0.21526	-0.29707	0.21195
1.0	-0.50000	-1.49461	-0.12218	0.18790	-0.28147	0.21807
1.0	-0.55000	-2.12545	-0.08136	0.15039	-0.25396	0.21191
1.0	-0.60000	-2.65685	-0.03506	0.10499	-0.21633	0.19462
1.0	-0.65000	-3.04305	0.01421	0.05408	-0.17062	0.16767
1.0	-0.70000	-3.23469	0.06403	0.00011	-0.11905	0.13277
1.0	-0.75000	-3.17885	0.11210	-0.05449	-0.06393	0.09182
1.0	-0.80000	-2.81912	0.15634	-0.10741	-0.00759	0.04684
1.0	-0.85000	-2.09562	0.19491	-0.15649	0.04768	-0.00008
1.0	-0.90000	-0.94503	0.22627	-0.19979	0.09973	-0.04687
1.0	-0.92000	-0.35037	0.23651	-0.21510	0.11919	-0.06509
1.0	-0.94000	0.32769	0.24533	-0.22914	0.13770	-0.08284
1.0	-0.95000	0.69941	0.24919	-0.23564	0.14655	-0.09150
1.0	-0.96000	1.09368	0.25268	-0.24179	0.15513	-0.10000
1.0	-0.98000	1.95217	0.25852	-0.25300	0.17139	-0.11644
1.0	-0.99990	2.90285	0.26279	-0.26265	0.18631	-0.13198
1.0	-0.50000	-1.49461	-0.12218	0.18790	-0.28147	0.21807
1.0	0.16670	2.55966	0.10667	0.11732	0.12915	-0.05406
1.0	0.83330	-2.38157	-0.18276	-0.14065	-0.02948	0.01568
1.0	-0.62500	-2.87110	-0.01064	0.08007	-0.19435	0.18225
1.0	-0.12500	2.81666	-0.06648	0.07174	-0.07745	-0.11271
1.0	0.37500	0.25072	0.18454	0.23312	0.29518	0.17825
1.0	0.87500	-1.57780	-0.21158	-0.17897	-0.07424	-0.02362

S	X	A01	A02	A03	A04	A05
1.2	0.99990	1.82638	0.85896	0.68228	0.63090	0.62844
1.2	0.95000	1.84072	0.92535	0.72095	0.66509	0.66199
1.2	0.90000	1.85792	0.99564	0.76099	0.70132	0.69774
1.2	0.85000	1.87831	1.07006	0.80260	0.73996	0.73601
1.2	0.80000	1.90235	1.14907	0.84612	0.78153	0.77728
1.2	0.75000	1.93061	1.23321	0.89200	0.82670	0.82215
1.2	0.70000	1.96378	1.32318	0.94083	0.87630	0.87139
1.2	0.65000	2.00277	1.41989	0.99343	0.93140	0.92603
1.2	0.60000	2.04874	1.52451	1.05094	0.99344	0.98749
1.2	0.55000	2.10329	1.63871	1.11496	1.06443	1.05780
1.2	0.50000	2.16868	1.76482	1.18792	1.14731	1.14006
1.2	0.45000	2.24828	1.90649	1.27369	1.24670	1.23931
1.2	0.40000	2.34769	2.06984	1.37904	1.37064	1.36457
1.2	0.35000	2.47754	2.26692	1.51770	1.53549	1.53479
1.2	0.30000	2.66490	2.52945	1.72709	1.78619	1.80351
1.2	0.25000	3.14159	3.14159	2.35619	2.55254	2.69981
1.2	0.20000	3.14159	3.14159	2.19911	2.32478	2.33420
1.2	0.15000	3.14159	3.14159	2.04204	2.11272	2.00159
1.2	0.10000	3.14159	3.14159	1.88496	1.91637	1.69960
1.2	0.05000	3.14159	3.14159	1.72788	1.73573	1.42589
1.2	0.	3.14159	3.14159	1.57080	1.57080	1.17810
1.2	-0.05000	3.14159	3.14159	1.41372	1.42157	0.95387
1.2	-0.10000	3.14159	3.14159	1.25664	1.28805	0.75084
1.2	-0.15000	3.14159	3.14159	1.09956	1.17024	0.56666
1.2	-0.20000	3.14159	3.14159	0.94248	1.06814	0.39898
1.2	-0.25000	3.14159	3.14159	0.78540	0.98175	0.24544
1.2	-0.30000	3.14542	3.13672	0.63451	0.90319	0.11369
1.2	-0.35000	3.15283	3.12709	0.48997	0.83189	0.00261
1.2	-0.40000	3.16238	3.11435	0.34988	0.76994	-0.09236
1.2	-0.45000	3.17363	3.09902	0.21375	0.71772	-0.17366
1.2	-0.50000	3.18630	3.08135	0.08137	0.67526	-0.24327
1.2	-0.55000	3.20023	3.06150	-0.04736	0.64245	-0.30296
1.2	-0.60000	3.21531	3.03960	-0.17245	0.61908	-0.35438
1.2	-0.65000	3.23145	3.01569	-0.29389	0.60491	-0.39906
1.2	-0.70000	3.24858	2.98982	-0.41163	0.59962	-0.43844
1.2	-0.75000	3.26668	2.96203	-0.52561	0.60289	-0.47387
1.2	-0.80000	3.28571	2.93230	-0.63574	0.61434	-0.50662
1.2	-0.85000	3.30565	2.90065	-0.74192	0.63357	-0.53788
1.2	-0.90000	3.32650	2.86705	-0.84402	0.66017	-0.56875
1.2	-0.92000	3.33510	2.85306	-0.88369	0.67276	-0.58122
1.2	-0.94000	3.34384	2.83875	-0.92268	0.68643	-0.59385
1.2	-0.95000	3.34826	2.83147	-0.94192	0.69366	-0.60025
1.2	-0.96000	3.35273	2.82411	-0.96098	0.70115	-0.60671
1.2	-0.98000	3.36176	2.80916	-0.99858	0.71687	-0.61984
1.2	-0.99990	3.36971	2.79396	-1.03528	0.73348	-0.63323
1.2	-0.50000	3.18630	3.08135	0.08137	0.67526	-0.24327
1.2	0.16670	3.14159	3.14159	2.09450	2.18180	2.10916
1.2	0.83330	1.88590	1.09592	0.81691	0.75349	0.74943
1.2	-0.62500	3.22325	3.02789	-0.23362	0.61086	-0.37747
1.2	-0.12500	3.14159	3.14159	1.17810	1.22718	0.65654
1.2	0.37500	2.40777	2.16297	1.44282	1.44630	1.44213
1.2	0.87500	1.86768	1.03231	0.78158	0.72031	0.71653

S	X	A11	A12	A13	A14	A15
1.2	0.99990	2.79362	1.03556	0.73359	0.63331	0.60233
1.2	0.95000	2.66406	1.08349	0.74076	0.63493	0.60162
1.2	0.90000	2.53440	1.13073	0.74457	0.63477	0.59923
1.2	0.85000	2.40480	1.17701	0.74486	0.63291	0.59515
1.2	0.80000	2.27516	1.22220	0.74149	0.62948	0.58930
1.2	0.75000	2.14536	1.26612	0.73429	0.62459	0.58158
1.2	0.70000	2.01525	1.30858	0.72311	0.61832	0.57183
1.2	0.65000	1.88468	1.34938	0.70777	0.61078	0.55985
1.2	0.60000	1.75347	1.38828	0.68806	0.60202	0.54538
1.2	0.55000	1.62140	1.42503	0.66376	0.59206	0.52806
1.2	0.50000	1.48820	1.45931	0.63458	0.58090	0.50747
1.2	0.45000	1.35352	1.49071	0.60016	0.56840	0.48300
1.2	0.40000	1.21692	1.51874	0.56001	0.55433	0.45387
1.2	0.35000	1.07775	1.54264	0.51341	0.53812	0.41891
1.2	0.30000	0.93493	1.56119	0.45903	0.51854	0.37608
1.2	0.25000	0.78540	1.57080	0.39270	0.49087	0.31907
1.2	0.20000	0.62832	1.57080	0.31416	0.45553	0.24819
1.2	0.15000	0.47124	1.57080	0.23562	0.42804	0.18202
1.2	0.10000	0.31416	1.57080	0.15708	0.40841	0.11938
1.2	0.05000	0.15708	1.57080	0.07854	0.39663	0.05910
1.2	0.	-0.00000	1.57080	0.00000	0.39270	0.00000
1.2	-0.05000	-0.15708	1.57080	-0.07854	0.39663	-0.05910
1.2	-0.10000	-0.31416	1.57080	-0.15708	0.40841	-0.11938
1.2	-0.15000	-0.47124	1.57080	-0.23562	0.42804	-0.18202
1.2	-0.20000	-0.62832	1.57080	-0.31416	0.45553	-0.24819
1.2	-0.25000	-0.78540	1.57080	-0.39270	0.49087	-0.31907
1.2	-0.30000	-0.93493	1.56119	-0.45903	0.51854	-0.37608
1.2	-0.35000	-1.07775	1.54264	-0.51341	0.53812	-0.41891
1.2	-0.40000	-1.21692	1.51874	-0.56001	0.55433	-0.45387
1.2	-0.45000	-1.35352	1.49071	-0.60016	0.56840	-0.48300
1.2	-0.50000	-1.48820	1.45931	-0.63458	0.58090	-0.50747
1.2	-0.55000	-1.62140	1.42503	-0.66376	0.59206	-0.52806
1.2	-0.60000	-1.75347	1.38828	-0.68806	0.60202	-0.54538
1.2	-0.65000	-1.88468	1.34938	-0.70777	0.61078	-0.55985
1.2	-0.70000	-2.01525	1.30858	-0.72311	0.61832	-0.57183
1.2	-0.75000	-2.14536	1.26612	-0.73429	0.62459	-0.58158
1.2	-0.80000	-2.27516	1.22220	-0.74149	0.62948	-0.58930
1.2	-0.85000	-2.40480	1.17701	-0.74486	0.63291	-0.59515
1.2	-0.90000	-2.53440	1.13073	-0.74457	0.63477	-0.59923
1.2	-0.92000	-2.58625	1.11194	-0.74346	0.63504	-0.60039
1.2	-0.94000	-2.63812	1.09301	-0.74180	0.63504	-0.60127
1.2	-0.95000	-2.66406	1.08349	-0.74076	0.63493	-0.60162
1.2	-0.96000	-2.69001	1.07395	-0.73959	0.63475	-0.60189
1.2	-0.98000	-2.74192	1.05476	-0.73684	0.63418	-0.60224
1.2	-0.99990	-2.79362	1.03556	-0.73359	0.63331	-0.60233
1.2	-0.50000	-1.48820	1.45931	-0.63458	0.58090	-0.50747
1.2	0.16670	0.52370	1.57080	0.26185	0.43635	0.20367
1.2	0.83330	2.36151	1.19224	0.74415	0.63194	0.59340
1.2	-0.62500	-1.81917	1.36908	-0.69847	0.60655	-0.55295
1.2	-0.12500	-0.39270	1.57080	-0.19635	0.41724	-0.15033
1.2	0.37500	1.14771	1.53126	0.53758	0.54654	0.43722
1.2	0.87500	2.46960	1.15400	0.74517	0.63404	0.59741

S	X	A21	A22	A23	A24	A25
1.2	0.99990	3.51555	0.60375	0.20042	0.06183	-0.00884
1.2	0.95000	2.89472	0.57712	0.13758	0.00314	-0.06607
1.2	0.90000	2.30047	0.54616	0.07070	-0.05589	-0.12298
1.2	0.85000	1.73414	0.51120	0.00044	-0.11435	-0.17895
1.2	0.80000	1.19586	0.47255	-0.07259	-0.17143	-0.23349
1.2	0.75000	0.68580	0.43059	-0.14774	-0.22627	-0.28612
1.2	0.70000	0.20420	0.38579	-0.22429	-0.27800	-0.33635
1.2	0.65000	-0.24867	0.33865	-0.30146	-0.32569	-0.38369
1.2	0.60000	-0.67240	0.28982	-0.37836	-0.36834	-0.42759
1.2	0.55000	-1.06653	0.24002	-0.45399	-0.40486	-0.46743
1.2	0.50000	-1.43042	0.19015	-0.52722	-0.43404	-0.50246
1.2	0.45000	-1.76326	0.14133	-0.59667	-0.45444	-0.53171
1.2	0.40000	-2.06393	0.09496	-0.66064	-0.46429	-0.55382
1.2	0.35000	-2.33085	0.05304	-0.71685	-0.46114	-0.56667
1.2	0.30000	-2.56143	0.01866	-0.76166	-0.44105	-0.56635
1.2	0.25000	-2.74889	-0.00000	-0.78540	-0.39270	-0.53996
1.2	0.20000	-2.89027	-0.00000	-0.78540	-0.31416	-0.48695
1.2	0.15000	-3.00022	-0.00000	-0.78540	-0.23562	-0.44571
1.2	0.10000	-3.07876	-0.00000	-0.78540	-0.15708	-0.41626
1.2	0.05000	-3.12588	-0.00000	-0.78540	-0.07854	-0.39859
1.2	0.	-3.14159	-0.00000	-0.78540	-0.00000	-0.39270
1.2	-0.05000	-3.12588	-0.00000	-0.78540	0.07854	-0.39859
1.2	-0.10000	-3.07876	-0.00000	-0.78540	0.15708	-0.41626
1.2	-0.15000	-3.00022	-0.00000	-0.78540	0.23562	-0.44571
1.2	-0.20000	-2.89027	-0.00000	-0.78540	0.31416	-0.48695
1.2	-0.25000	-2.74889	-0.00000	-0.78540	0.39270	-0.53996
1.2	-0.30000	-2.56143	-0.01866	-0.76166	0.44105	-0.56635
1.2	-0.35000	-2.33085	-0.05304	-0.71685	0.46114	-0.56667
1.2	-0.40000	-2.06393	-0.09496	-0.66064	0.46429	-0.55382
1.2	-0.45000	-1.76326	-0.14133	-0.59667	0.45444	-0.53171
1.2	-0.50000	-1.43042	-0.19015	-0.52722	0.43404	-0.50246
1.2	-0.55000	-1.06653	-0.24002	-0.45399	0.40486	-0.46743
1.2	-0.60000	-0.67240	-0.28982	-0.37836	0.36834	-0.42759
1.2	-0.65000	-0.24867	-0.33865	-0.30146	0.32569	-0.38369
1.2	-0.70000	0.20419	-0.38579	-0.22429	0.27800	-0.33635
1.2	-0.75000	0.68580	-0.43059	-0.14774	0.22627	-0.28612
1.2	-0.80000	1.19586	-0.47255	-0.07259	0.17143	-0.23349
1.2	-0.85000	1.73414	-0.51120	0.00044	0.11435	-0.17895
1.2	-0.90000	2.30047	-0.54616	0.07070	0.05589	-0.12298
1.2	-0.92000	2.53482	-0.55904	0.09788	0.03230	-0.10030
1.2	-0.94000	2.77364	-0.57126	0.12450	0.00867	-0.07750
1.2	-0.95000	2.89472	-0.57712	0.13758	-0.00314	-0.06607
1.2	-0.96000	3.01692	-0.58281	0.15050	-0.01494	-0.05462
1.2	-0.98000	3.26464	-0.59366	0.17586	-0.03850	-0.03168
1.2	-0.99990	3.51555	-0.60375	0.20042	-0.06183	-0.00884
1.2	-0.50000	-1.43042	-0.19015	-0.52722	0.43404	-0.50246
1.2	0.16670	-2.96699	-0.00000	-0.78540	-0.26185	-0.45818
1.2	0.83330	1.55123	0.49868	-0.02367	-0.13361	-0.19735
1.2	-0.62500	-0.46420	-0.31441	-0.34000	0.34771	-0.40611
1.2	-0.12500	-3.04342	-0.00000	-0.78540	0.19635	-0.42951
1.2	0.37500	-2.20174	0.07329	-0.68990	-0.46453	-0.56159
1.2	0.87500	2.01380	0.52916	0.03595	-0.08524	-0.15111

S	X	A31	A32	A33	A34	A35
1.2	0.99990	3.02928	-0.22902	-0.45646	-0.49197	-0.50789
1.2	0.95000	1.68167	-0.26212	-0.48564	-0.49683	-0.49880
1.2	0.90000	0.51411	-0.28902	-0.50554	-0.48942	-0.47758
1.2	0.85000	-0.47917	-0.30886	-0.51541	-0.46942	-0.44451
1.2	0.80000	-1.30688	-0.32095	-0.51478	-0.43679	-0.40016
1.2	0.75000	-1.97784	-0.32475	-0.50336	-0.39176	-0.34533
1.2	0.70000	-2.50095	-0.31989	-0.48112	-0.33482	-0.28114
1.2	0.65000	-2.88526	-0.30621	-0.44829	-0.26679	-0.20899
1.2	0.60000	-3.13999	-0.28379	-0.40542	-0.18883	-0.13062
1.2	0.55000	-3.27462	-0.25303	-0.35343	-0.10254	-0.04819
1.2	0.50000	-3.29893	-0.21472	-0.29372	-0.01001	0.03563
1.2	0.45000	-3.22311	-0.17018	-0.22828	0.08603	0.11752
1.2	0.40000	-3.05800	-0.12148	-0.15996	0.18189	0.19316
1.2	0.35000	-2.81542	-0.07182	-0.09292	0.27244	0.25662
1.2	0.30000	-2.50911	-0.02667	-0.03393	0.34953	0.29850
1.2	0.25000	-2.15984	-0.	0.00000	0.39270	0.29452
1.2	0.20000	-1.78442	-0.	0.00000	0.39270	0.23562
1.2	0.15000	-1.37131	-0.	0.00000	0.39270	0.17671
1.2	0.10000	-0.92991	-0.	0.00000	0.39270	0.11781
1.2	0.05000	-0.46967	-0.	0.00000	0.39270	0.05890
1.2	0.	-0.00000	-0.	0.00000	0.39270	0.00000
1.2	-0.05000	0.46967	-0.	0.00000	0.39270	-0.05890
1.2	-0.10000	0.92991	-0.	0.00000	0.39270	-0.11781
1.2	-0.15000	1.37130	-0.	0.00000	0.39270	-0.17671
1.2	-0.20000	1.78442	-0.	0.00000	0.39270	-0.23562
1.2	-0.25000	2.15984	-0.	0.00000	0.39270	-0.29452
1.2	-0.30000	2.50911	-0.02667	0.03393	0.34953	-0.29850
1.2	-0.35000	2.81542	-0.07182	0.09292	0.27244	-0.25662
1.2	-0.40000	3.05800	-0.12148	0.15996	0.18189	-0.19316
1.2	-0.45000	3.22311	-0.17018	0.22828	0.08603	-0.11752
1.2	-0.50000	3.29893	-0.21472	0.29372	-0.01001	-0.03563
1.2	-0.55000	3.27462	-0.25303	0.35343	-0.10254	0.04819
1.2	-0.60000	3.13999	-0.28379	0.40542	-0.18883	0.13062
1.2	-0.65000	2.88526	-0.30620	0.44829	-0.26679	0.20899
1.2	-0.70000	2.50095	-0.31989	0.48112	-0.33482	0.28114
1.2	-0.75000	1.97784	-0.32475	0.50336	-0.39176	0.34533
1.2	-0.80000	1.30688	-0.32095	0.51478	-0.43679	0.40016
1.2	-0.85000	0.47917	-0.30886	0.51541	-0.46942	0.44451
1.2	-0.90000	-0.51411	-0.28902	0.50554	-0.48942	0.47758
1.2	-0.92000	-0.95974	-0.27906	0.49875	-0.49388	0.48751
1.2	-0.94000	-1.43380	-0.26803	0.49039	-0.49635	0.49552
1.2	-0.95000	-1.68167	-0.26212	0.48564	-0.49683	0.49880
1.2	-0.96000	-1.93686	-0.25596	0.48051	-0.49683	0.50160
1.2	-0.98000	-2.46947	-0.24291	0.46916	-0.49535	0.50572
1.2	-0.99990	-3.02928	-0.22902	0.45646	-0.49197	0.50789
1.2	-0.50000	3.29893	-0.21472	0.29372	-0.01001	-0.03563
1.2	0.16670	-1.51290	-0.	0.00000	0.39270	0.19639
1.2	0.83330	-0.77360	-0.31379	-0.51639	-0.45992	-0.43091
1.2	-0.62500	3.02824	-0.29607	0.42806	-0.22896	0.17046
1.2	-0.12500	1.15355	-0.	0.00000	0.39270	-0.14726
1.2	0.37500	-2.94560	-0.09650	-0.12594	0.22824	0.22688
1.2	0.87500	-0.00377	-0.29987	-0.51176	-0.48100	-0.46249

S	X	A41	A42	A43	A44	A45
1.2	0.99990	3.00045	-0.14883	-0.12929	-0.02990	0.05188
1.2	0.95000	0.82469	-0.10386	-0.06663	0.05049	0.13877
1.2	0.90000	-0.79702	-0.05533	-0.00183	0.13009	0.22063
1.2	0.85000	-1.93100	-0.00543	0.06219	0.20536	0.29349
1.2	0.80000	-2.64498	0.04349	0.12253	0.27287	0.35371
1.2	0.75000	-3.00307	0.08901	0.17622	0.32930	0.39788
1.2	0.70000	-3.06575	0.12861	0.22036	0.37154	0.42299
1.2	0.65000	-2.88976	0.15986	0.25226	0.39684	0.42657
1.2	0.60000	-2.52802	0.18048	0.26953	0.40297	0.40687
1.2	0.55000	-2.02950	0.18851	0.27031	0.38845	0.36305
1.2	0.50000	-1.43907	0.18256	0.25352	0.35277	0.29549
1.2	0.45000	-0.79717	0.16206	0.21917	0.29682	0.20623
1.2	0.40000	-0.13951	0.12776	0.16890	0.22347	0.09958
1.2	0.35000	0.50370	0.08253	0.10693	0.13861	-0.01661
1.2	0.30000	1.10931	0.03320	0.04224	0.05376	-0.12792
1.2	0.25000	1.66897	-0.00000	-0.00000	-0.00000	-0.19635
1.2	0.20000	2.17650	-0.00000	-0.00000	-0.00000	-0.19635
1.2	0.15000	2.58883	-0.00000	-0.00000	-0.00000	-0.19635
1.2	0.10000	2.89278	-0.00000	-0.00000	-0.00000	-0.19635
1.2	0.05000	3.07892	-0.00000	-0.00000	-0.00000	-0.19635
1.2	0.	3.14159	-0.00000	-0.00000	-0.00000	-0.19635
1.2	-0.05000	3.07892	-0.00000	-0.00000	-0.00000	-0.19635
1.2	-0.10000	2.89278	-0.00000	-0.00000	-0.00000	-0.19635
1.2	-0.15000	2.58883	-0.00000	-0.00000	-0.00000	-0.19635
1.2	-0.20000	2.17650	-0.00000	-0.00000	-0.00000	-0.19635
1.2	-0.25000	1.66897	-0.00000	-0.00000	-0.00000	-0.19635
1.2	-0.30000	1.10931	-0.03320	0.04224	-0.05376	-0.12792
1.2	-0.35000	0.50370	-0.08253	0.10693	-0.13861	-0.01661
1.2	-0.40000	-0.13951	-0.12776	0.16890	-0.22347	0.09958
1.2	-0.45000	-0.79717	-0.16206	0.21917	-0.29682	0.20623
1.2	-0.50000	-1.43907	-0.18256	0.25352	-0.35277	0.29549
1.2	-0.55000	-2.02950	-0.18851	0.27031	-0.38845	0.36305
1.2	-0.60000	-2.52802	-0.18048	0.26953	-0.40297	0.40687
1.2	-0.65000	-2.88976	-0.15986	0.25226	-0.39684	0.42657
1.2	-0.70000	-3.06575	-0.12861	0.22036	-0.37154	0.42299
1.2	-0.75000	-3.00307	-0.08901	0.17622	-0.32930	0.39788
1.2	-0.80000	-2.64498	-0.04349	0.12253	-0.27287	0.35371
1.2	-0.85000	-1.93101	0.00543	0.06219	-0.20536	0.29349
1.2	-0.90000	-0.79702	0.05533	-0.00183	-0.13009	0.22063
1.2	-0.92000	-0.21078	0.07503	-0.02782	-0.09858	0.18875
1.2	-0.94000	0.45796	0.09437	-0.05374	-0.06659	0.15568
1.2	-0.95000	0.82469	0.10386	-0.06663	-0.05049	0.13877
1.2	-0.96000	1.21377	0.11322	-0.07943	-0.03434	0.12165
1.2	-0.98000	2.06134	0.13144	-0.10471	-0.00206	0.08691
1.2	-0.99990	3.00045	0.14883	-0.12929	0.02990	0.05188
1.2	-0.50000	-1.43907	-0.18256	0.25352	-0.35277	0.29549
1.2	0.16670	2.46259	-0.00000	-0.00000	-0.00000	-0.19635
1.2	0.83330	-2.21294	0.01113	0.08290	0.22894	0.31518
1.2	-0.62500	-2.72895	-0.17163	0.26285	-0.40241	0.41971
1.2	-0.12500	2.75503	-0.00000	-0.00000	-0.00000	-0.19635
1.2	0.37500	0.18554	0.10622	0.13897	0.18194	0.04199
1.2	0.87500	-1.42066	-0.03041	0.03046	0.16848	0.25841

APPENDIX 4.

Tables of $C_m^{(n)}$ and $S_m^{(n)}$ in Section 3, Part III.

$R_0(\beta)$	$R_1(\beta)$	$R_2(\beta)$
$C_0^{(0)} = 4.08181$	$C_0^{(1)} = -2.79420$	$C_0^{(2)} = -1.25926$
$C_1^{(0)} = 0.42090$	$C_1^{(1)} = -0.24261$	$C_1^{(2)} = -0.24657$
$C_2^{(0)} = -2.02739$	$C_2^{(1)} = -0.79307$	$C_2^{(2)} = -0.56473$
$C_3^{(0)} = -0.16202$	$C_3^{(1)} = -0.00904$	$C_3^{(2)} = -0.00304$
$C_4^{(0)} = 0.15225$	$C_4^{(1)} = -0.02945$	$C_4^{(2)} = -0.02611$
$C_5^{(0)} = -0.02309$	$C_5^{(1)} = 0.$	$C_5^{(2)} = 0.$
$C_6^{(0)} = 0.00326$	$C_6^{(1)} = 0.$	$C_6^{(2)} = 0.$
$S_m^{(0)} = 0.$ (m=1,2,...)	$S_m^{(1)} = 0.$ (m=1,2,...)	$S_m^{(2)} = 0.$ (m=1,2,...)

$R_3(\beta)$	$R_4(\beta)$	$R_5(\beta)$
$C_0^{(3)} = 4.08181$		
$C_1^{(3)} = 0.42090$	$S_1^{(4)} = 0.34632$	$S_1^{(5)} = -0.40807$
$C_2^{(3)} = -2.02739$	$S_2^{(4)} = 1.24215$	$S_2^{(5)} = -0.46714$
$C_3^{(3)} = -0.16202$	$S_3^{(4)} = -0.12137$	$S_3^{(5)} = 0.21549$
$C_4^{(3)} = 0.15225$	$S_4^{(4)} = -0.01830$	$S_4^{(5)} = 0.03044$
$C_5^{(3)} = -0.02309$	$S_5^{(4)} = -0.04067$	$S_5^{(5)} = 0.09550$
$C_6^{(3)} = 0.00326$	$S_6^{(4)} = -0.00383$	$S_6^{(5)} = 0.01577$
$S_m^{(3)} = 0.$ (m=1,2,...)	$C_m^{(4)} = 0.$ (m=0,1,2,...)	$C_m^{(5)} = 0.$ (m=0,1,2,...)

APPENDIX 4 (cont'd.)

$R_6(\beta)$	$R_7(\beta)$	$R_8(\beta)$
$C_0^{(6)} = -3.61963$		
$C_1^{(6)} = 1.46974$	$S_1^{(7)} = 1.50595$	$S_1^{(8)} = 1.00755$
$C_2^{(6)} = -1.06303$	$S_2^{(7)} = 0.04600$	$S_2^{(8)} = 0.72053$
$C_3^{(6)} = 0.07831$	$S_3^{(7)} = 0.05229$	$S_3^{(8)} = -0.03182$
$C_4^{(6)} = -0.03876$	$S_4^{(7)} = -0.00101$	$S_4^{(8)} = 0.05085$
$S_m^{(6)} = 0.$ (m=1,2,...)	$C_m^{(7)} = 0.$ (m=0,1,2,...)	$C_m^{(8)} = 0.$ (m=0,1,2,...)